

In-vitro Synthesis and Reconstitution of Cytochrome b_0_3 Ubiquinol Oxidase in Artificial Membranes

Dissertation
Zur Erlangung des Grades
Doktor der Naturwissenschaften

Am Fachbereich Biologie
Der Johannes Gutenberg-Universität Mainz

Ahu ARSLAN YILDIZ
geboren am 20.12.1980 in Turkey

Mainz, 2010

Dekan: Prof. Dr. Erwin Schmidt

1. Berichterstatter: Prof. Dr. Eva K. Sinner
2. Berichterstatter: Prof. Dr. Harald Paulsen
3. Prüfer: Prof. Dr. Wolfgang Knoll
4. Prüfer: Prof. Dr. Elmar Jaenicke

Tag der mündlichen Prüfung: 29.01.2010

Abbreviations

ATP	Adenosine triphosphate
PD	Parkinson's Disease
Cyt- b_0_3	Cytochrome b_0_3 ubiquinol oxidase
NADH	Nicotinamide adenine dinucleotide
UQ	Ubiquinone
UQH ₂	Ubiquinol
Cyt- <i>c</i>	Cytochrome <i>c</i>
E.coli	Escherichia coli
Heme	Heme or Haem molecule
Cyt- <i>bd</i>	Cytochrome <i>bd</i> ubiquinol oxidase
<i>cyo</i>	Cytochrome encoding operon
Cu _A	Copper site in subunit II
Cu _B	Copper of binuclear site
CFPS	Cell-free protein synthesis
tRNA	Transfer RNA
GTP	Guanidine triphosphate
BLMs	Black lipid membranes
sBLM	Supported bilayer lipid membrane
tBLM	Tethered lipid bilayer membrane
SPR	Surface Plasmon Resonance Spectroscopy
SPFS	Surface Plasmon Enhanced Fluorescence Spectroscopy
θ_c	Critical angle
θ_m	Minimum angle
TIR	Total internal reflection
ϵ_d	Dielectric constant
<i>n</i>	Refractive index
CA	Contact angle
pJRHisA	Subunit II histidine tagged enzyme with natural promoter
pRCO3	Fused subunit II-I-III enzyme with natural promoter
pETcyo	Subunit II histidine tagged enzyme with T7 promoter
LB	Luria Bertani media

KOH	Potassium hydroxide
PES	Polyethylene sulfonate
X-Gal	Bromo-chloro-indolyl-galactopyranoside
IPTG	Isopropyl β -D-1-thiogalactopyranoside
RT	Room temperature
rpm	Round per minute
NaAc	Sodium acetate
EtOH	Ethanol
TAE	Tris-Acetate-EDTA buffer
kb	kilo base pairs
Ni-NTA	Nickel-Nitrilotriacetic acid
BCA	Bicinchoninic acid
mRNA	Messenger RNA
SDS	Sodium dodecyl sulfate
PVDF	Polyvinylidene fluoride
Ab	Antibody
DMSO	Dimethyl sulfoxide
HCl	Hydrochloric acid
K_M	Michaelis-Menten affinity constant
V_{max}	Michaelis-Menten velocity
PDMS	Polydimethyl sulfoxide
LaSFN9	High refractive index glass
HeNe	Helium/Neon
λ	Wavelength
TM	Transversal magnetic (p) polarization
P19	Laminin Peptide P19
EDC	N-(3-Dimethylaminopropyl)-N'-ethylcarbodiimide Hydrochloride
NHS	N-Hydroxysuccinimide
DMPE	1,2-Dimyristoyl- <i>sn</i> -glycero-3-phosphoethanolamine
PBS	Phosphate Buffered Saline (Buffer)
PC	L- α -Phosphatidylcholine from soybean
1°Ab	Primary antibody
2°Ab	Secondary antibody

PentaHis 1°Ab	Primary antibody responds to five histidine residues
Cy5	Fluorescence Cyanine dye
Alexa Fluor 647	Fluorescence Alexa Fluor dye
DPePE	1,2-Dipentadecanoyl- <i>sn</i> -glycero-3-phosphoethanolamine
DPPE	1,2-Dipalmitoyl- <i>sn</i> -glycero-3-phosphoethanolamine
DPhyPE	1,2-Diphytanoyl- <i>sn</i> -glycero-3-phosphoethanolamine
DPalPE	1,2-Dipalmitoleoyl- <i>sn</i> -glycero-3-phosphoethanolamine
DLPE	1,2-Dilinolenoyl- <i>sn</i> -glycero-3-phosphoethanolamine
DAPE	1,2-Diarachidonoyl- <i>sn</i> -glycero-3-phosphoethanolamine
DDPE	1,2-Didocosaheptaenoyl- <i>sn</i> -glycero-3-phosphoethanolamine
TE	<i>E. coli</i> Total Extract
AFM	Atomic force microscopy
FR	Farnesyl Transferase
<i>cyoA</i>	Subunit II encoding operon
<i>cyoB</i>	Subunit I encoding operon
<i>cyoC</i>	Subunit III encoding operon
<i>cyoD</i>	Subunit IV encoding operon
<i>cyoE</i>	FR encoding operon
T7	T7 promoter
aa	Amino acid
bp	Base pair
kDa	kilo Dalton
PEG	Polyethylene glycol
BSA	Bovine Serum Albumine
DTT	Sodium hydrosulfite or dithionite
e ⁻	Electron

Table of Contents

Acknowledgements	i
Abbreviations	ii
1 Introduction	1
1.1 Overview	1
1.1.1 Aim of the Work	3
1.2 Literature Review	4
1.2.1 Membrane Proteins	4
1.2.2 Bioenergetics and Respiratory Chain.....	5
1.2.2.2 Cyt- <i>bo</i> ₃	8
1.2.3 Working with Proteins	10
1.2.3.1 Cell-free Protein Synthesis	10
1.2.4 Membranes.....	12
1.2.4.1 Biological Membranes	12
1.2.4.2 Model Membranes	14
1.2.5 Characterization Methods	15
1.2.5.1 Surface Plasmon Resonance Spectroscopy (SPR).....	15
1.2.5.2 Surface Plasmon Enhanced Fluorescence Spectroscopy (SPFS).....	19
1.2.5.3 Contact Angle	22
2 Materials & Methods	23
2.1 Strains and Plasmids	23
2.2 Cell Growth for Plasmid Extraction or <i>In-vivo</i> Expression	23
2.2.1 Bacterial Media Preparation	23
2.2.2 Bacterial Growth for pJRHisA, pRCO ₃ and pETcyo plasmids.....	24
2.3 Plasmid Extraction	25
2.3.1 Extraction by Promega Kit.....	25
2.3.2 Ethanol Precipitation.....	26
2.3.3 Gel Electrophoresis Analysis	26
2.3.4 Restriction Enzyme digestion	27
2.4 Purification of <i>In-vivo</i> Cytochrome <i>bo</i>₃ Ubiquinol Oxidase	28
2.4.1 Purification of Histidine Tagged Enzyme.....	28
2.4.2 Preparation of Cytoplasmic Membranes.....	28

2.5 <i>In-vitro</i> Expression of Cytochrome bo_3 Ubiquinol Oxidase	29
2.5.1 Promega E.coli Kit.....	29
2.5.2 Qiagen Insect Kit	30
2.5.3 Acetone Precipitation.....	31
2.5.4 BODIPY-FL Labelling	31
2.6 Immuno Blotting	32
2.6.1 Coomassie Staining.....	34
2.7 Spectroscopic Quantification of Enzyme	34
2.7.1 Reduction of UQ Substrate	34
2.7.2 Spectrophotometric Analysis of Cyt- bo_3	35
2.7.2.1 Reduced Minus Oxidized Spectra	35
2.7.2.2 Enzyme Activity Assay via Spectroscopic detection.....	35
2.7.3 Enzyme Activity Assay via Oxygen Electrode.....	35
2.7.4 Sample Preparation of <i>in-vitro</i> Expressed Cyt- bo_3 for Spectrophotometric Analysis and Enzyme Activity Assay	36
2.8 SPR/SPFS Measurements	36
2.8.1 Preparation of PDMS Spacer	36
2.8.2 Preparation of Gold Substrates	36
2.8.3 SPR/SPFS Setup	37
2.8.4 Assembly of Flow Cell	39
2.8.5 Scan and Kinetic Mode of SPR/SPFS	40
2.8.6 Experimental SPR/SPFS Protocol	41
2.9 Contact Angle Measurements	45
3 Results & Discussion	47
3.1 Membrane Construction Strategies	47
3.1.1 General Remarks of tethered Bilayer Lipid Membranes (tBLM).....	47
3.1.2 Peptide Spacer.....	47
3.1.3 Monolayer Formation	50
3.1.3.1 DMPE Optimization	51
3.1.3.2 Phospholipid Optimization	53
3.1.4 Bilayer Formation	55
3.1.5 Conclusion of Membrane Construction	60
3.2 Plasmid DNA Overview	61
3.3 Plasmid Extraction for <i>in-vitro</i> Expression and General Analysis	69
3.3.1 Cell growth for Plasmid DNA Isolation	69
3.3.2 Isolation of Plasmid DNA.....	70
3.3.3 Gel Electrophoresis Analysis	71

3.4 Purification of Histidine Tagged Cytochrome bo_3 Ubiquinol Oxidase	74
3.4.1 Isolation of Histidine Tagged Cytochrome bo_3	74
3.4.2 Preparation of Cytoplasmic Membranes.....	82
3.4.3 Conclusion of Cyt- bo_3 Purification.....	84
3.5 <i>In-vitro</i> Expression of Histidine Tagged Cytochrome bo_3 Ubiquinol Oxidase and Western Blot Analysis	84
3.5.1 Expression of Cytochrome bo_3 via Promega E.coli Kit.....	84
3.5.2 Expression of Cytochrome bo_3 via Qiagen Insect Kit	87
3.5.3 Expression and Characterization of Non-Histidine Tagged Cytochrome bo_3 via BODIPY-FL Labelling	88
3.5.4 Conclusion of <i>In-vitro</i> Expression of Cyt- bo_3	90
3.6 Observation of Histidine Tagged Cytochrome bo_3 Expression in Artificial Membranes by Surface Plasmon Enhanced Fluorescent Spectroscopy	91
3.6.1 Kinetic Mode Measurements	92
3.6.2 Membrane-Antibody Interaction	93
3.6.3 Incorporation of Isolated Enzyme.....	95
3.6.4 Detection of <i>in-vitro</i> Expression of the Cytochrome bo_3 in Real Time.....	98
3.6.4.1 In-vitro Expression of Cyt- bo_3 for pJRHSA plasmid.....	98
3.6.4.2 In-vitro Expression of Cyt- bo_3 for pETcyo plasmid.....	99
3.6.5 Western Blot Analysis of SPFS	101
3.6.6 Conclusion of SPFS detection of Cyt- bo_3 in Artificial Membranes	103
3.7 Spectroscopic Features of Cytochrome bo_3	104
3.7.1 Spectrophotometric Analysis of Isolated Cytoplasmic Membranes	104
3.7.2 Spectrophotometric Analysis of <i>in-vitro</i> Expressed Cytochrome bo_3	106
3.8 Enzymatic Properties of Cytochrome bo_3	107
3.8.1 Ubiquinol/Ubiquinone Quantification	108
3.8.2 Enzyme Activity Assay of Isolated Cytoplasmic Membranes	109
3.8.3 Enzyme Activity Assay of <i>in-vitro</i> Expressed Cytochrome bo_3	115
3.8.4 Conclusion Enzymatic Activity of <i>in-vitro</i> Expressed Cyt- bo_3	117
4 General Conclusion & Outlook	119
List of Tables	121
List of Figures	122
References	127

1 Introduction

1.1 Overview

Mitochondria have been known as “power house” of the eukaryotic cells¹ since they supply all chemical energy requirements of cells in adenosine triphosphate (ATP) form to support cellular functions². Besides supplying cellular energy, mitochondria are engaged with cellular differentiation, cell cycle, cell growth, signaling and cell death³ processes. It has been well documented that a mitochondrion is connected to several human diseases⁴, so called mitochondrial disorders^{5,6}. These diseases can be of a quite different nature; one well known example might be the “Parkinson’s Disease” (PD)⁷. Numerous studies have been reported^{8,9} about reduced Complex I and Complex IV activities of respiratory chain in PD patients. It has been estimated that about 80% of mitochondrial diseases are based on reduced activity of respiratory chain or dysfunction.

The respiratory chain, so called the “Electron Transport Chain”, is a series of four-membrane bound protein complexes; each one is comprised of multi-subunit enzyme complex that is integrated in the inner membrane of mitochondria. Cytochrome c oxidase or namely Complex IV is the terminal enzyme of respiratory chain in mitochondria and it catalyzes the reduction of molecular oxygen to water. Cytochrome b_0 ubiquinol oxidase (Cyt- b_0) is the homolog counterpart of Cytochrome c oxidase in bacterial system^{10,11}. Respiratory oxidases have been the object of intensive studies during the past years. Series of reactions takes place through electron transport chain complexes to contribute ATP synthesis where membranes play a crucial role in this mechanism to maintain the proton concentration gradient *via* creating closed and connected architectures¹². It is not only important to maintain the proton gradient but also to maintain the structural and functional integrity of the proteins. Especially for membrane

¹ McBride, H. M., Neuspiel, M., Wasiak, S., (2006) *Curr. Biol.*, 16, 14, 551.

² Henze, K., Martin, W., (2003) *Nature*, 426, 6963, 127.

³ Pizzo, P., Pozzan, T., (2007) *Trends Cell Biol.*, 10, 511.

⁴ Taylor, R. W., Turnbull, D. M., (2005) *Nat. Rev. Genet.*, 6, 5, 389.

⁵ Zeviani, M., Di Donato, S., (2004) *Brain*, 127, 2153.

⁶ Gardner, A., Boles, R. G., (2005) *Curr. Psych. Reviews*, 1, 3, 255.

⁷ Sherer, T. B., Betarbet, R., Greenamyre, J. T., (2002) *Neuroscientist*, 8, 3, 192.

⁸ Benecke, R., Strümper, P., Weiss, H., (1993) *Brain*, 116, 6, 1451.

⁹ Haas, R. H., Nasirian, F., Nakano, K., Ward, D., Pay, M., (1995) *Ann. Neurol.*, 37, 714.

¹⁰ Garcia-Horsman, J. A., Barquera, B., Rumbley, J., Ma, J., Gennis, R. B., (1994) *J. Bacteriol.*, 176, 18, 5587.

¹¹ Gennis, R. B., (1991) *Biochimica Biophysica Acta*, 1058, 21.

¹² Riisama, S., *Structural and Functional Studies of Bacterial Heme-Copper Oxidases*, Academic Dissertation, (2000) University of Helsinki.

CHAPTER I : INTRODUCTION

proteins, the membrane structure is an essential factor for correct folding and for the observation of functionality¹³.

Research about membrane proteins is facing severe obstacles, therefore still just few examples of membrane protein species have been characterized in suitable experimental platforms^{14,15}. The mimic of a biological membranes such as solid supported lipid membranes are widely used as a platform to investigate protein membrane interactions^{16,17}. The major challenge is to preserve their structural integrity while the expression, isolation and reconstitution processes occur¹⁸.

On the other hand, it is very well known the *in-vitro* translation systems may have advantages over cell based gene expression for example, when the over-expressed product is toxic to the host cell or when missing post-translational modification in bacterial expression systems corrupts the functionality of mammalian proteins. It is a reasonable hypothesis that lack of available membrane space prohibit functional expression. By combining these two major approaches; solid supported membrane system and *in-vitro* expression system, we are able to address membrane protein species, since we introduce a platform for membrane protein synthesis, namely the *in-vitro* synthesis of membrane proteins into a peptide supported membrane system¹⁹. The reconstitution of membrane proteins in lipid bilayers generally results in different protein conformations. As an alternative, we are exploring this system as pioneers in Eva Sinner's Lab, in order to create closer model to the cellular membranes and to mimic their function, such as protein insertion, protein function and ligand interactions.

¹³ Bowie, J. U., (2005) Nature, 438, 581.

¹⁴ Knoll, W., Köper, I., Naumann, R., Sinner, E. K., (2008) Electrochimica Acta, 53, 23, 6680.

¹⁵ Sinner, E. K., Knoll, W., (2001) Curr. Op. Chem. Biol., 5, 6, 705.

¹⁶ Giess, F., Friedrich, M. G., Heberle, J., Naumann, R., (2004) Biophysical Journal, 87, 5, 3213.

¹⁷ Vockenroth, I. K., Atanasova, P. P., Jenkins, A. T. A., Köper, I., (2008) Langmuir, 24, 2, 496.

¹⁸ Bowie, J. U., (2001) Curr. Op. Struct. Biol., 11, 397.

¹⁹ Robelek, R., Lemker, E., Wiltschi, B., Kirste, V., Oesterhelt, D., Sinner, E.K., (2007) Angewandte Chemie-International Edition, 46(4), 605.

1.1.1 Aim of the Work

The aim of this project is to synthesize fully functional Cyt-bo₃ in artificial membrane surface by maintaining its structural integrity as its natural form. This study is divided into three parts.

I. In the first part optimization of the suitable membrane structure is aimed, although the very same system¹⁹ was used previously, it is quite difficult to insert large membrane proteins such as Cyt-bo₃ with large internal and external membrane domains. Thus, it is necessary to provide good equilibrium in between high packing density and native-like fluidity.

II. The second and the prominent part of this study consists in application of the *in-vitro* expression of active Cyt-bo₃ in artificial membrane surface by using this optimized membrane system. Both *in-vitro* expression and insertion of a membrane protein is a quite complicated process and they are major topics of the related field. Here these two major approaches are combined to increase the efficiency and to decrease the disadvantages.

III. The final part consists in the characterization and analysis of enzyme functionality to see the potential of such a strategy for protein research and commercial applications in several fields.

1.2 Literature Review

1.2.1 Membrane Proteins

Membrane proteins can be divided into two main groups; integral and peripheral membrane proteins²⁰. Integral proteins are very firmly associated with the membrane and removable only by agents that interfere with hydrophobic interactions such as detergents, organic solvents or denaturing agents. Most integral proteins contain residues with hydrophobic side chain that interact with membrane phospholipids for anchoring the protein to the membrane and most of the integral proteins span the entire phospholipid bilayer. Two different types of membrane spanning domains are found in transmembrane proteins; one or more α -helices or less commonly multiple β -strands. When the polypeptide chain of integral membrane protein spans the membrane multiple times, the core of the protein is generally hydrophilic which permits the passage of water soluble molecules and the surface is hydrophobic that permits interaction with the interior of lipid bilayer²¹. Peripheral membrane proteins associate with the membrane through electrostatic interactions and hydrogen bonding with the hydrophilic domains of integral membrane proteins or with the polar head groups of membrane lipids. They do not interact directly with the hydrophobic core of the phospholipid bilayer. They can be released by relatively mild agents that interfere with the electrostatic interactions or break hydrogen bonds.

Several families of integral proteins in the plasma membrane provide specific points of attachment between cells, or between a cell and respective extracellular matrix protein species. The ability of cells to receive and act on signals from beyond the plasma membrane is fundamental to life. Cells receive constant input from membrane proteins that act as information receptors, sampling the surrounding for pH, osmotic strength, and the availability of food, oxygen, light and the presence of hazardous chemicals. In all these cases, signal represents “information” that is detected by specific receptors and converted to a “cellular response” which always involves a chemical process. This conversion of information into a chemical change, signal transduction, is a universal property of all living cells. These processes are remarkably specific and sensitive such as enzyme-substrate interaction. This specificity is generally achieved by membrane proteins.

²⁰ Nelson, D. L., Cox, M. M., (2005) Lehninger Principles of Biochemistry, 4th Edt., W. H. Freeman Co, NewYork.

²¹ Lodish, H., Berk, A., Zipursky, S. L., Matsudaira, P., Baltimore, D., Darnell, J., (2000) Molecular Cell Biology, 4th Edt., W. H. Freeman Co., NewYork.

1.2.2 Bioenergetics and Respiratory Chain

Living cells and organisms must perform work to stay alive, to grow and to reproduce. The ability to harness energy and to channel it into biological work is a fundamental property of all living organisms which can be confined under the term Bioenergetics. Bioenergetics is a huge subject of the field of biochemistry, which concerns energy flow through living systems which includes different cellular and metabolic processes that leads to production and utilization of energy such as ATP²⁰. Electron transfer in oxidation-reduction reactions involve the loss of electrons by one chemical species which is thereby oxidized, and the gain of electrons by another species which is reduced in return. The flow of electrons in oxidation-reduction reactions is responsible directly or indirectly for all “work” done by living organisms which means responsible for the production of energy as well. The path of electron flow in metabolism is complex. Electrons move from various metabolic intermediates to specialized electron carrier in enzyme catalyzed reactions. These electron carriers are called as “electron transport chain” or “respiratory chain”.

Electron transport chain connects a chemical reaction in between an electron donor and an electron acceptor to transfer H⁺ ions across the membrane through a set of mediating biochemical reactions. Respiratory chain is situated in the mitochondrial inner membrane in eukaryotes and in the outer membrane (more exactly cell-wall) in prokaryotes.

Electron transfer from NADH to molecular oxygen is highly favorable and large amount of energy is released when electrons are transported along the respiratory chain from NADH to molecular oxygen. Enzymes of respiratory chain conserve this energy via translocating protons across the membrane which generates an electrochemical proton gradient across the respective membrane. Here membrane has an important role by forming a closed or protected system which proton gradient can be maintained¹². The controlled flow of protons drive ATP synthesis and this is called the “chemiosmotic theory”²².

Mitochondrial respiratory chain is composed of energy-transducing, multi-subunit enzyme complexes, shown in Figure 1.1; Complex I-IV, each designated to couple the redox potential energy from the oxidation of substrates to the reduction of product and mobile electron carriers which shuttle electrons in between the complexes during this process²³. The first enzyme of the respiratory chain is Complex I, known as NADH:ubiquinone oxidoreductase, which transfers electrons from nicotinamide adenine dinucleotide (NADH) to

²² Mitchell, P., (1961) Nature, 191, 144.

²³ Saraste, M., (1999) Science, 283, 1488.

CHAPTER I : INTRODUCTION

ubiquinone (UQ) and couples this reaction for translation of protons across the membrane²⁴. Complex II, succinate:ubiquinone reductase, is also a member of citric acid cycle. It catalyzes electron transfer from succinate to ubiquinone. Complex III, ubiquinol:cytochrome *c* oxidoreductase, is commonly referred to the cytochrome *bc*₁ complex. This complex translocates net one proton across the membrane per electron transported to cytochrome *c*^{25,26}. Complex IV, cytochrome *c* oxidase, is the last enzyme of mitochondrial respiratory chain. This cytochrome *aa*₃ type of oxidase catalyzes the reduction of molecular oxygen to water^{27,28}. Furthermore, it couples this redox reaction for translocation of one proton across the mitochondrial membrane per each electron transported to molecular oxygen.

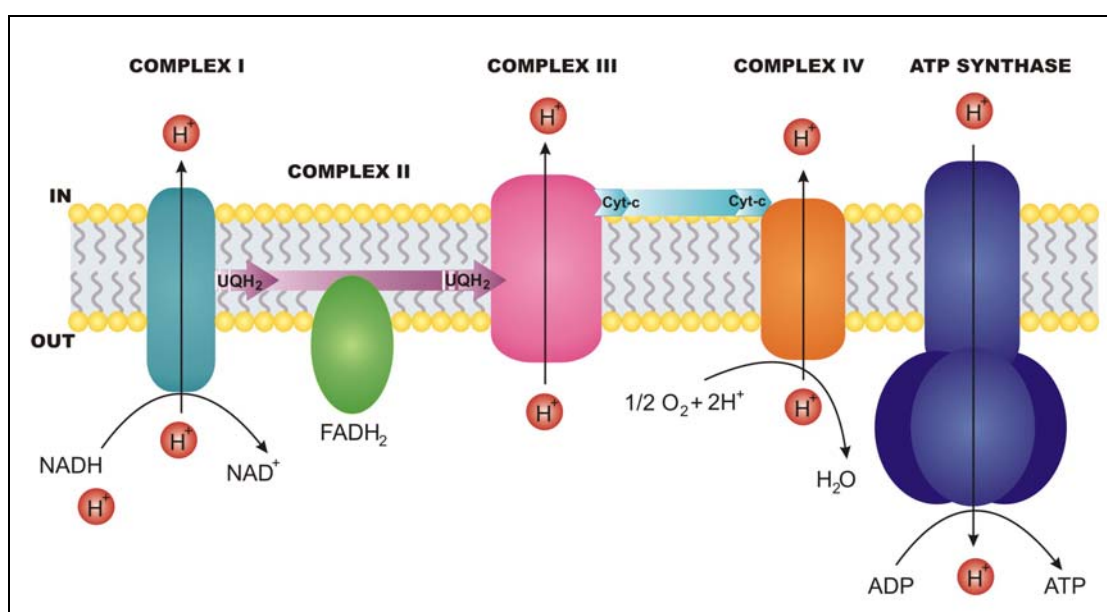


Figure 1.1 Simplified view of mitochondrial respiratory chain

In the mitochondrial respiratory chain, there are two mobile electron carriers; ubiquinone (UQ) and cytochrome *c* (Cyt-*c*). UQ is a small, hydrophobic, two-electron and two-proton carrier present in the lipid bilayer. UQ is able to act between two-electron donor and one-electron acceptor system. Cyt-*c* is a small, soluble protein with a covalently attached heme C. It is a one-electron carrier that found in intermembrane space of mitochondria or periplasm of bacteria, and transfers electrons between cytochrome *bc*₁ complex and cytochrome *c* oxidase.

²⁴ Brandt, U. (1997) *Biochim. Biophys. Acta*, 1318, 79.

²⁵ Mitchell, P., (1976) *J. Theor. Biol.*, 62, 327.

²⁶ Trumppower, B. L., (1990) *J. Biol. Chem.*, 265, 11409.

²⁷ Babcock, G. T., Wikström, M., (1992) *Nature*, 356, 301.

²⁸ Ferguson-Miller, S., Babcock, G. T., (1996) *Chem. Rev.*, 96, 2889.

In contrast to the mitochondria, bacteria are more various in their energy production modes. They usually have branched respiratory pathways and use several terminal oxidases¹⁰. Differentiation of two system, mitochondria and bacterial systems, has been shown in.

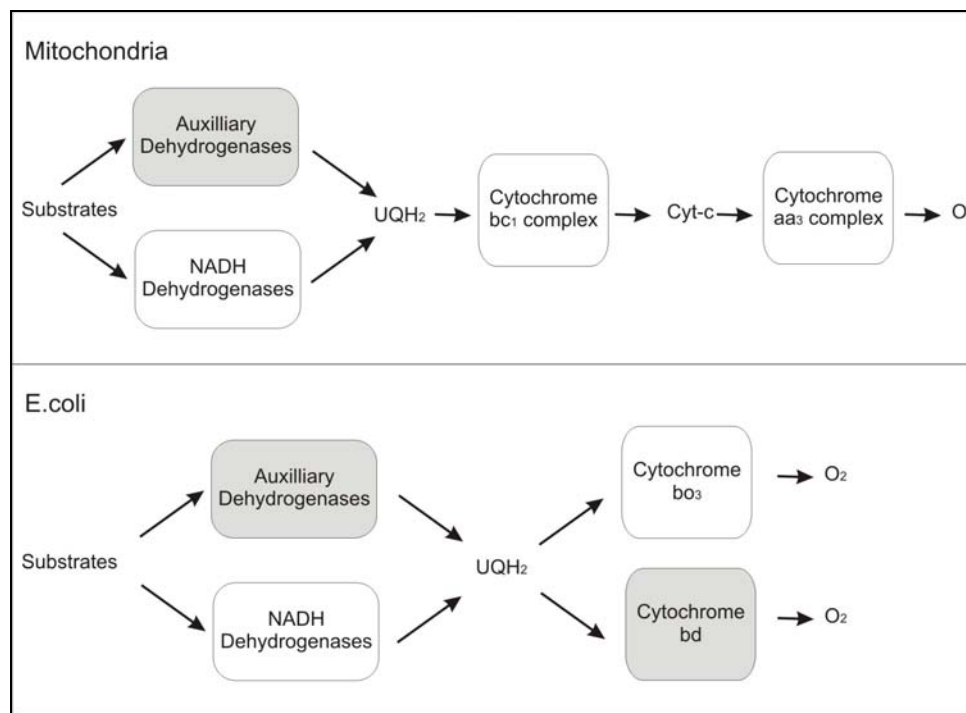


Figure 1.2 Aerobic respiratory chains of mitochondria and *E. coli*

1.2.2.1 Terminal Oxidases

Bacterial respiratory systems are branched, having a number of distinct terminal oxidases rather than single cytochrome c oxidase, which is present in most eukaryotic mitochondrial system. It has been recognized past several years that most of the bacterial oxidases are closely related members of a single superfamily called “Heme-Copper Oxidase Superfamily”. This is despite the fact that, bacterial oxidases differ in their substrates; quinol versus Cyt-c, oxygen affinities, heme types and metal compositions. The heme-copper oxidase superfamily also includes the eukaryotic mitochondrial oxidases. Cytochrome c oxidase catalyzes the four-electron reduction of molecular oxygen to two molecules of water and utilizes the free energy available from this reaction to pump protons across the membrane. Although bacterial oxidases typically contain only 3 or 4 subunits, in contract to the 13-subunit

mammalian enzyme, the bacterial oxidases catalyze the reduction of molecular oxygen and pump protons as efficiently as the mitochondrial oxidases do²⁹.

All aerobic bacterial species examined so far, have multiple respiratory oxidases. The different respiratory oxidases allow the cells to customize their respiratory systems to meet the demands of a variety of environmental growth conditions. For example, *E.coli* has two different respiratory oxidases, cytochrome *bd* and cytochrome *bo*₃. Cyt-*bd* has a substantially higher affinity for O₂ than Cyt-*bo*₃ has and it induced to high levels when the oxygen tension of growth medium is low.

1.2.2.2 Cyt-*bo*₃

The *E.coli* cytochrome *o* complex is a four-subunit enzyme that catalyzes the two-electron oxidation of UQ within the bacterial cytoplasmic membrane and the four-electron reduction of molecular oxygen to water. The oxidase contains two heme prosthetic groups and one copper. The three mitochondrially encoded subunits of the eukaryotic cytochrome *c* oxidases, subunit I, II, III, each have a homologue in the quinol oxidase. For example, the sequence of subunit I of *bo*₃ type quinol oxidase from *E.coli* is 40% identical to the sequence of bovine *aa*₃ type cytochrome *c* oxidase and followed by subunit II on the order of 23-30%. The sequence of the *cyo* operon which has been given completely in materials section, has clearly shown a phylogenetic relationship between the heme *b* containing ubiquinol oxidase from *E.coli* and the *aa*₃ type family of cytochrome *c* oxidase¹¹.

Cyt-*bo*₃ is a four subunit enzyme, compared to as many as thirteen subunits found in the mammalian enzyme. Subunit I has been shown to be the location of the three redox active metal centers, heme *b*, heme *o* and Cu_B. Subunit I from *E.coli* contains 15 transmembrane spanning domains. Subunit II has 2 transmembrane spanning domains and a large C-terminal hydrophilic domain in the periplasm. Subunit III and subunit IV have five and three transmembrane spans respectively. Subunit IV has little or no sequence homology with other oxidases and its function is unknown. Latest structure determination and x-ray structure at 3.5°A is given in Figure 1.3³⁰.

²⁹ Hendler, R. W., Pardhasaradhi, K., Reynafarje, B., Ludwig, B., (1991) *Biochys. J.*, 60, 415.

³⁰ Abramson, J., Riistama, S., Larsson, G., Jasaitis, A., Svensson-Ek, M., Laakkonen, L., Puustinen, A., Iwata, S., Wikström, M., (2000) *Nature Structural Biology*, 7, 10, 910.

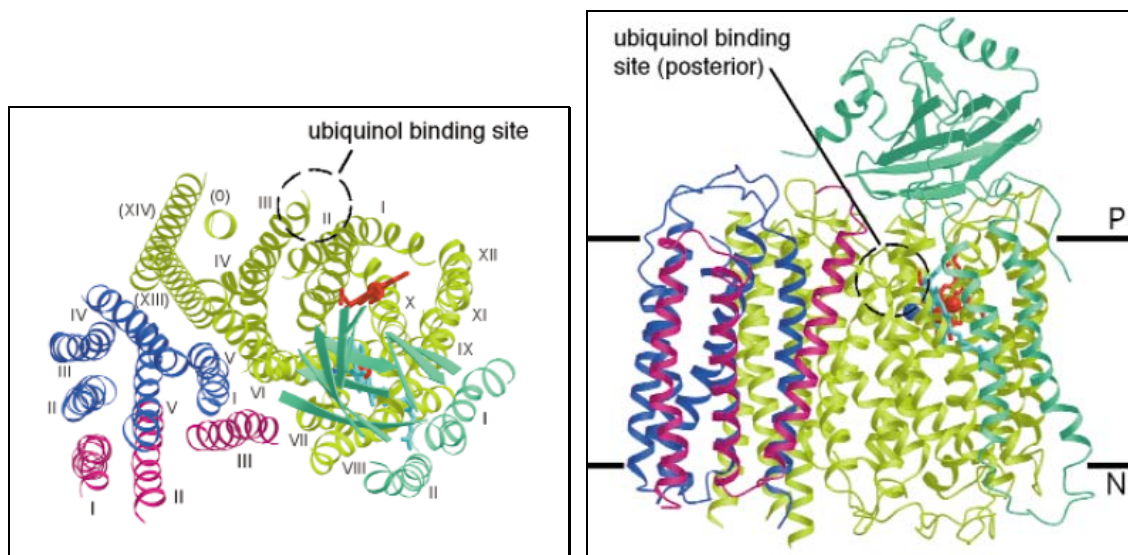


Figure 1.3 Overall structure of ubiquinol oxidase from *E.coli*

Cyt- bo_3 is a structural and functional homologue of the mitochondrial cytochrome *c* oxidase despite containing one redox metal center less than cytochrome *c* oxidase as it lacks the Cu_A site in subunit II. All redox centers, shown in Figure 1.4, are located within the largest subunit, subunit I.

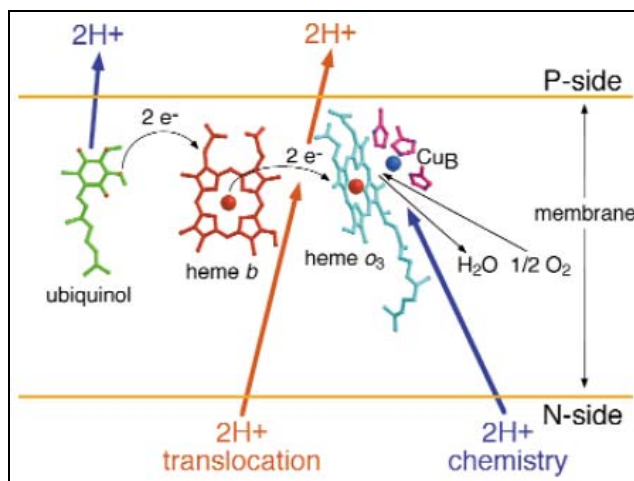


Figure 1.4 Schematic representation of electron and proton transfer in ubiquinol oxidase

1.2.3 Working with Proteins

Understanding of protein structure and function has been derived from the study of many individual proteins. Because of the vast variations of knowledge about its genetics, *E.coli* is the system of choice for expression of many heterologous proteins³¹. Genetic manipulations are straight forward, cultures of *E.coli* are easily and inexpensively grown and many foreign proteins are well-tolerated and may be expressed at high levels. During the past 20 years, several hundred recombinant proteins have been expressed in *E.coli* using several vector systems. Factors that influence the choice of a system for expression of particular protein in *E.coli* can be listed mainly as; size of the protein, amount of protein needed, whether active protein is required.

To study a protein in detail, the researcher must be able to separate it from other proteins from the cellular context and must have the techniques to determine its properties. A pure preparation is essential before a protein's properties and activities can be determined. The source of a protein is generally tissue or microbial cells. Given the fact that cells contain thousands of different kinds of proteins. Methods for separating proteins take advantage of properties that vary from one protein to the next, including size, color, charge and binding properties. All purification procedures require a method for quantifying or assaying the protein of interest in the presence of other proteins. To purify a protein, it is essential to have a way of detecting and quantifying that protein at each step of the procedure. Whether the expressed protein is to be used in structural and functional studies, it is best to have target as a soluble protein. Overexpression of foreign proteins from cloned genes in heterologous hosts, such as *E.coli*, often leads to the formation of insoluble intracellular aggregates of expressed protein.

A common strategy to avoid some of the problems associated with expression difficulties, purification process and functioning is to express the protein of interest by using a cell-free system.

1.2.3.1 Cell-free Protein Synthesis

Cell-free protein synthesis³² (CFPS) is a rapid and high throughput technology for obtaining proteins from their genes. *In-vitro* protein translation using cell extracts has become an important tool for molecular biology by playing a central role in a wide variety of applications. CFPS or namely *in-vitro* synthesis refers to protein production by using lysates

³¹ Sambrook, J., Russell, D. W., (2001) Molecular Cloning A Laboratory Manual, 3rd Edt., Cold Spring Harbor Laboratory Press, NewYork.

³² Nirenberg, M. W., Matthaei, J. H., (1961) Proc. Natl. Acad. Sci., 47, 1588.

CHAPTER I : INTRODUCTION

that provides the cellular machinery necessary for synthesis. Ribosomes, tRNAs, GTP, ATP, Mg⁺², K⁺, initiation, elongation and termination factors are among the requirements for a translation system. These are provided by lysates, commercially available or home-made, which can be obtained from prokaryotic or eukaryotic sources.

CFPS is a useful alternative to *in-vivo* synthesis for the analysis and production of proteins³³. Some of them include better protein yield, an optimal environment in terms of co- and post-translational modifications, cell viability concerns, ease of use, cost and time saving. The biggest advantage comparing to the protein production in living cells, is that CFPS is the fastest way to obtain an expressed protein (phenotype) from a gene (genotype) of a protein. In *in-vivo* protein expression, a large part of the metabolic resources are dedicated towards basic cellular processes. However in an *in-vitro* production system, all those resources are optimized towards to the production of protein of interest. There are no cell walls in *in-vitro* expression system, it is an open system which allows the addition of components to create most optimal environment for the protein production. There is no cell growth in *in-vitro* expression system and hence even proteins considered toxic or inhibitory to the host cell can be expressed. In most cases enough protein can be produced in few hours. No elaborate setup is required for the synthesis and there is no need for further purification steps.

One of the potential and most far-reaching impacts of *in-vitro* expression could be in the area of membrane protein production³⁴. Membrane proteins account for nearly a third of the genes encoded by most fully sequenced genomes. However only a handful of integral membrane protein structures (<80) have been observed and characterized. Over expression of membrane proteins *in-vivo* frequently results in cell toxicity largely owing to their hydrophobicity, protein aggregation, misfolding and low yield. In some cases, the over expression of integral membrane proteins such as ion channel proteins, transporters and receptors can disrupt the integrity of the cell membrane and lead to cell lysis. What is exciting is that nearly all of these obstacles can be overcome by cell-free expression. *In-vitro* expression offers a unique opportunity to use the highly efficient bacterial transcription and translation machinery while introducing natural mammalian or other synthetic lipids. In addition to all these facts, *in-vitro* expression can circumvent the problem of post-translational modification. The presence of mild detergents or lipid mixtures during the reaction notably eased aggregation and insolubility issues and does not interfere with the translation activity.

³³ Spirin, A. S., Swartz, J. R., (2008) Cell-free Protein Synthesis, WILEY-VCH Verlag GmbH & Co.

³⁴ Katzen, F., Chang, G., Kudlicki, W., (2005) Trends in Biotechnology, 23, 3, 150.

1.2.4 Membranes

1.2.4.1 Biological Membranes

The boundaries of cells are formed by *biological membranes*, the barriers that define the inside and the outside of a cell³⁵. These barriers prevent molecules generated inside the cell from leaking out and unwanted molecules from diffusing in. Membranes are dynamic structures in which proteins float in a sea of lipids³⁶ (Figure 1.5).

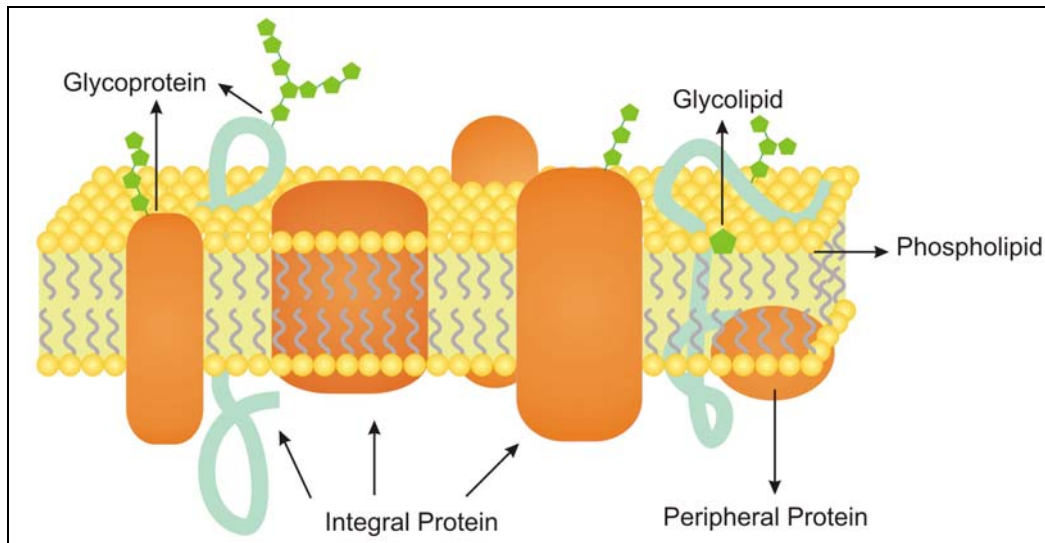


Figure 1.5 Schematic representation of a cell membrane

The lipid components of the membrane form the permeability barrier, and protein components act as a transport system of pumps and channels that endow the membrane with selective permeability. Biological membranes serve several additional important functions indispensable for life, such as energy storage and information transduction, that are dictated by the proteins associated with them. Membranes are as diverse in structure as they are in function. However they do have in common a number of important attributes;

- Membranes are sheet-like structures, only two molecules thick. The thickness of most membranes is between 60°A and 100°A.
- Membrane lipids are relatively small molecules that have both hydrophilic and hydrophobic moieties.

³⁵ Berg, J. M., Tymoczko, J. L., Stryer, L., (2002) Biochemistry, 5th Edt., W. H. Freeman Co., New York.

³⁶ Singer, S. J., Nicolson, G. L., (1972) Science, 175, 720.

CHAPTER I : INTRODUCTION

- Membranes consist mainly of lipids and proteins. They also contain carbohydrates that are linked to lipids and proteins.
- Membranes are fluid structures. Lipid molecules diffuse rapidly in the plane of the membrane, as do proteins, unless they are anchored by specific interactions. Membranes can be regarded as two-dimensional solutions of oriented proteins and lipids.
- Specific proteins mediate distinctive functions of membranes. Proteins serve as pumps, channels, receptors, energy transducers and enzymes. Membrane proteins are embedded in lipid bilayers, which create suitable environment for their activity.

Lipids differ remarkably from the other groups of biomolecules. They have a variety of biological roles; they serve as highly concentrated energy stores, signal molecules and components of the membrane. The three major kinds of membrane lipids are phospholipids, glycolipids and cholesterol. Phospholipids are the major class of membrane lipids and they are abundant in all biological membranes. A phospholipid³⁷ molecule is constructed from four components; a fatty acid, a backbone which fatty acids are attached, a phosphate and an alcohol group attached to the phosphate. The fatty acid components provide hydrophobic barrier, whereas the remainder of the molecule has hydrophilic properties to enable interaction with the environment.

Membrane formation is a consequence of the amphipathic nature of the molecules. Their polar head groups favor contact with water, whereas their hydrocarbon tails interact with one another. One way is to form a micelle³⁸, a globular structure in which polar head groups are surrounded by water and hydrocarbon tails are inside. Alternatively, the strongly opposed preferences of the hydrophilic and hydrophobic moieties of membrane lipids can be satisfied by forming a lipid bilayer³⁹. The hydrophobic tails of each individual sheet interact with one another, forming a hydrophobic interior that acts as a permeability barrier. The hydrophilic head groups interact with the aqueous medium on each side of the bilayer. The favored structure for most phospholipids in aqueous media is biomolecular sheet rather than a micelle. The reason is that, two fatty acyl chains of phospholipids are too bulky to fit into the interior of a micelle. The formation of lipid bilayer is a self assembly process. In other words, the structure of a lipid bilayer is inherent in the structure of the constituent lipid molecule. The

³⁷ Helm, C. A., Israelachvili, J. N., (1993) *Methods in Enzymology*, 220, 130.

³⁸ Tanford, C., (1980) *The hydrophobic effect: Formation of Micelles and Biological Membranes*, 2nd Edt., John Wiley & Sons Inc.

³⁹ Israelachvili, J. N., Marcelja, S., Horn, R. G., (1980) *Quarterly Reviews of Biophysics*, 13, 121.

growth of lipid bilayer architectures from phospholipids is a rapid and spontaneous process in water. Hydrophobic interactions are the major driving force for the formation of lipid bilayer. Recall that, hydrophobic interactions also play a dominant role in the folding, insertion and functioning of proteins.

1.2.4.2 Model Membranes

For the systematic study of membranes and membrane related processes, various model systems have been proposed that allow an facile characterization of the membrane architecture by minimizing the number of parameters involved^{40,41}. The first model systems developed, can be described as non-supported membranes such as liposomes, giant vesicles and black lipid membranes. Liposomes are spherically assembled bilayers where the hydrophobic part is buried inside⁴². Their limitation for electrochemical characterizations, since their inner compartment is very small and inaccessible and their limited lifetime is an important drawback for practical applications. Planar lipid membranes or black lipid membranes (BLMs) have been established to overcome these limitations^{43,44}. BLMs are assemblies of two opposing monolayers spanning on aperture which separates two aqueous compartments.

The BLM technique has been successfully used to study the membrane active substances^{45,46}. Unlike liposomes, it provides a direct access to both sides of the membrane and this allows modifying each side. Nevertheless, the main drawback of BLMs is their inherent instability. Long time measurements and robust sensing devices using BLMs are still not feasible⁴⁷. Stability problems of model membranes have been overcome by using solid supports⁴⁸ underneath the membrane. Another advantage of this system is to use various surface analytical tools for the characterization.

Supported bilayer lipid membranes⁴⁹ (sBLM) can be divided into two subgroups; the so-called “solid supported bilayers” which are separated from the solid support by only a thin

⁴⁰ Chan, Y. H. M., Boxer, S. G., (2007) *Current Opinion in Chemical Biology*, 11, 6, 581.

⁴¹ Förch, R., Schönherr, H., Jenkins, A. T. A., (2009) *Surface Design: Applications in Bioscience and Nanotechnology*, WILEY-VCH Verlag GmbH & Co.

⁴² Edwards, D. A., Schneck, F., Zhang, I., Davis, A. M. J., Chen, H., Langer, R., (1996) *Biophys. J.*, 71, 1208.

⁴³ Ottava, A., Tvarozek, V., Racek, J., Sabo, J., Ziegler, V., Hianik, T., Tien, H., (1997) *Supramolecular Science*, 4, 101.

⁴⁴ Winterhalter, M., (2000) *Current Opinion in Colloid & Interface Science*, 5, 250.

⁴⁵ Kasianowicz, J. J., Brandin, E., Branton, D., Deamer, D. W., (1996) *Proc. Natl. Acad. Sci.*, 102, 12377.

⁴⁶ Subrahmaniam, Y., Alves, I. D., Salgado, G. F. J., Lau, P. W., Wysocki, R. J., Salamon, Z., Tollin, G., Hruby, V. J., Brown, M. F., Saavedra, S. S., (2005) *JACS Comm.*, 127, 5320.

⁴⁷ Heyse, S., Stora, T., Schmid, E., Lakey, J. H., Vogel, H., (1998) *Biochimica Biophysica Acta*, 88507, 319.

⁴⁸ Sackmann, E., (1996) *Science*, 271, 43.

⁴⁹ Knoll, W., Frank, C. W., Heibel, C., Naumann, R., Offenhauser, A., Rühle, J., Schmidt, E. K., Shen, W. W., Sinner, A., (2000) *Reviews in Molecular Biotechnology*, 74, 137.

water layer and the alternative type of bilayer which is separated from solid support by a spacer such as small polymer layer or a thin tethering layer that composed of heterogeneous molecules. Since separation of a bilayer from solid support by a thin water layer does not provide any ion reservoir under the membrane, it does not suit for functional analysis of electrogenic membrane proteins and in addition, this model system does not provide enough space for the functional incorporation of complex membrane proteins.

Tethered lipid bilayer membranes^{50,51} (tBLM) provide a reservoir place for insertion of the protein. The inner leaflet of tBLM is covalently coupled to the solid support via spacer group. Such systems have been shown to provide excellent stability and electrical properties⁵², as well as high efficiency to incorporate membrane proteins¹⁶ which is satisfactory for biosensing applications.

1.2.5 Characterization Methods

1.2.5.1 Surface Plasmon Resonance Spectroscopy (SPR)

Over the last two decades, surface plasmon resonance (SPR) has attracted a great deal of attention^{53,54}. It has been widely used as a detection technique in biosensor applications^{55,56} as well as for characterizing molecular interactions at the interface between analytes and a sensor surface. It has been shown this system is an effective optical tool for the characterization of the thin films, as well as for the sensitive detection of kinetic binding processes.

Surface plasmons are surface waves which can be excited at the interface between a metal and a dielectric and the exact excitation conditions strongly depend on the optical properties of the system. This measurable response of the system permits the sensitive monitoring of processes near interface. Under certain conditions, the energy carried by photons is transferred to packets of electrons, called plasmon, on a metal surface like Au, Ag, Al, Cu, etc. This energy transfer occurs only at a specific resonance wavelength, namely at the wavelength where the quantum energy carried by the photons exactly equals the quantum

⁵⁰ Raguse, B., Braach-Maksvytis, V., Cornell, B. A., King, L. G., Osman, P. D. J., Pace, R. J., Wieczorek, L., (1998) *Langmuir*, 14, 648.

⁵¹ Köper, I., (2007) *Molecular BioSystems*, 3, 10, 651.

⁵² Atanasov, V., Atanasov, P., Vockenroth, I., Knorr, N., Köper, I., (2006) *Bioconjugated Chem.*, 17, 631.

⁵³ Raether, H., (1988) *Surface Plasmon on Smooth and Rough Surfaces and on Gratings*, Springer, Berlin.

⁵⁴ Ulman, A., (1991) *An Introduction to Ultrathin Organic Films*, Academic Press, London.

⁵⁵ Neumann, T., (2001) *Strategies for Detecting DNA Hybridisation Using Surface Plasmon Fluorescence Spectroscopy*, Dissertation Thesis, Johannes Gutenberg University.

⁵⁶ Vockenroth, I. K., (2007) *Investigation of Tethered Bilayer Lipid Membranes for Their Potential Use in Biosensing Devices*, Dissertation Thesis, University of Bath.

energy level of plasmon. In order to understand the excitation of surface plasmons by light, total internal reflection and the dispersion relation of surface plasmons has to be discussed.

If a light beam reaches to a surface which divides two media with different refractive indices n_1 and n_2 , a part of the incident light is transmitted and the other part is reflected as shown in Figure 1.6. The angle of the incident light is equal to the angle of reflected light. If a transmission occurs from a medium with a high refractive index to a medium with a low refractive index, the angle of transmitted light is higher than the angle of the incoming light. This phenomenon can be described by Snell's law;

$$n_1 \sin \theta_1 = n_2 \sin \theta_2$$

The critical angle, θ_c is the angle where the angle of the transmitted light θ_2 reaches 90° . This angle is the limit of total internal reflection. This angle can be calculated according to Snell's law;

$$\sin \theta_c = \frac{n_2}{n_1}$$

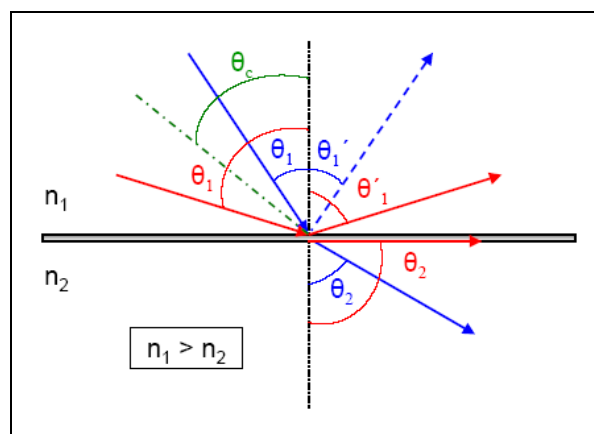


Figure 1.6 Reflection at the glass/dielectric interface

According to Maxwell's theory, above θ_c , the optical E-field along the propagation direction E_x , has the usual oscillatory character of an electromagnetic mode. The component perpendicular to the interface, E_z , however does not to fall zero abruptly, but decays exponentially with a decay length l , which is a function of the angle of incidence.

$$l = \frac{\lambda}{2\pi\sqrt{(n \cdot \sin \theta)^2 - 1}} \quad \theta > \theta_c$$

Such an electromagnetic field distribution is called as an evanescent field. The decay length is in the order of wavelength of incoming light.

If the beam reaches to metal surface in contact with dielectric, as described in previous paragraph, a part will be reflected and the other part will be transmitted. Additionally, it can lead to an interaction in between the light and the electrons of the metal. This produces a collective movement of the nearly free electron gas of metal. Because of their charge, these electrons keep a certain distance from each other and a pseudo lattice is created. Electrons can only move in a collective manner in this lattice. These collective excitation states of the quasi free electrons of metal are described as “Surface Plasmon Polaritons”.

A graphical representation of the dispersion of free photons and surface plasmon modes is given in Figure 1.7. The dispersion of photons in the bulk is given as a straight line (A). The surface Plasmon dispersion curve (SP1) approaches a maximum angular frequency that is attributed to the plasma frequency of the employed metal. Increasing the angle θ from 0° to the grazing angle tunes the curve. Because of the asymptotically approach of surface plasmon dispersion curve, SP1, to the line A at very low energies, the momentum matching conditions for resonant surface plasmon excitation can not be met which means that coupling of the modes is not possible only by changing the angle of incidence itself.

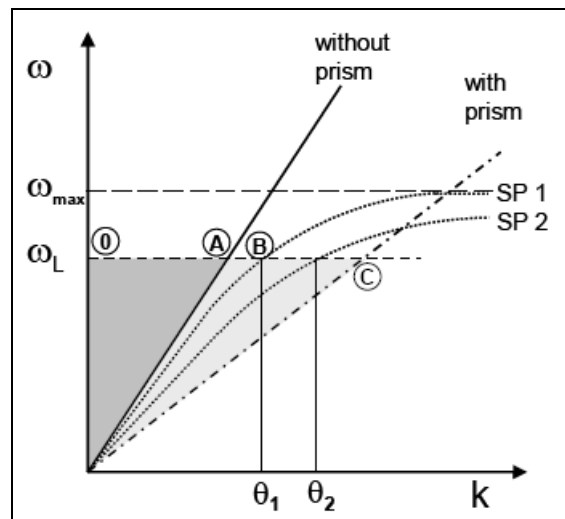


Figure 1.7 Dispersion relation of free photons and surface plasmons⁵⁶

There are two coupling techniques to overcome this problem; prism coupling and grating coupling⁵⁷. A common way to increase the momentum of light is a method based on prism coupling⁵⁸. Using this method, photons are not coupled directly to the metal/dielectric interface but via the evanescent tail of light upon total internal reflection at base of a high refractive index prism. The geometry experimentally used in this work is the Kretschmann configuration⁵⁹, shown in section 2.8.3 (Figure 2.2). By using this configuration, the evanescent field close to the surface causes a very intensive and sensitive interaction with the surface. Therefore, SPR is a suitable tool for the investigation of optical properties of thin films and layers.

Excitation of surface plasmon polaritons requires efficient coupling between the metal and the prism. The evanescent field resulting from total internal reflection overlaps with the surface plasmon mode and resonance is achieved by tuning the angle of incidence. Figure 1.8 shows a typical evanescent excitation with total internal reflection (TIR) of a plane wave at a glass prism with a dielectric constant ϵ_d in contact with a dielectric medium of $\epsilon_d < \epsilon_p$. In the presence of metal interface, while sweeping through a range of angles, plasmon resonance shows a sharp decrease in the reflectivity spectrum at the resonance angle.

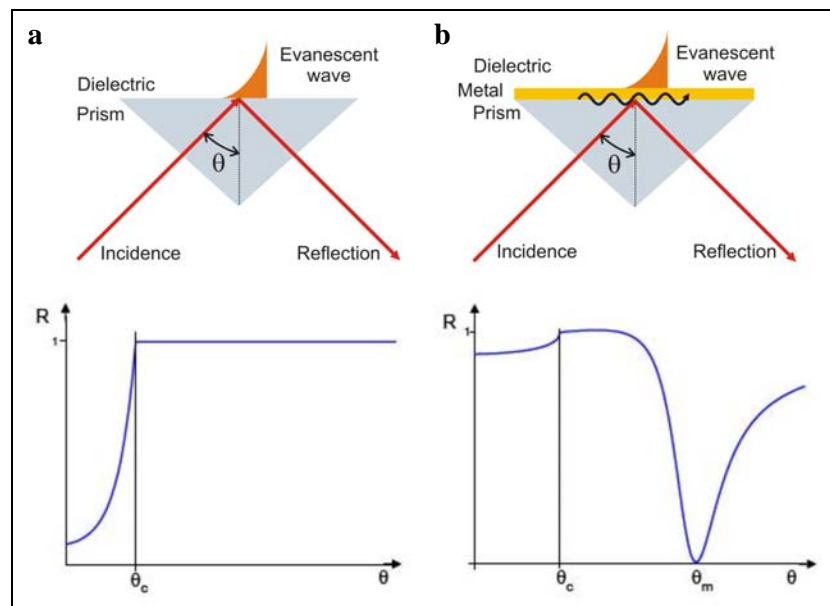


Figure 1.8 Total internal reflection (a) at a glass prism in contact with a dielectric, (b) at a metal film

⁵⁷ Knoll, W., (1998) Annual Reviews of Physics and Chemistry, 49, 569.

⁵⁸ Otto, A., (1968) Zeitschrift für Physik, 216, 398.

⁵⁹ Kretschmann, E., (1971) Zeitschrift für Physik, 241, 313.

In the scan mode, reflectivity changes are measured as a function of the incident angle. Changes in the refractive index occurring at the metal film due to the adsorption or binding on this film are detected as a shift in the minimum angle θ_m . The deposition of an ultra thin layer of a material with a higher refractive index than the ambient dielectric is equivalent to an increase of the overall refractive index integrated over the evanescent field. The net effect is a slight shift of the resonance angle in order to again couple resonantly to surface plasmon modes. In a kinetic measurement, the change in intensity of reflected light is measured at a constant angle. The formation of a new layer results in an increase in intensity of reflected light. This increase in intensity corresponds to a shift of a resonance angle. In a typical kinetic curve, there is only very slight change in reflectivity when the curve reaches to plateau. Kinetic measurements allow the investigation of adsorption processes. Moreover, qualitative aspects of the adsorption can be observed. For example, a fast adsorption results in a very sharp slope.

1.2.5.2 Surface Plasmon Enhanced Fluorescence Spectroscopy (SPFS)

Analytical methods incorporating fluorescence based detection are widely used in chemical as well as biochemical research due to the extraordinary sensitivity, signal amplification and the favorable time scale on which fluorescence occur. A number of processes can be observed by monitoring their influence on a fluorescent probe during the fluorescent lifetime which is typically in range of 10ns. The SPR method offers a label-free, non-invasive and real time detection of various biomolecular events. Detection limit and sensitivity problems occur with SPR, when an analyte does not form a closed layer or a thick layer enough to be monitored as a change in reflectivity minimum⁶⁰. Recently surface plasmon enhanced fluorescence spectroscopy (SPFS) was introduced⁶¹ which overcomes this sensitivity limitations of SPR by combining it with the indirect detection methods of fluorescence⁶². SPFS uses the enhanced electromagnetic field obtained by SPR to excite fluorescent dyes in close proximity to the metal/dielectric interface. The evanescent surface plasmon field excites fluorophores within the vicinity of this field. The optical excitation follows the strength of the evanescent field and reaches its maximum near the maximum resonant angle of surface plasmons. The fluorescence peak is observed at a slightly lower angle than the actual resonance angle, the reflectivity minimum is only shifted due to an absorptive loss or damping in the metal film.

⁶⁰ Spinke, J., Liley, M., Guder, H. J., Angermaier, L., Knoll, W., (1993) *Langmuir*, 9, 1821.

⁶¹ Attridge, J. W., Daniels, P. B., Deakon, J. K., Robins, G. A., Davidson, G. P., (1991) *Biosensors & Bioelectronics*, 6, 201.

⁶² Liebermann, T., Knoll, W., (2000) *Colloids and Surfaces*, 171, 115.

The fluorescence emission from the fluorophore molecules is strongly dependent upon the distance from the metal surface. The ones that are close to the metal surface are quenched and most of the excited state energy is dissipated as heat^{63,64}. For the fluorophores lying at intermediate distances from the metal surface, some of their energy can be used in back coupling of a surface plasmon mode. And as a last case, at sufficient separation distances (>20nm) free emission of the dye nominates. Some of the distance dependent energy transfer mechanisms are summarized in Figure 1.9. The layer architecture which is used for SPFS needs to be designed and optimized according to these distance related effects to guarantee the binding of the fluorophores within a distance in between 30 and 100 nm from the metal surface which is inside the evanescent field but out of the quenching distance⁶⁵.

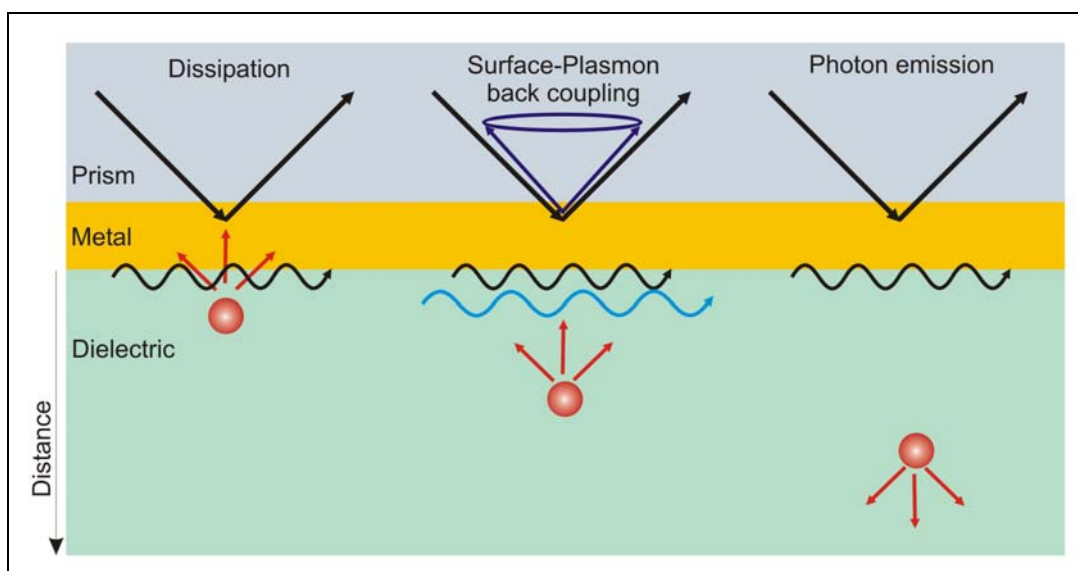


Figure 1.9 Major decay channels for fluorophores in close proximity to metal film

1.2.5.2.1 Fluorescence

Fluorescence is well characterized phenomenon which describes the emission of photons from the molecules that undergo a transition from electronically excited state to the ground state. Three-step process is responsible for fluorescence which is illustrated in Figure 1.10 which is named as Jablonski diagram.

⁶³ Knobloch, H., Brunner, A., Leitner, A., Aussenegg, F., Knoll, W., (1993) *Journal of Chemical Physics*, 98, 10093.

⁶⁴ Vasilev, K., Knoll, W., Kreiter, M., (2004) *Journal of Chemical Physics*, 120, 3439.

⁶⁵ Yu, F., Yao, D., Knoll, W., (2003) *Analytical Chemistry*, 75, 2610.

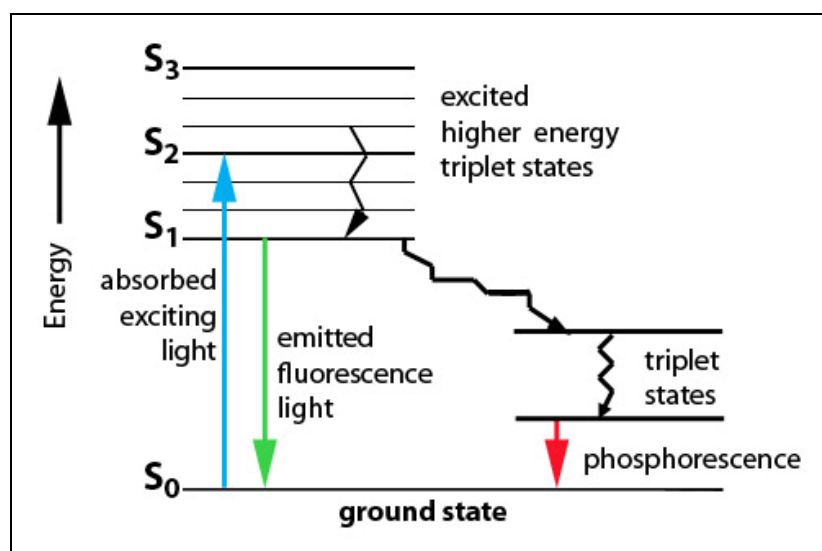


Figure 1.10 Jablonski energy level diagram

A fluorophore may exist in several electronic states. Upon absorption of a photon's energy, the fluorophore is excited from the ground state (S_0) to one of the vibrational level of a higher state (S_1). Through a fast internal conversion process, the fluorophore relaxes rapidly towards the lowest vibrational level of S_1 . This process is typically in the range of 10^{-12} s or less so therefore it is completed before emission occurs, as fluorescence life times are 10^{-8} s. Emission results from the lowest vibrational state of S_1 . From there molecule can decay to different vibrational levels of S_0 by emitting the energy. Examination of Jablonski diagram reveals that the energy of the emission is typically less than that of the absorption. Hence, fluorescence typically occurs at lower energies or longer wavelengths. By comparing absorption and emission spectra, this red shift can be observed. This so called Stokes' shift can be explained by energy loss between two processes due to the rapid internal conversion in the excited state and the subsequent decay of the fluorophore to the higher vibrational levels of S_0 . This shift is a prerequisite for the sensitivity of the fluorescence technique, as it allows distinguishing the emitted photons from the excitation photons against a low background⁶⁶.

⁶⁶ Lakowicz, J. R., (1999) Principles of Fluorescence Spectroscopy, 2nd Edt., Kluwer Academic/Plenum, NewYork.

1.2.5.3 Contact Angle

Contact angle (CA) measurements consist of the analysis of the shape of a droplet on a surface⁶⁷. This method reveals information about hydrophilicity of surfaces. Wetting of a surface is a sensitive process and it depends strongly on the chemical composition of a surface. CA measurements can quantify the wettability as these measurements react sensible on small changes of the surface. The CA is a measure for the energetic interaction between solid and liquid and thus gives information about the hydrophobicity and hydrophilicity of a surface⁶⁸. If a solvent shows complete wetting, this is called spreading and a film is generated. For incomplete wetting, a droplet is created so CA can be determined. The outer form of droplet results from the minimization of free energy of the surface and the gas phase. This relation is described by the Young equation;

$$\gamma_{SV} - \gamma_{SL} = \gamma_{LV} \cdot \cos \theta$$

where γ_{SV} is the solid-vapor interfacial energy, γ_{SL} is the solid-liquid interfacial energy, γ_{LV} is the liquid-vapor interfacial energy and θ is the CA.

Figure 1.11 shows the wetting situation for hydrophobic and hydrophilic surfaces. On extremely hydrophilic surfaces, a water droplet spread completely. Hydrophobic surfaces show CA higher than 90° .

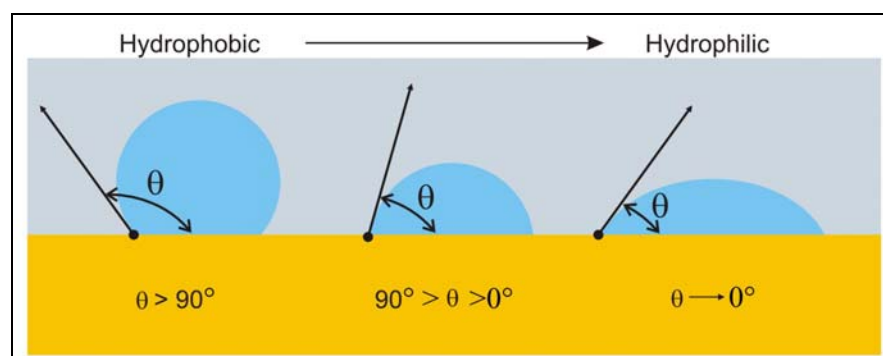


Figure 1.11 Contact angles of hydrophilic and hydrophobic surfaces

⁶⁷ Sell, P. J., Neumann, A. W., (1966) *Angewandte Chemie*, 78, 321.

⁶⁸ De Gennes, P., (1985) *Reviews of Modern Physics*, 57, 827.

2 Materials & Methods

2.1 Strains and Plasmids

A number of strains have been used in this work. *E.coli* strains pJRHisA, pRCO3 and pETcyo, gifts from Prof. R. B. Gennis, University of Illinois, were used in this study. They are summarized in Table 2.1.

Table 2.1 Bacterial strains and plasmids

<i>Strain/ Plasmid</i>	<i>Relevant Properties</i>	<i>Source or Reference</i>
pJRHisA	histidine-tag at the end of <i>cyoA</i>	pJT39, Rumbley et al., 1997 ^{1,4}
pRCO3		RG129, Gennis et al., 1992 ²
pETcyo	histidine-tag at the end of <i>cyoA</i> , T7	pET-17b, Rienstra et al., 2006 ³

2.2 Cell Growth for Plasmid Extraction or *In-vivo* Expression

2.2.1 Bacterial Media Preparation

Corresponding media components in 1L Luria Bertani (LB) media are shown in Table 2.2, and 2.3 for pJRHisA and pRCO3 respectively. MilliQ water (Millipore, Direct-Q 3 System) was used for the preparation of all solutions and pH of the media was adjusted to pH 7.0 by addition of KOH. All solutions, which were not heat sensitive, were autoclaved at 121°C for 20 min in Varioklav Steam Sterilizer (Thermo Scientific). Heat sensitive solutions or media were filtered through 0.22µm, PES disposable filter sterilization system (Corning Co.).

M63 minimal media (which is given in Table 2.4) was used to cultivate *E.coli* cells with pETcyo plasmid. Ready to use X-Gal (Cat No: R0941) and IPTG (Cat No: R1171) solutions were purchased from Fermentas.

Table 2.2 Growth media for pJRHisA plasmid^{1,4}

<i>Component</i>	<i>Amount in 1L LB Broth</i>
CuSO ₄	125 mg (or 500µM)
Lactic Acid	3% (V/V)
Ampicillin	100mg (final concentration 100µg/ml)

¹ Rumbley, J. N., Furlong Nickels, E., Gennis, R.B., (1997) *Biochim Biophys Acta*, 1340, 131.

² Ma, J., Lemieux, L., Gennis, R. B., (1993) *Biochemistry*, 32, 7692.

³ Frericks, H. L., Zhou, D. H., Yap, L. L., Gennis, R. B., (2006) *Journal of Biomolecular NMR*, 36, 55.

⁴ Rumbley, J. N., Analysis of Heme-Copper Ligation, Quinol Activity and Ligand Binding Kinetics of Cytochrome b₃ Quinol Oxidase from *E.coli*, Dissertation Thesis (1995), University of Illinois at Urbana-Champaign.

CHAPTER II : MATERIALS & METHODS

Table2.3 Growth media for pRCO3 plasmid^{2, 5}

<i>Component</i>	<i>Amount in 1L LB Broth</i>
Lactic Acid	0.3% (V/V)
Ampicillin	100mg (final concentration 100µg/ml)

Table2.4 M63 Minimal media / Growth media for pETcyo plasmid³

<i>Component</i>	<i>Amount in 1L</i>
Glycine	100 mg
Glycerol	2 g
NH ₄ Cl	2 g
KH ₂ PO ₄	3 g
K ₂ HPO ₄	7 g
MgSO ₄	120.4 mg (or 1mM)
CuSO ₄	2.5 mg (or 10µM)
FeSO ₄	8.3 mg (or 30µM)
Thiamine (VitaminB1)	10 mg
Ampicillin	100mg (final concentration 100µg/ml)

2.2.2 Bacterial Growth for pJRHisA, pRCO3 and pETcyo plasmids

Cells which are carrying pJRHisA and pRCO3 plasmids were grown aerobically in a 2L baffled flask with a total volume of 1L LB media which contains supplementary salt. Inoculation of a small flask was done directly from frozen glycerol stock and grown overnight at 37°C. 10 ml of overnight culture was transferred to inoculate 1L of LB broth. Cells were grown with vigorous shaking (250-300rpm) at 37°C in a New Brunswick Innova-44 incubator shaker. Cells were harvested approximately at mid-logarithmic phase by centrifugation at 4500 rpm for 20min in a Heraeus Labofuge 400R centrifuge. The supernatant was discarded and cell pellets were either used for other applications or stored at -80°C.

E.coli cells carrying pETcyo plasmid were plated directly from frozen glycerol stocks on LB agar plates containing Ampicillin (100µM/ml), X-Gal and IPTG for blue/white

⁵ Lemieux, L. J., Calhoun, M. W., Thomas, J. W., Ingledeu, W. J., Gennis, R. B., (1992) The Journal of Biological Chemistry, 267-3, 2105.

CHAPTER II : MATERIALS & METHODS

screening⁶ of colonies. Individual blue colonies were picked for inoculation of small flask and transferred in 1L media as described above. Cells were grown aerobically in 1L M63 minimal media which is given in Table2.4. Supplementation of trace metals and vitamins was optimized and determined to be critical for heme production and increased production of active enzyme. IPTG induction was done at early-logarithmic phase. Over expression of Cyt-bo₃ was complete 4 h after induction and cells were pelleted at 4500 rpm for 20min. Pellets were stored at -80°C for further applications.

2.3 Plasmid Extraction

2.3.1 Extraction by Promega Kit

High quality plasmid DNA was prepared with PureYield Plasmid Midiprep System, Promega (Cat No: A2492). Plasmid extraction was done by using the alkaline lysis method and as indicated by the manual of the kit, centrifugation method was used for DNA purification. Since all pBR322 derivatives are classified as low copy plasmid⁷, generally 250ml or 500ml bacteria culture was used for the extraction. Related chemicals and volumes which have been used were given in Table2.5.

Table2.5 Volumes of solutions required to create lysate

<i>Solution Name</i>	<i>Volume</i>
Bacteria Culture	101-250 ml
Cell Resuspension Solution	6 ml
Cell Lysis Solution	6 ml
Neutralization Solution	10 ml
Endotoxin Removal Wash	5 ml
Column Wash Solution	20ml
Nuclease Free Water	400-600µl

For plasmid DNA isolation, 250 ml of overnight culture was centrifuged at 4500 rpm for 20 min. The bacterial pellet was resuspended in Cell Resuspension Solution. For cell lysis Cell Lysis Solution was added and mixed by inverting the tube 3-5 times, incubation was done for 3 min at RT. Solution was neutralized by addition of Neutralization Solution and inverting

⁶ Sambrook, J., Russell, D.W., (2001) Molecular Cloning: A Laboratory Manual, 3rd Edt., Cold Spring Harbor Laboratory Press, Cold Spring Harbor, New York.

⁷ Austin, S., Friedman, S., Ludtke, D., (1986) Journal of Bacteriology, 168-2, 1010.

3-5 times. Neutralization was complete after 2-3 minutes incubation at RT. Cell debris was removed by centrifugation at 3500 rpm for 5 min with PureYield Clearing Column. Filtered lysate containing DNA was poured into PureYield Binding Column and centrifuged for 3 min at 3500 rpm. Endotoxin Removal Wash was added to remove substantial amount of protein, RNA and other endotoxin contaminants, and centrifuged at 3500 rpm for 3 min. Column Wash Solution was added to the column and followed by centrifugation at 3500 rpm for 5 min and additional 10 min run was performed to ensure the removal of ethanol. Nuclease-free water was added to the column and DNA was collected after centrifugation at 4000 rpm, 5min.

2.3.2 Ethanol Precipitation

For subsequent applications, such as *in-vitro* expression, higher concentration of plasmid DNA and purity was needed. Therefore, ethanol precipitation was performed after plasmid extraction. This treatment of the plasmid DNA was carried out as following;

- Add 1/10 volume of NaAc (3M, pH 4.8) to the low concentration plasmid DNA and mix gently.
- Add 2 volume of 95-100 % EtOH and mix gently.
- Place sample at -80°C for 30 min.
- Centrifugate the sample at 12,000 rpm (4°C) for 30min.
- Decant supernatant and drain samples on a paper towel on the bench.
- Resuspend DNA in nuclease free water for desired concentration.

2.3.3 Gel Electrophoresis Analysis

Extracted plasmid DNA and restricted linear DNA samples were separated in horizontal gel electrophoresis chamber (Agagel Mini, Biometra) according to their molecular size. 1% agarose was boiled in 1xTAE buffer (30ml) for 2-3 min and after cooling down at ~60°C and 3µl of SYBRSafe DNA stain (Invitrogen, Cat No: S33102) was applied. 1xTAE buffer was used as electrophoresis buffer as well. DNA samples were diluted with loading buffer, amounts and markers which have been used were given in Table2.6. Gel electrophoresis was carried out at 120V during 55 min.

CHAPTER II : MATERIALS & METHODS

Table2.6 Sample preparation for agarose gel

<i>Component</i>	<i>Amount</i>
DNA Sample	5 μ l
MilliQ water	5 μ l
6x Loading buffer (Fermentas)	2 μ l
Hyper Ladder I (Bioline)	7 μ l
GeneRuler 1kb Plus DNA Ladder (Fermentas)	7 μ l

2.3.4 Restriction Enzyme digestion

All plasmids were checked *via* restriction enzyme digestion, pJRHSA and pRCO3 plasmids were digested with either FastDigest ClaI(Bsu15I) (Fermentas, Cat No: FD0144) or EcoRI (Fermentas, Cat No: ER0279), and pETcyo was digested with ClaI, EcoRI, BamHI (Fermentas, Cat No: ER0059), BglII (Fermentas, Cat No: ER0081), HindIII (Fermentas, Cat No: ER0501). All pipetting schemes for restriction digests were given in Table2.7.

Table2.7 Restriction digest scheme

<i>Component</i>	<i>ClaI digest</i>	<i>EcoRI digest</i>	<i>BamHI digest</i>	<i>BglII digest</i>	<i>HindIII digest</i>	<i>ClaI-EcoRI double digest</i>
DNA	2 μ l	2 μ l	1 μ l	1 μ l	1 μ l	2 μ l
ClaI	1 μ l	-	-	-	-	1 μ l
EcoRI	-	1 μ l	-	-	-	1 μ l
BamHI	-	-	2 μ l	-	-	-
BglII	-	-	-	2 μ l	-	-
HindIII	-	-	-	-	2 μ l	-
10X Recom. Buffer	2 μ l	2 μ l	2 μ l	2 μ l	2 μ l	2 μ l
Nuclease free water	16 μ l	16 μ l	16 μ l	16 μ l	16 μ l	15 μ l
Incubation	37°C, 5min	37°C, 2hrs	37°C, 3hrs	37°C, 3hrs	37°C, 3hrs	37°C, 2hrs
Deactivation	65°C, 5min	65°C,20min	65°C,20min	65°C,20min	65°C,20min	65°C,20min

2.4 Purification of *In-vivo* Cytochrome *bo*₃ Ubiquinol Oxidase

2.4.1 Purification of Histidine Tagged Enzyme

All his-tag mutants were expressed in *E.coli* as mentioned before in section 2.2.2. Metal affinity chromatography was employed to purify expressed Cyt-*bo*₃. In a single step, Cyt-*bo*₃ was purified by using Ni-NTA Fast Start Kit (Qiagen, Cat No: 30600). Purification both under native and denaturing conditions was carried out as explained in Qiaexpress Ni-NTA Fast start Handbook. All the solution volumes which have been used during purification were given in Table2.8.

Table2.8 Volumes of Solutions Required for His-tag protein purification

<i>Solution Name</i>	<i>Denaturing Conditions</i>	<i>Native Conditions</i>
Bacteria Culture	250 ml	250 ml
Lysis Buffer (Native or Denaturing)	10 ml	10 ml
Wash Buffer (Native or Denaturing)	4 ml (x2)	4 ml (x2)
Elution Buffer (Native or Denaturing)	1 ml (x2)	1 ml (x2)

Purification process was performed as following, cell pellets were thawed in ice for 15 min and resuspended in Lysis buffer. Native sample was incubated on ice for 30 min and denaturing sample was incubated at room temperature for 1 hr. Samples were mixed gently 2-3 times and centrifuged at 9000 rpm for 30 min. The cleared lysate was applied to Ni-NTA Spin Columns and gravity flow was applied to collect flow-through fraction. Column was washed 2 times with Wash buffer. All bound his-tagged proteins were eluted from the column by Elution buffer, than they were kept at -80°C for further applications. At each step samples were collected from each fraction and stored for SDS-Page analysis. Proteins were detected by Western Blot analysis and protein concentration was determined *via* BCA Protein Assay (Pierce Co.).

2.4.2 Preparation of Cytoplasmic Membranes

Cells were carrying either pJRHisA or pETcyo plasmids were grown in 2L shaker flasks containing 1L corresponding media. Cell pellets were resuspended in 50mM K₂HPO₄ (pH 8.3) containing EasyPack Protease Inhibitor Cocktail Tablet (Roche, Cat No: 4693132), 1 tablet for each 50ml solution. The volume of buffer used for resuspending cells was 2-3 times the volume of cell culture used. Cells were broken either using BeadBeater (Biospec) or ultrasonic homogenizer (Bandelin, Sonoplus HD2200).

CHAPTER II : MATERIALS & METHODS

Cell debris was removed by centrifugation at 9000 rpm for 15 min (Eppendorf 5810R centrifuge) at 4°C. Membranes were pelleted by centrifugation of supernatant at 47,000 rpm in Beckman UltraMax ultracentrifuge at 4°C for 3 hrs. Pellet was resuspended in 50mM K₂HPO₄ (pH 8.3) and solubilized by addition of TritonX-100 (1%) and octyl glucoside (1.25%). The solution was mixed 1-2 hrs, prior to solubilization of membrane pellet, and kept in ice. Solution was centrifuged again at 30,000 rpm, 4°C for 20 min to remove all insoluble material. Amicon Ultra-15 Centrifugal Filter (Millipore, Cat No: UF905024) was used to concentrate the final solution at 4500 rpm for 15 min. Concentrated supernatant was stored at -80°C and used as a positive control for further applications such as, spectroscopic analysis and enzyme activity assay.

2.5 *In-vitro* Expression of Cytochrome *bo*₃ Ubiquinol Oxidase

2.5.1 Promega E.coli Kit

E.coli T7 S30 Extract System for Circular DNA (Promega, Cat No: L1130) has been used for *in-vitro* expression of Cyt-*bo*₃. The concentration of DNA was optimized by using dsDNA measurement option of BioPhotometer plus (Eppendorf). Since the *in-vitro* expression reaction is extremely sensitive to nuclease contamination, either RNase and DNase free tubes and pipet tips were used or autoclaved. Additionally, Bacillol AF (BODE Chemie) solution was used for disinfecting the working environment. All components were thawed in ice and mixed in appropriate volumes as described in the product manual. Pipetting scheme is given in Table2.9.

Table2.9 *In-vitro* expression pipetting scheme (Promega Kit)

<i>Component</i>	<i>Amount</i>
DNA Template	≤ 4μg
S30 Premix without amino acids	20μl
T7 S30 Extract, circular	15μl
Amino Acid mixture (Minus Met or Cys or Leu)	5μl
Rnasin Ribonuclease Inhibitor (Promega, Cat No: N2111)	1μl
Nuclease-Free water to final volume of	50 μl

All components were mixed gently prior to use and centrifuged for 5 sec in a Minispin Plus centrifuge (Eppendorf) to collect reaction mixture at the bottom of the tube. Incubation was done at 37°C in Thermomixer Comfort (Eppendorf) heating plate for 2hrs. Reaction was

CHAPTER II : MATERIALS & METHODS

stopped by placing the tube in ice and kept at -80°C either for further applications or directly analyzed *via* Western Blot analysis.

2.5.2 Qiagen Insect Kit

Another *in-vitro* expression kit, EasyXpress Insect Kit (Qiagen, Cat No: 32561) was used for comparison purpose. *In-vitro* reaction was carried out as described in the handbook of the kit. In the original protocol, procedure was divided into two different sections, *in-vitro* transcription and *in-vitro* translation. Both for transcription and translation reactions, pipetting schemes are given in Table2.10 and Table2.11.

Table2.10 Transcription reaction pipetting scheme (Qiagen Kit)

<i>Component</i>	<i>Transcription Reaction</i>
DNA Template (circular)	1.5 μg
5x Transcription Buffer	5 μl
5x NTP Mix	5 μl
20x Enzyme Mix	1.25 μl
Nuclease-Free water to final volume of	25 μl

Table2.11 Translation reaction pipetting scheme (Qiagen Kit)

<i>Component</i>	<i>Translation Reaction</i>
Template mRNA (obtained from transcription)	12 μl
EasyXpress Insect Reaction Buffer	5 μl
EasyXpress Insect Extract	20 μl
Insect EasyXpress Energy Mix	5 μl
Nuclease-Free water to final volume of	50 μl

All reaction components were thawed in ice and pipetted together, they were mixed gently and centrifuged shortly to collect all reaction mixture at the bottom of the tube. *In-vitro* transcription reaction was carried out at 37°C for 120 min and further treatment was done as explained in handbook. After obtaining eluate of mRNA, immediately proceeded with *in-vitro* translation reaction. Again all components were thawed in ice and mixed gently and reaction mixture was incubated in Thermomixer for 90 min at 27°C and 500rpm. Reaction mixture was kept at -80°C for other applications or analyzed *via* Western Blot.

2.5.3 Acetone Precipitation

Acetone precipitation was done to all *in-vitro* samples to minimize the interference of lipids. 5µl of *in-vitro* reaction mixture was mixed gently with 20µl pure acetone and was kept in ice for 15 min. Solution was centrifuged at 40,000 rpm for 5min. Supernatant was removed and pellet was dried under vacuum for 45 min. Cell pellet was dissolved in SDS buffer and proceeded with Western Blot analysis.

2.5.4 BODIPY-FL Labelling

Fluorescent labeling method was used to observe *in-vitro* expressed protein, since pRCO3 plasmid encodes only Cyt-bo₃ mutant without tag. FluoroTect™ Green_{Lys} *in-vitro* Translation Labeling System (Promega, Cat No: L5001) was used for fluorescent labeling of *in-vitro* synthesized Cyt-bo₃. Reaction was carried out as explained in product handbook. Following protocol was applied and component volumes were given in Table2.12.

Table2.12 Volumes of components for *in-vitro* expression by using FluoroTect Labeling

<i>Component</i>	<i>Amount</i>
DNA Template	≤ 4µg
S30 Premix without amino acids	20µl
T7 S30 Extract, circular	15µl
Amino Acid mixture (Minus Met or Cys or Leu)	5µl
Rnasin Ribonuclease Inhibitor (Promega, Cat No: N2111)	1µl
FluoroTect™ Green _{Lys} tRNA	1-5µl
Nuclease-Free water to final volume of	50 µl

All components were thawed by quick hand warming, especially FluoroTect™ Green_{Lys} tRNA, and they are except FluoroTect™ Green_{Lys} tRNA mixed gently. After quick centrifugation, FluoroTect™ Green_{Lys} tRNA was added to the mixture and incubated at 37°C for 2hrs. Reaction was terminated by placing the tube on ice and reaction mixture was used directly for SDS-Page analysis or it was kept at -80°C for further applications. Since FluoroTect™ Green_{Lys} is sensitive to extreme heating, to perform SDS-Page analysis samples were denatured at 70°C for only 2-3 min.

2.6 Immuno Blotting

All *in-vitro* and *in-vivo* expressed Cyt-bo₃ samples were examined *via* SDS-Page gel electrophoresis. Sample preparation, buffers and running conditions were given in Table2.13 and Table2.14. During western blot process, XCell SureLock chamber system (Invitrogen) was used for gel electrophoresis, iBlot Dry Blotting system (Invitrogen) was used for the transfer of the gel to the membrane and WesternBreeze Chemiluminescent Kit – Anti Mouse (Invitrogen, Cat No: WB7104) was used for chemiluminescent detection.

Table2.13 Sample preparation for SDS-Page gel

<i>Component</i>	<i>Amount</i>
Protein Sample	5µl
Sample Reducing Agent (Invitrogen, Cat No: NP0009)	1.6µl
4X LDS Buffer (Invitrogen, Cat No: NP0008)	4µl
Milli-Q water	5.4µl
MagicMark™ XP Western Protein Standard (Invitrogen, Cat No: LC5602)	3µl
SeeBlue Plus2 (Invitrogen, Cat No: LC5925)	7µl
6xHis Protein Ladder (Qiagen, Cat No: 34705)	5µl
BenchMark His-tag Protein Ladder (Invitrogen, Cat No: 10748-010)	2µl

Cyt-bo₃ samples were mixed as given above and incubated at 70°C for 10 min, then centrifuged at 13,000 rpm for 1 min. 16µl of each sample and sufficient amount of marker was loaded to the gel.

Table2.14 Running conditions for SDS-Page gel

<i>Gel Type</i>	<i>Running Buffer</i>	<i>Power settings</i>	<i>Run Time</i>
NuPAGE®	NuPAGE® MOPS	200V	55 min
10% Bis-Tris gel (Invitrogen, Cat No: NP0302)	SDS Running Buffer (1X) (Invitrogen, Cat No: NP0001)	500mA	

After gel electrophoresis, pre-run gel containing protein samples and standards was placed on the PVDF transfer membrane (Invitrogen, Cat No: IB4010-02) of the anode stack. Sandwich system was completed with pre-soaked filter paper and cathode stack as described in

CHAPTER II : MATERIALS & METHODS

the manual. Following parameters were used for the gel transfer, program P3 (20V) and 7min. At the end of transfer, membrane was placed immediately into the milliQ water.

Western Breeze kit and protocol was used for immuno blotting and procedure was carried out as following;

- Rinse membrane with 20ml of milliQ water for 5min and repeat once.
- Place membrane in 10ml of appropriate Blocking Solution for 30min on a rotary shaker.
- Rinse membrane with 20ml of milliQ water for 5min and repeat once.
- Incubate the membrane with 10ml of Primary antibody solution overnight or at least 2-3 hrs. The Primary Antibody which has been used was PentaHis Ab (BSA-free) Mouse monoclonal IgG (Qiagen, Cat No: 34660) and it was diluted to a concentration 1:2000.
- Decant antibody solution and wash membrane with 20ml of Antibody Wash solution for 5min, repeat 3 times.
- Incubate the membrane with 10ml of Secondary Antibody Solution for 30 min.
- Decant secondary antibody solution and wash membrane with 20ml of Antibody Wash solution for 5min, repeat 3 times.
- Rinse membrane with 20ml of milliQ water for 2min and repeat twice.
- Place membrane on a sheet of transparency which was provided in the kit, do not allow the membrane to dry out.
- Apply 2.5ml of Chemiluminescent Substrate to the membrane surface and allow the development of reaction for few minutes.
- Blot excess solution from membrane surface with the filter paper, do not allow the membrane dry out completely.
- Cover membrane with another transparency to finish membrane sandwich.
- Expose membrane with suitable imager and program.

CHAPTER II : MATERIALS & METHODS

To complete western blotting procedure, LAS 3000 Imaging System (Fuji) was used and exposure details are given in Table2.15.

Table2.15 Exposure conditions for Western Blotting

<i>Exposure Type</i>	<i>Interval Time</i>	<i>Sensitivity/Resolution</i>	<i>Dark box settings</i>
Increment	3-5 min	Standard	Chemiluminescent Method
			Light: none
			Filter: through
			Iris: F2.8

2.6.1 Coomassie Staining

After gel electrophoresis, instructions were followed as explained in the manual of SimplyBlue™ SafeStain product (Invitrogen, Cat No: LC6060). Gel was removed completely from gel cassette and was rinsed 3 times with 100ml milliQ water for 5min. Then, it was stained in 20-25 ml of SimplyBlue staining solution up to 3 hrs. For over night incubation, 20% NaCl (w/v) solution was added to the staining solution. After staining the gel, it was washed with 100ml milliQ water for 1hr. Image was displayed immediately.

2.7 Spectroscopic Quantification of Enzyme

2.7.1 Reduction of UQ Substrate

Enzyme activity of Cyt-bo₃ was monitored *via* UV-Vis spectroscopy. Ubiquinone-1 or in other words Coenzyme-Q (Sigma, Cat No: C7956) was used as an analog of substrate. Ubiquinone (UQ) was reduced as explained elsewhere ^{4,8}.

20mg UQ was dissolved in 3ml absolute ethanol and 3ml, 0.1M K₂HPO₄ (pH 6.5). 15µl, 1.2M HCl was added in this mixture and the solution was bubbled for 10 min with N₂. A few grains of sodium hydrosulfite/dithionite (Acros, Cat No:169590256) and sodium borohydride (Sigma-Aldrich, Cat No: 452882) were added till solution become colorless, than the solution was bubbled again with N₂ for 10min. Solution was extracted with 3ml cyclohexane three times and top phase was collected. Extracted material was dried under N₂ stream. Colorless oily residue was resuspended in 2.5ml DMSO containing 6mM HCl. Final

⁸ Rieske, J. S., (1967) Methods in Enzymology, 239.

concentration for Ubiquinol-1 (UQH₂) was 30 mM. Aliquots were stored at -20°C for few months.

2.7.2 Spectrophotometric Analysis of Cyt-bo₃

2.7.2.1 Reduced Minus Oxidized Spectra

Difference spectra and kinetic measurements were performed on Lambda 900 UV-Vis Spectrophotometer (Perkin Elmer). Solubilized and concentrated Cyt-bo₃ membrane samples which obtained from pJRHisA and pETcyo plasmids were used. The reduced minus oxidized spectra were taken with relatively high concentrations of Cyt-bo₃, such as > 2-3 μM. For the oxidized spectra, *in-vivo* expressed enzyme samples were used without any treatment. To reduce oxidized samples, a few grains of dithionite or concentrated solution of dithionite (30-60μl) was added to the sample and mixed gently. A spectrum was taken after 1-2 min.

2.7.2.2 Enzyme Activity Assay *via* Spectroscopic detection

The spectrophotometric detection of enzyme activity was done by using reduced analog UQH₂ as a substrate. Activity of Cyt-bo₃ was monitored and calculated by means of oxidation of UQH₂ at 275nm ($\Delta E=12.25\text{mM}^{-1}\text{cm}^{-1}$)⁹. The assay was carried out in 50mM K₂HPO₄ (pH 7.0) which contains 2μM dithionite to maintain reduced ubiquinol, at ambient temperature. Enzyme kinetics was observed in different concentrations of UQH₂ from 50μM to 250μM. Enzymatic reaction was initiated with the addition of 50nM, 30μl of Cyt-bo₃ sample to the 1ml of substrate solution and the reaction kinetic was followed during 2min. K_M and V_{max} values were calculated by plotting the Lineweaver-Burk plots, data was obtained at least four independent measurements.

Calibration curve was obtained from UQ stock solution. Standard solutions were prepared at varying concentrations from 5μM to 1mM and measured at 278nm. Conditions were kept same with the enzymatic activity measurements.

2.7.3 Enzyme Activity Assay *via* Oxygen Electrode

Activity of Cyt-bo₃ was measured with respect to oxygen consumption as well. For the measurement of oxygen consumption rate YSI 5300A Oxygen Electrode Micro System (Yellow Life Sciences) was used. Substrate solutions were prepared in different concentrations varying from 50μM to 500μM UQH₂ in 50mM K₂HPO₄ buffer (pH 7.0). Activity measurement was started with the addition of 3μl of *in-vivo* expressed Cyt-bo₃ sample to the 600μl and

⁹ Redfearn, E. R., (1967) Methods in Enzymology, 10, 381.

recorded during 2-3 min. At least two independent measurements were obtained for the enzymatic activity calculations. For the calculation of *in-vitro* expressed enzyme activity, 500 μ M UQH₂ was used and oxygen consumption was recorded with the addition of 10-25 μ l of Cyt-b₀₃.

2.7.4 Sample Preparation of *in-vitro* Expressed Cyt-bo3 for Spectrophotometric Analysis and Enzyme Activity Assay

In-vitro expression of Cyt-b₀₃ was done as explained in section 2.5.1 and samples were used with and without purification process for the activity measurement. Purification was done as mentioned before in section 2.4.2 with small modifications. 350-400 μ L *in-vitro* expression mix was resuspended in 50mM K₂HPO₄ (pH 8.3). The volume of buffer used for resuspension was 2-3 times the volume of the mix. Debris was removed by centrifugation at 10,000 rpm for 15 min at 4°C. Cyt-b₀₃ or membranes were pelleted by centrifugation of supernatant at 47,000 rpm at 4°C for 3 hrs. Pellet was resuspended in 50mM K₂HPO₄ (pH 8.3) and solubilized by addition of TritonX-100 (1%) and octyl glucoside (1.25%). The solution was mixed in ice for 1-2 hrs to solubilize the protein.

2.8 SPR/SPFS Measurements

2.8.1 Preparation of PDMS Spacer

Sylgard 184 Silicon Elastomer (Dow Corning GmbH) was used for the preparation of PDMS spacer ring. Base silicon elastomer and curing agent were mixed in 10:1 ratio and homogenized by vortexing. All bubbles were removed by using a desiccator system which is connected to a vacuum pump. After removal of bubbles, small amount of PDMS mixture was filled in ellipse shaped molds and evenly spreaded in the mold. Filled molds were placed in an 80°C oven for 5 min so PDMS becomes more viscous and goes into crevasses. Cured PDMS was peeled off from the mold after 48 hrs incubation at room temperature.

2.8.2 Preparation of Gold Substrates

LaSFN9 glass substrates which has a refractive index value $n=1.845$ (Schott AG) were used as a substrate for gold evaporation. Before the evaporation of gold following procedure was applied to clean glass slides;

- Place glass slides in a container and rinse with 2% Hellmanex (Hellma GmbH) solution for 15min in ultrasonic bath.
- Rinse 15 times with milliQ.

- Rinse again with 2% Hellmanex solution for 15min in ultrasonic bath.
- Rinse 20 times with milliQ.
- Rinse 2 times with Ethanol (Sigma-Aldrich, HPLC grade).
- Dry with N₂ flow.
- Use directly for evaporation or store under Argon.

Edwards FL 400 was used for the gold evaporation process. 50nm gold film was deposited on glass substrates by electro-thermal evaporation.

2.8.3 SPR/SPFS Setup

A home-made Surface Plasmon Resonance (SPR) was used in Kretschmann configuration¹⁰ for all SPR measurements. After modification of the system with some small additions, setup was used at the same time for Surface Enhanced Fluorescence Spectroscopy (SPFS) measurements as well.

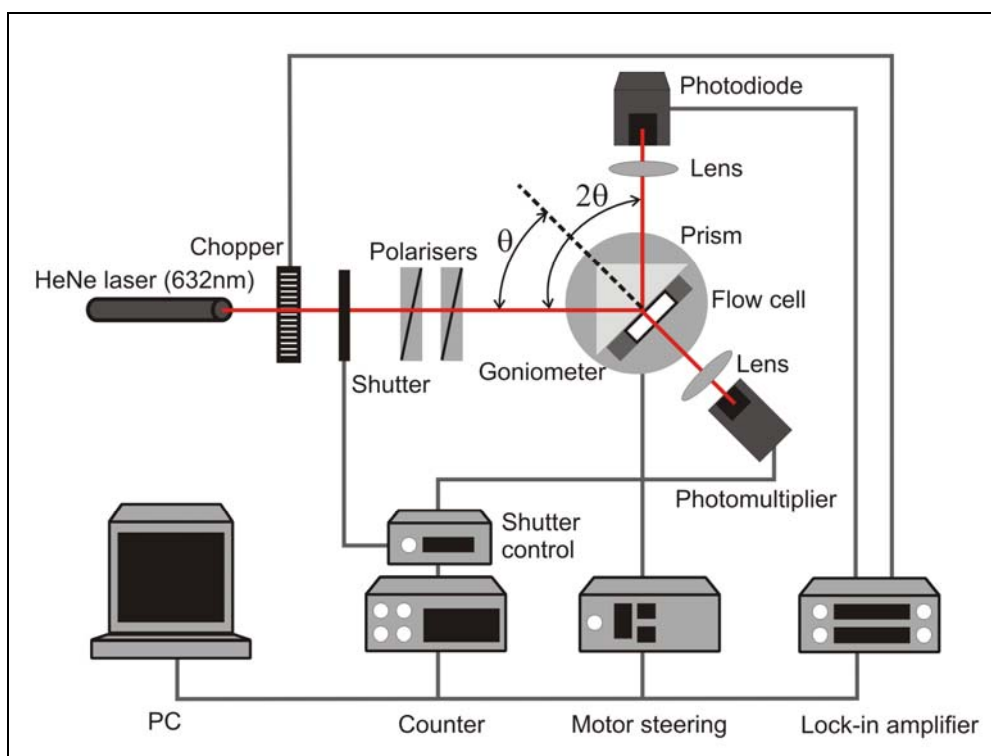


Figure 2.1 Schematic representation of SPR/SPFS setup

¹⁰ Kretschmann, E., Raether, H., (1968) Z. Naturforsch. A., 23, 2135.

All details of a typical SPR/SPFS setup are shown in Figure 2.1. HeNe laser (Uniphase, $\lambda=632.8\text{nm}$) was used and it was coupled to the system through LaSFN9 prism (Schott AG, $n=1.845$) at the same wavelength. The excitation beam passes through two polarizers (Glan-Thompson) which adjust the intensity of the incident light and TM polarization. Chopper was connected to a lock-in amplifier. The reflected light which was focused by a lens (Ovis, $f=50\text{mm}$) was then detected by a photodiode. The sample and the flow cell were fixed on a goniometer which has xy tilting table to enable the movement at an angle θ and to adjust sample holder. Based on reflection law, sample motor and detector motor were fixed at θ and 2θ respectively for the adjustment of the setup which has been shown in Figure 2.2.

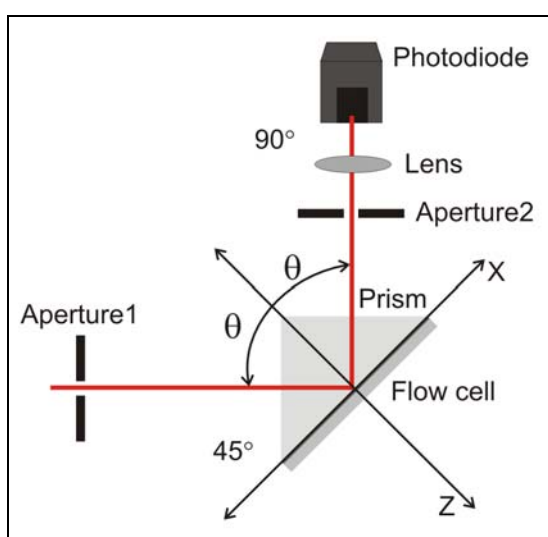


Figure 2.2 Alignment of SPR/SPFS setup

A photomultiplier was used to detect the fluorescence intensity and was connected to a counter. It was fixed directly in front of the sample. A shutter was used during fluorescence measurement to prevent bleaching of fluorophore in the sample. All experiments were carried out in a black-box to avoid photons which is coming from the environment. A photograph of the setup is given in Figure 2.3.

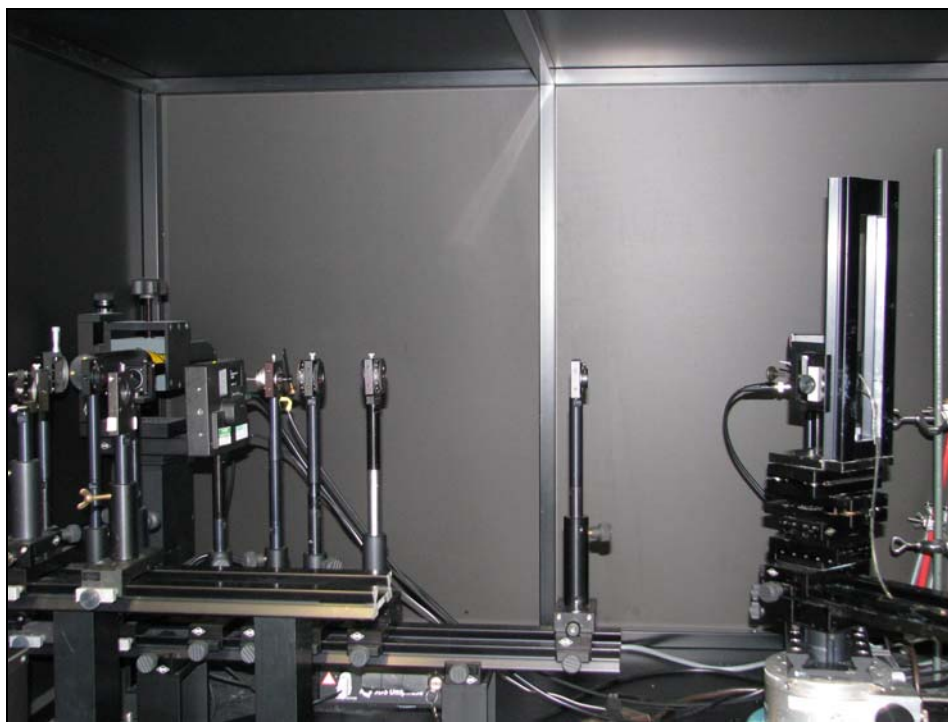


Figure 2.3 A photograph of SPR/SPFS setup

2.8.4 Assembly of Flow Cell

All experiments were carried out in a same flow cell. As it has been shown in Figure 2.4, all components such as gold substrate, quartz glass, prism and PDMS ring were sandwiched together. PDMS ring provides a reservoir volume about 50 μ l for the aqueous environment. LaSFN9 prism and glass substrate which was coated with gold film were sandwiched by using one drop of index matching oil (Cargille Labs) which has the refractive index $n=1.7$. Flow cell was connected to a peristaltic pump *via* Tygon® tubing with needles for a continuous flow through the flow cell.

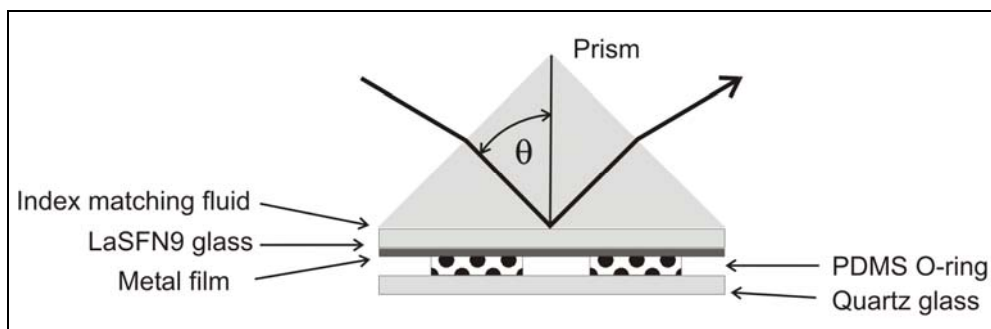


Figure 2.4 Assembly of flow cell

2.8.5 Scan and Kinetic Mode of SPR/SPFS

Home-made Wasplas (MPIP, Mainz) software has been engaged for detection and Winspall (MPIP, Mainz) software has been selected for data evaluation. Scan curve is obtained by plotting the reflected intensity versus incident angle. Fitting has been done for the obtained scan curve according to Fresnel equation by using Winspall which simulates the expected reflectivity curve to calculate thickness of metallic and dielectric layers. Addition of a new layer affects the refractive index of a dielectric layer and it results with the shift of minima. This shift has been considered as an introduction of a new layer and refractive index of a new layer or thickness can be calculated *via* fitting of the curve.

A typical reflectivity scan curve and corresponding kinetic curve are given in Figure 2.5. Refractive index or thickness of the additional layer can be simulated and compared with respect to this angular dependence of reflectivity. Relation in between angle change ($\Delta\theta$) and thickness (d) or refractive index (n) is given in equation 2.1. However, this relation shows that either refractive index or thickness can only be detected by using an additional method.

$$\Delta\theta \propto n \cdot d \tag{Eq 2.1}$$

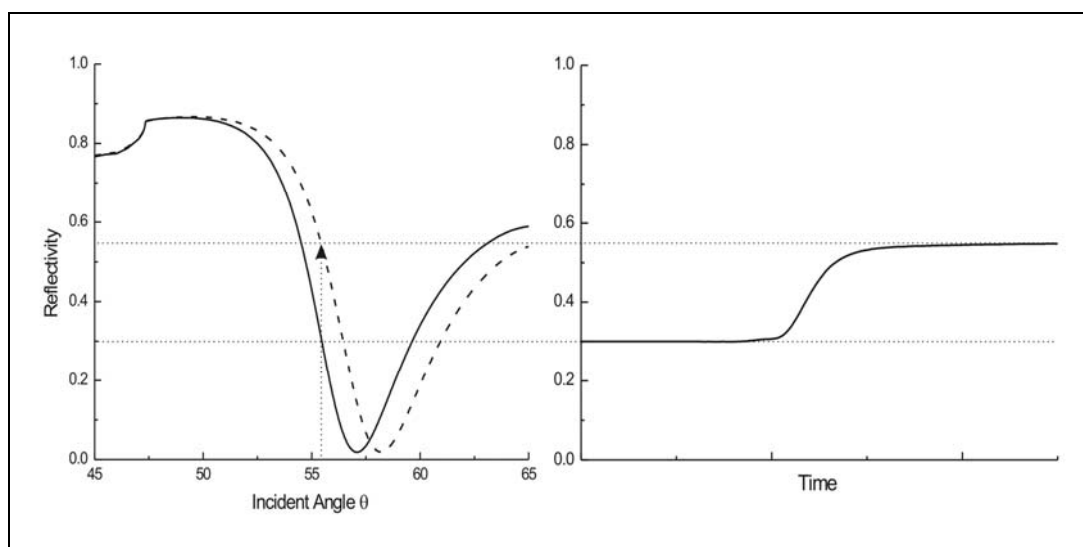


Figure 2.5 Scan curve and Kinetic curve

Kinetics of reaction on the surface is obtained by plotting the reflectivity change versus time during addition of another layer. Kinetic curve shows the interaction in between surface and additional material at a fixed angle. For this purpose, the incident angle was fixed at 30% reflectivity and the reflectivity was detected during incubation period. For the all kinetic

measurements, 30% reflectivity region was chosen, since the change in reflectivity is nearly linear at this point, so the change in reflectivity is really high and sensitive to the additions at this angle.

Counter-scan and kinetic was observed by attaching a photomultiplier to the goniometer while performing normal scan and kinetic measurement. Photomultiplier collects the fluorescence intensity and both counter-scan curve and kinetic curve was obtained by plotting same curves as mentioned before by plotting fluorescence intensity instead reflected intensity. Counter-scan curve and kinetic curve before and after addition of fluorescent sample is given in Figure 2.6

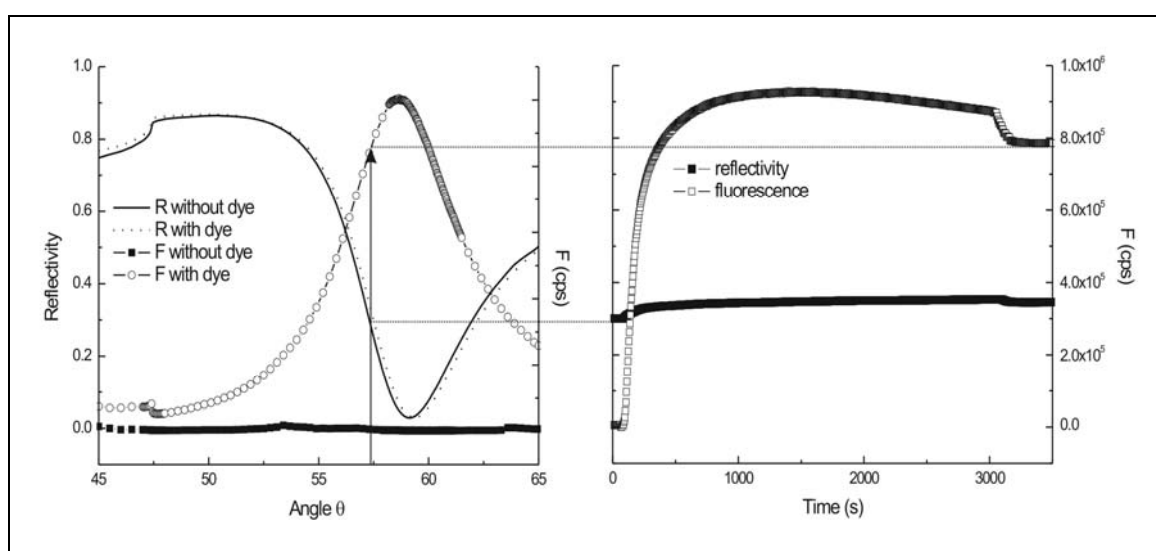


Figure 2.6 Fluorescence Scan curve and Kinetic curve

2.8.6 Experimental SPR/SPFS Protocol

All solutions were prepared fresh for the SPR/SPFS experiments and they were diluted just before adding to the system. Following reagents have been used in the membrane assembly and *in-vitro* synthesis;

Laminin Peptide P19 (Cys-Laminin A chain 2091-2108)

Cys-Ser-Arg-Ala-Arg-Lys-Gln-Ala-Ala-Ser-Ile-Lys-Val-Ala-Val-Ser-Ala-Asp-Arg

Sigma, Cat No: C 6171

Stock Solution: 0.1 mg/ml in milliQ water, store at -20°C

Working Solution: 0.01 mg/ml in milliQ water, dilute before use

N-(3-Dimethylaminopropyl)-N'-ethylcarbodiimide Hydrochloride (EDC)

Fluka, Cat No: 03449

Stock Solution & Working Solution: 0.4M in milliQ water, store at -20°C

N-Hydroxysuccinimide (NHS)

Fluka, Cat No: 56480

Stock Solution & Working Solution: 0.1M in milliQ water, store at -20°C

1,2-Dimyristoyl-*sn*-glycero-3-phosphoethanolamine (DMPE)

Sigma, Cat No: P 5693 or Avanti Polar Lipids, Cat No: 850745X

Stock Solution: 2 mg/ml in PBS (Dulbecco's Phosphate Buffered Saline 1X, GIBCO/Invitrogen, Cat No: 14040-083) with 0.1% TritonX-100 (Sigma, Cat No: T9284), store at -20°C

Working Solution: 0.2 mg/ml in PBS, dilute before use

When it is in powder form, lipid was directly dissolved in PBS buffer which contains TritonX-100 and solution was mixed *via* vortex or ultrasonic bath was used till complete solubilization. At the end solution was milky suspension since the solubility was low. When it is dissolved form in chloroform, solvent was evaporated completely by N₂ stream and PBS was added together with TritonX-100. Solution was frozen in liquid nitrogen, than it was thawed in water bath (35°C). It was mixed well by vortexing and this treatment was done at least three times to get high solubility of DMPE.

L- α -Phosphatidylcholine from soybean (PC)

Fluka, Cat No: 61757

Stock Solution: 100 mg/ml, 10% in chloroform, store at -20°C

Working Solution: 1.0 mg/ml in PBS, dilute before use

Same procedure was performed since lipid is dissolved in chloroform, chloroform was evaporated by N₂ stream and PBS was added. Solution was mixed well by vortexing. Freeze & thaw cycle was done at least three times.

Western Blocking Reagent

Roche, Cat No: 11921673001

Stock Solution: 10X concentrated blocking solution

Working Solution: 0.5% (V/V) in PBS, dilute before use

PentaHis Ab (BSA free) Mouse monoclonal IgG (1°Ab)

Qiagen, Cat No: 34660

Stock Solution: 0.2 µg/µl in milliQ water, store at -20°C

Working Solution: 2.0% (V/V) in 200µl PBS, dilute before use

Cy5-Conjugated Secondary Antibody Goat-Antimouse IgG H+L (2°Ab)

Chemicon Int., Cat No: AP181S

Stock Solution: 1.5 mg/ml in milliQ water, store at 4°C

Working Solution: 3.0% (V/V) in 200µl PBS, dilute before use

PentaHis Alexa Fluor 647 Conjugate (1°Ab)

Qiagen, Cat No: 35370

Stock Solution: 200 µg/ml, store at 4°C

Working Solution: 3.0% (V/V) in 200µl PBS, dilute before use

During measurements, SPR Scan was performed always just before and after addition of new layer or component. SPR Kinetic was performed during addition and incubation of a new component. Self assembly of the Tethered Bilayer Lipid Membrane (tBLM) was carried out step by step as follows;

- Assemble the sample holder and the flow cell as explained in section 2.8.4
- Rinse surface of the gold substrate and flow cell with 1ml milliQ water
- Perform scan each time after rinsing and before addition of a new layer
- Pump 500µl of P19 solution to the flow cell with the flow rate 0.105 ml/min and incubate for 45min
- Rinse surface with 1ml milliQ water
- Add 500µl of a 1:1 EDC/NHS mixture to the flow cell and incubate for 10min

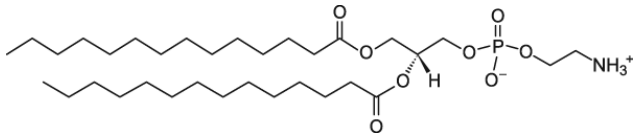
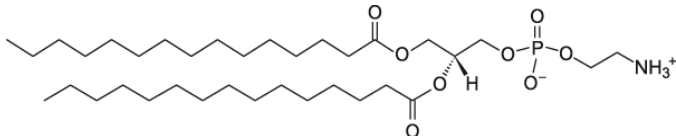
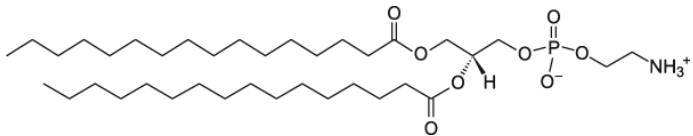
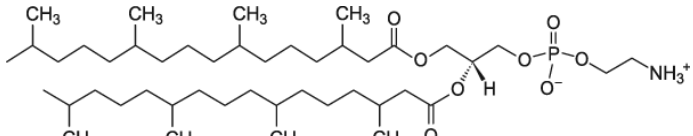
- Do not rinse after EDC/NHS addition step
- Add 1ml of DMPE solution to the flow cell without rinsing to exchange all EDC/NHS mixture with DMPE solution, incubate for 60min
- Rinse surface with 1ml PBS buffer
- Extrude 500 μ l of PC solution by using extruder
- Add PC vesicles to the system and incubate for 90min
- Rinse surface with 1ml PBS buffer
- Prepare *in-vitro* mix as explained in section 2.5.1 and add into flow cell immediately. Incubate for 120 min at 37°C.
- Rinse with 1ml PBS buffer and collect *in-vitro* mix for western blot analysis
- Add 1ml, 0.5% Western Blocking Reagent and incubate for 60min
- Rinse with 1ml PBS buffer
- Add 200 μ l of 1°Ab solution (PentaHis) or for the direct detection PentaHis Alexa Fluor 647 Conjugate, incubate for 60 min.
- Install photomultiplier to the system before addition of any fluorescent labeled component
- Rinse with 1ml PBS buffer
- Add 200 μ l of 2°Ab solution, Cy5 Conjugate and incubate for 45 min. Skip this step if you are using PentaHis Alexa Fluor 647 Conjugate instead PentaHis 1°Ab
- Rinse with 1ml PBS buffer and perform fluorescent scan for the detection of protein-antibody complex

2.9 Contact Angle Measurements

DSA10 (Krüss CA, Germany) was selected as an experimental setup. OCA software (DataPhysics, Filderstadt, Germany) was used for the calculation and analysis of the contact angle. Sessile drop method has been used and 3µl drop was dispensed on the surface, it was recorded *via* CCD camera. In average 3-5 measurements were taken for each slide.

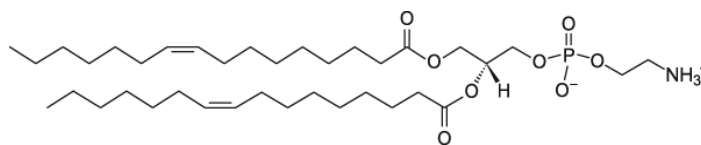
A membrane was generally assembled as previously stated in section 2.8.6 with minor modifications. The main difference of the protocol was flash rinsing with ethanol after formation of monolayer and bilayer to remove excess lipids from the surface. Contact angle was obtained after addition of each layer. Various lipids which have been listed in Table 2.16 were used as a monolayer instead of DMPE layer and stock solutions were prepared in a same way as explained previously for DMPE. For the coupling of P19 spacer and lipid monolayer, different time and concentration combinations and preparation methods were examined such as coupling in a tube than assembling on a gold surface which will be discussed later on the following chapters.

Table 2.16 Chemical structures of Lipid Monolayer Components

<i>Lipid Monolayer</i>	<i>Literature Name & Structure</i>
DMPE	1,2-Dimyristoyl- <i>sn</i> -glycero-3-phosphoethanolamine 
DPePE	1,2-Dipentadecanoyl- <i>sn</i> -glycero-3-phosphoethanolamine 
DPPE	1,2-Dipalmitoyl- <i>sn</i> -glycero-3-phosphoethanolamine 
DPhyPE	1,2-Diphytanoyl- <i>sn</i> -glycero-3-phosphoethanolamine 

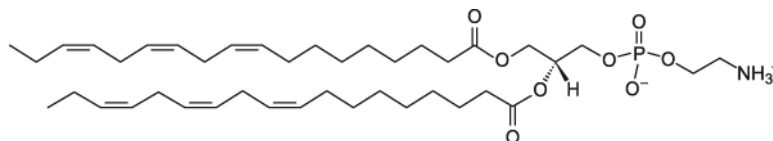
DPalPE

1,2-Dipalmitoleoyl-*sn*-glycero-3-phosphoethanolamine



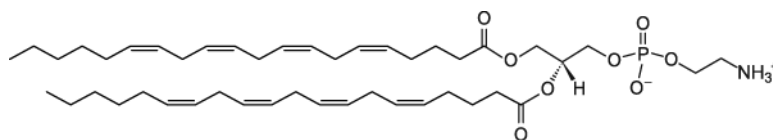
DLPE

1,2-Dilinolenoyl-*sn*-glycero-3-phosphoethanolamine



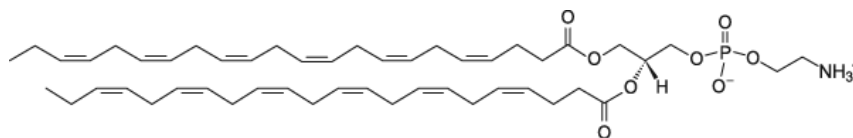
DAPE

1,2-Diarachidonoyl-*sn*-glycero-3-phosphoethanolamine



DDPE

1,2-Didocosahexaenoyl-*sn*-glycero-3-phosphoethanolamine



3 Results & Discussion

3.1 Membrane Construction Strategies

3.1.1 General Remarks of tethered Bilayer Lipid Membranes (tBLM)

To attain functionality of membrane proteins, various models of a complex membrane system were experienced and optimized. Here the strategy is to mimic cellular membrane rather a simple model that is away from complexity with respect to natural counterpart. The mimic of a biological membranes such as solid supported lipid membranes are widely used as a platform to investigate protein membrane interactions¹⁻⁴.

Tethered bilayer lipid membrane (tBLM) is composed of a monolayer which is attached to the surface *via* peptide spacer and a bilayer. Flexible and hydrophilic peptide spacer provides reservoir space in between the membrane structure and solid support and it assists the incorporation of proteins which contains huge outer membrane parts. The main aspect of optimizing tBLM is to obtain “good” membrane structure which shows a high performance to integrate membrane proteins while preserving their functionality. The definition of a “good” means inserted membrane protein behaves as in its natural environment, so we can say that tBLM structure is suitable for further studies. Recently, it has been shown that previously developed tBLMs has a high insulating properties and nearly ideal electrical properties⁵. However, the most important fact is incorporation of membrane proteins with a large outer membrane parts. For this reason optimization of the system was necessary to find the right balance in between all membrane components.

We are able to address membrane protein species, since we introduce a platform for membrane protein synthesis, namely the *in-vitro* synthesis of membrane proteins into a peptide supported membrane system. As an alternative, we are exploring this system for the first time to create closer model to the cellular membranes and to mimic their function.

3.1.2 Peptide Spacer

In this project, Laminin Peptide P19 is employed as a spacer, since it is composed of amino acids providing high hydrophilicity and high compatibility to protein molecules by

¹ Sackmann, E., (1996) *Science*, 271, 43.

² Sinner, E. K., Knoll, W., (2001) *Current Opinion in Chemical Biology*, 5, 705.

³ Zhao, J., Tamm, L. K., (2003) *Langmuir*, 19, 1838.

⁴ Munro, J. C., Frank, C. W., (2004) *Langmuir*, 20, 10567.

⁵ Schiller, S., Naumann, R., Lovejoy, K., Kunz, H., Knoll, W., (2003) *Angewandte Chemie International Edition*, 42, 208.

means of its peptide structure. Two parameters; incubation time and concentration of P19 were investigated to maximize the formation of highly ordered, dense membrane structure which enables insertion of Cyt-bo₃ while keeping its functionality.

Optimal incubation time and P19 concentration was investigated by contact angle (CA) and SPR methods. All data has been calculated from 10 independent measurements and OriginPro 7.5 software was used to calculate mean values and standard deviations. CA results of time optimization are shown in Figure 3.1 and P19 concentration was kept constant at 0.01 mg/ml for each measurement. Characteristic value for bare gold which is around 79° was obtained by measuring static CA immediately after evaporation of gold layer. Regarding to bare gold, P19 layer shows a hydrophilic behavior and possess lower CA values as expected. Very slight change in CA value was observed in between 20min and 45 min incubation time; however to get the highest packing density, 45min incubation period was chosen. It was detected that longer incubation times such as 2hours or overnight cause defects in gold layer which results with the removal of some of the gold layer from the surface.

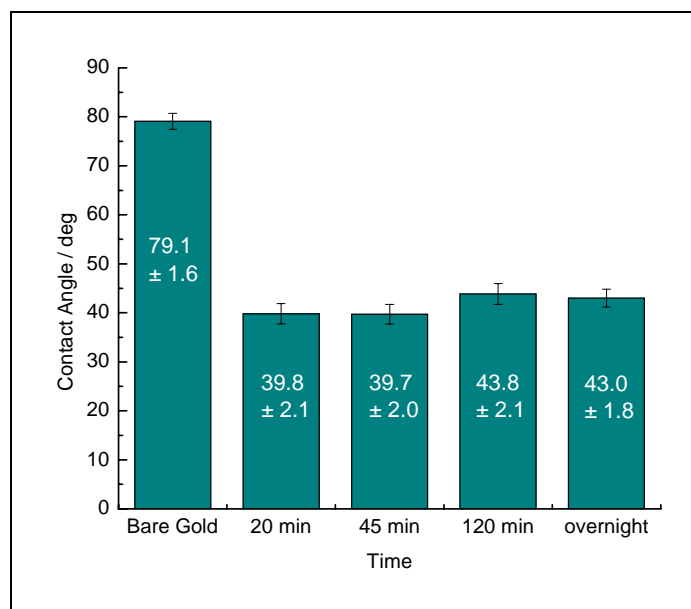


Figure 3.1 Contact angles of P19 for different incubation times

To detect the CA of each sample, sessile drop method was used and the shape of a 3 μ l drop was monitored for each sample *via* CCD camera. Relevant images were given in Figure 3.2 for different assembly times of P19.



Figure 3.2 CCD images of (a) bare gold, (b) 20min, (c) 45min, (d) 120min, (e) overnight incubation period of 0.01mg/ml P19

CA results of different P19 concentrations at a fixed time interval (45min) were given in Figure 3.3. A significant difference was observed in between high and low concentrations of P19 solutions. Higher concentrations leads to lower CA values, as predicted they form more ordered layers than the low concentration set. Although 0.1 mg/ml solution has a lower CA value than 0.01 mg/ml, we prefer 0.01 mg/ml P19 as a working solution. The most important fact is, there is not so much difference in between these two solutions in terms of CA which is shown in Figure 3.4 (b and c). That was also supported *via* SPR measurements; there was not considerable reflectivity difference in between 0.1mg/ml and 0.01mg/ml with respect to lower concentrations, the corresponding SPR kinetic curve for P19 assembly was given in Figure 3.5. Another advantage of using lower concentration is to avoid any unfavorable interactions caused by excess free P19 molecules. CCD camera images of concentration optimization were given in Figure 3.4.

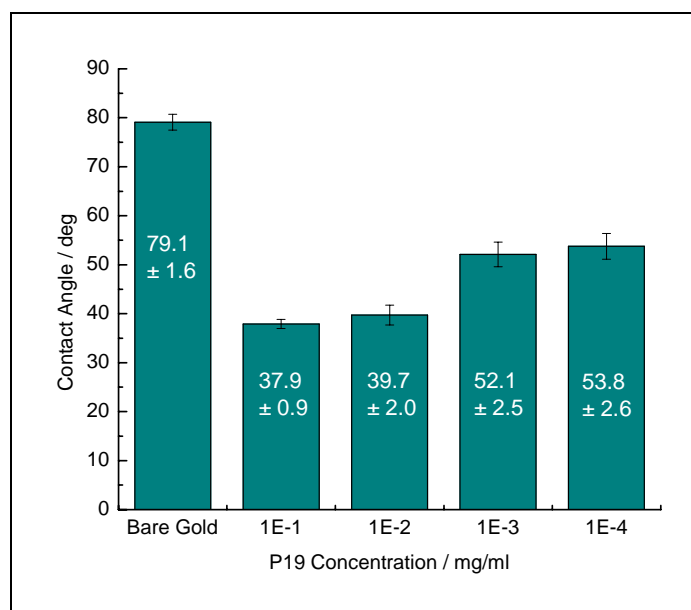


Figure 3.3 Contact angles of P19 for different concentrations

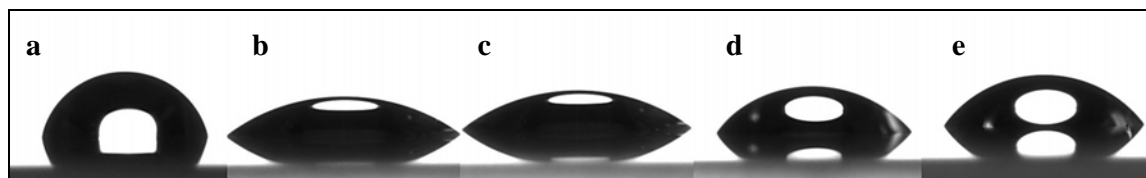


Figure 3.4 CCD images of (a) bare gold, (b) 0.1mg/ml, (c) 0.01mg/ml, (d) 0.001mg/ml, (e) 0.0001mg/ml P19

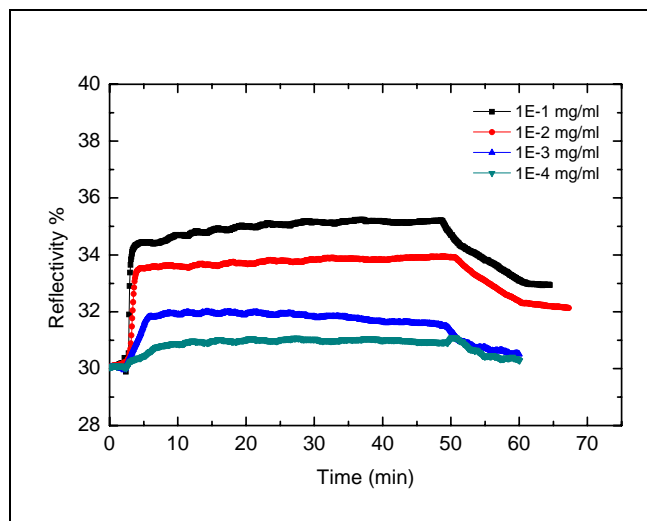


Figure 3.5 Kinetic SPR curve of P19 assembly

3.1.3 Monolayer Formation

Artificial membrane synthesis was performed by subsequent building steps which is depicted in Figure 3.6 to investigate the protein incorporation and functioning. The formation of spacer layer was followed by EDC-NHS coupling step or in other words amine coupling reaction. EDC-NHS coupling is the most common method of amide bond formation. The most important advantage of this method is; all components are water soluble and it gives a great opportunity to work with bio-mimicking systems.

On the surface, attached P19 molecules bearing carboxyl groups at the open end, through this carboxyl groups reactive succinimide ester structure was obtained *via* activation with 1:1 mixture of EDC:NHS. Succinimide ester is a reactive group that can react spontaneously with any free amine group. Thereby EDC-NHS coupling produces a peptide or amide bond in between P19 molecule and the corresponding phospholipid molecule. Synthetic mechanism and details are given in Figure 3.6 and Figure 3.7.

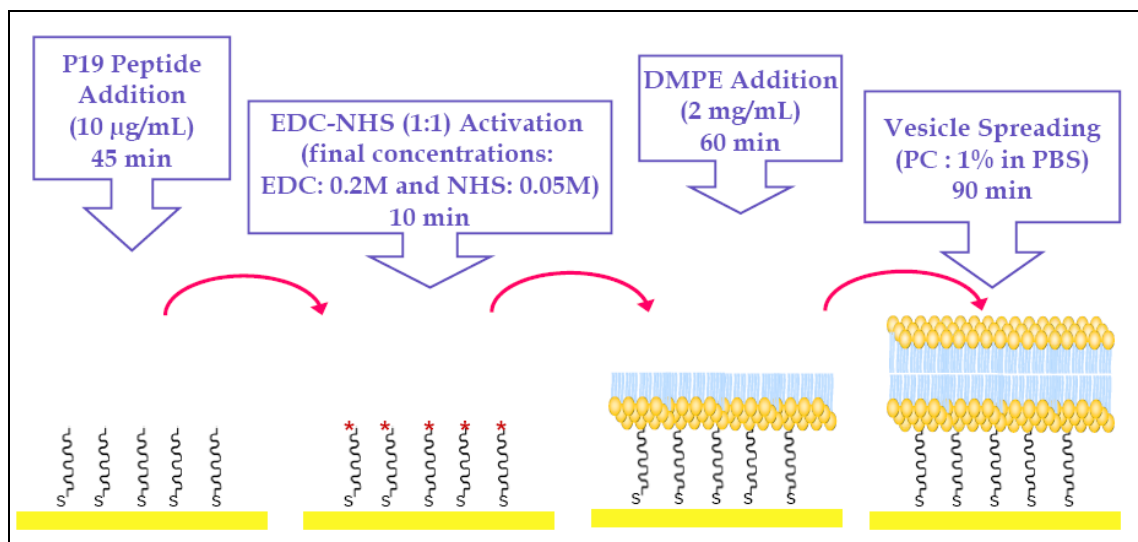


Figure 3.6 Membrane formation steps

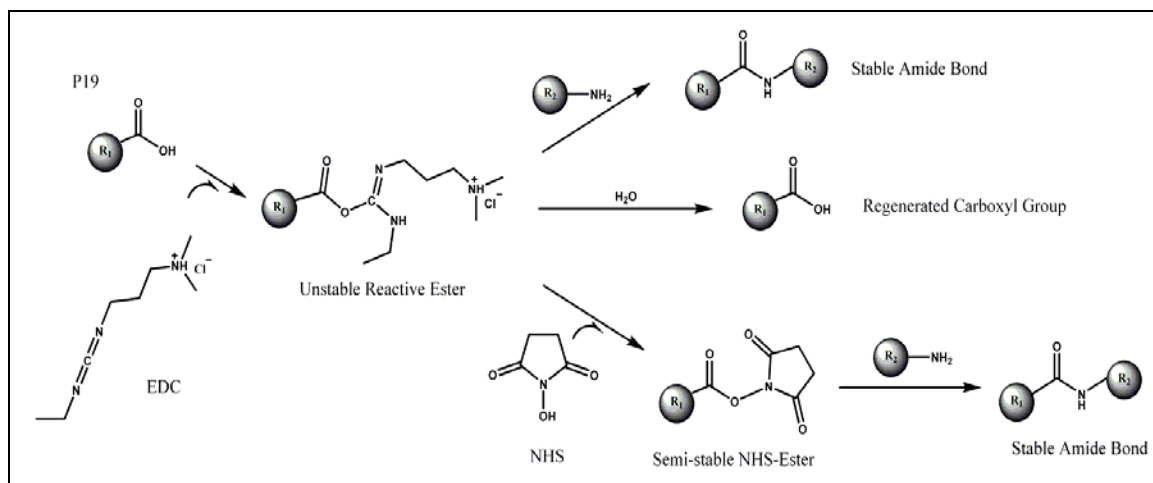


Figure 3.7 Reaction Mechanism for EDC-NHS coupling

3.1.3.1 DMPE Optimization

In this work, DMPE was used mainly as a phospholipid monolayer. The dependency of DMPE:TritonX ratio on the monolayer formation was optimized. Effect of detergent (TritonX) was explored in two different DMPE concentrations. CA results of this optimization were given in Figure 3.8.

Since DMPE is not completely soluble in water, TritonX was used to obtain the highest solubility of DMPE. The highest CA value was measured for DMPE layer when the highest

CHAPTER III : RESULTS & DISCUSSION

TritonX concentration was chosen; however increasing DMPE concentrations did not yield CA values as high as expected. As it was shown in the graph, CA values for 2mg/ml DMPE concentration are higher than 0.2 mg/ml. In other words regarding the standard deviations, obtained CA values are still far from enough hydrophobicity than expected and this may be because of the inhomogeneity of the previous layer or surface. For this reasons 0.2 mg/ml DMPE was used with DMPE:TritonX 2:1 ratio in all experimental procedure. Corresponding CA images are shown in Figure 3.9.

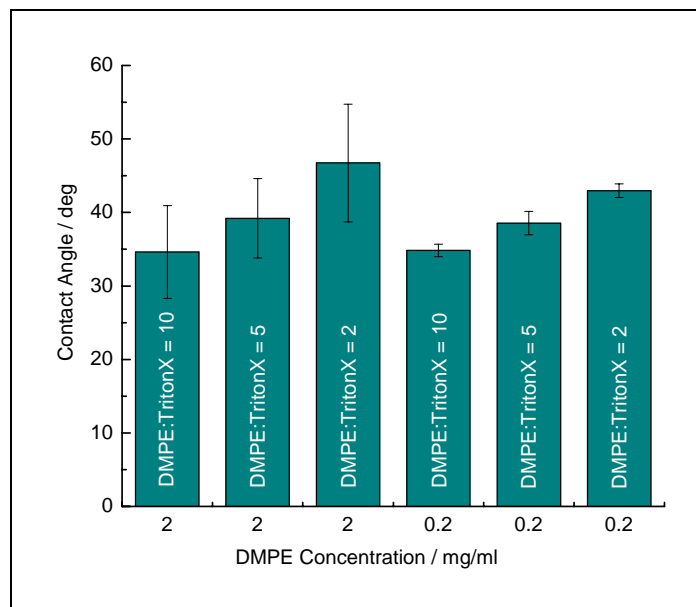


Figure 3.8 Contact Angles of different DMPE:TritonX mixing ratio

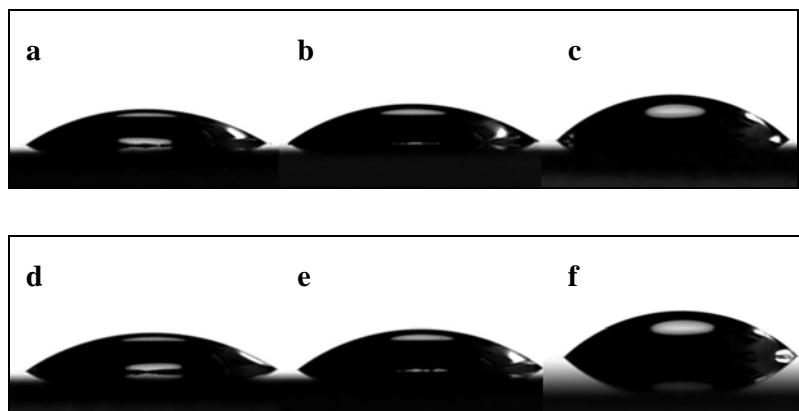


Figure 3.9 CCD images of (a) 2 mg/ml, DMPE:TritonX 10:1, (b) 2 mg/ml, DMPE:TritonX 5:1, (c) 2 mg/ml, DMPE:TritonX 2:1, (d) 0.2 mg/ml, DMPE:TritonX 10:1, (e) 0.2 mg/ml, DMPE:TritonX 5:1, (f) 0.2 mg/ml, DMPE:TritonX 2:1

3.1.3.2 Phospholipid Optimization

Two main issues for monolayer formation were investigated. First how to do the assembly of spacer and the monolayer and second, what is the effect of various phospholipid length and structure on membrane formation. To accomplish this, two different routes were followed; assembly of P19 and phospholipids on the surface which corresponds to the membrane assembly protocol that has been explained in section 2.8.6 and assembly of P19 and phospholipids after EDC-NHS coupling which refers to mix all components beforehand instead of layer by layer assembly. Our main concern was the increase of the hydrophobicity of the monolayer to facilitate vesicle spreading on top of it. In this direction a series of phospholipid structures which was shown in section 2.9, has been examined as well instead of DMPE. This will help to get an insight of the influence of varied structures on membrane formation and how they differ or resemble. CA results have been given in Figure 3.10-Figure 3.13 for all these varied conditions.

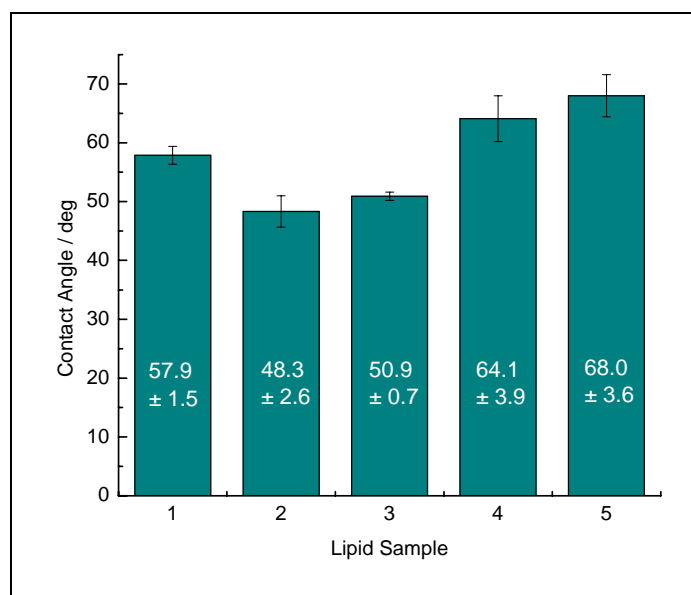


Figure 3.10 Contact Angles of (1)DMPE, (2)DPePE, (3)DPPE, (4)DPalPE, (5)DPhyPE for EDC-NHS coupled samples before assembly

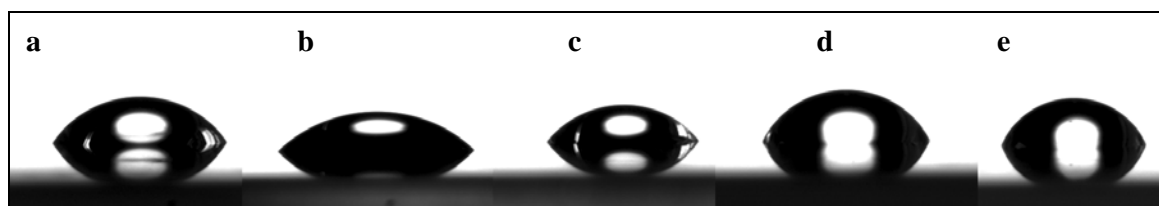


Figure 3.11 CCD images of (a)DMPE, (b)DPePE, (c)DPPE, (d)DPalPE, (e)DPhyPE monolayer for EDC-NHS coupled samples before assembly

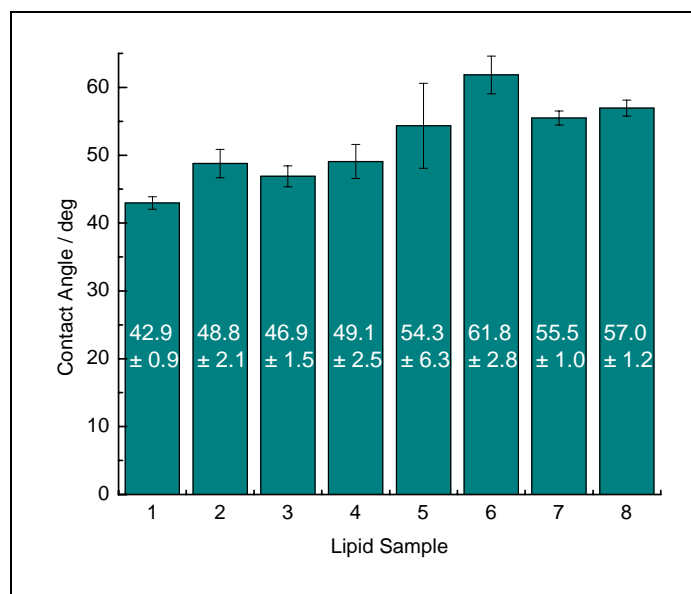


Figure 3.12 Contact Angles of (1)DMPE, (2)DPePE, (3)DPPE, (4)DPalPE, (5)DPhyPE, (6)DLPE, (7)DAPE, (8)DDPE monolayer *via* self assembly

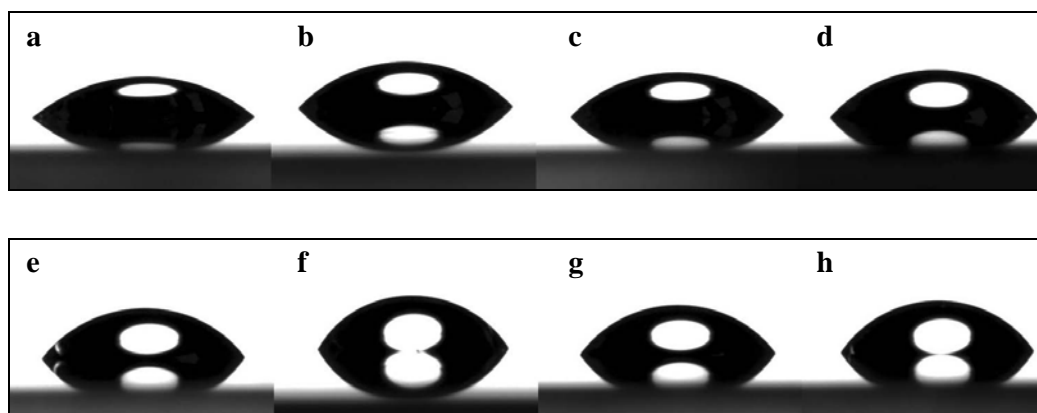


Figure 3.13 CCD images of (a)DMPE, (b)DPePE, (c)DPPE, (d)DPalPE, (e)DPhyPE, (f)DLPE, (g)DAPE, (h)DDPE monolayer *via* self assembly

As it is shown in figures, mixing all components and treating the surface with this mixture (Figure 3.10, Figure 3.11) yields higher CA values with respect to the step by step assembly (Figure 3.12, Figure 3.13) method. However disregarding high CA values, mixing all components beforehand has one crucial drawback; inhomogeneous surface coverage. Since EDC-NHS coupling was done in a test tube *via* mixing it was not easy to control reaction products at the end. Although they produce higher CA values, inhomogeneity on surface is still

an important issue, therefore it relatively shows us this method is not reliable for the formation of artificial membrane structure.

On the other hand, changing the phospholipid structure shows a significant difference in CA values. As predicted, longer alkyl chains, double bonds and branched structures predominantly govern the increase in hydrophobicity. The main challenge for these molecules was solubility and accordingly formation of inhomogeneous surfaces. So, again TritonX was used to solubilize phospholipids and to get rid of excess lipids from the surface flash rinsing was done with ethanol. According to the promising ones, SPR measurements were screened to have a detailed idea about formation of monolayer. These results are going to be presented in the following section together with the bilayer results.

3.1.4 Bilayer Formation

It has been known that for the vesicle fusion monolayer platform must be hydrophobic enough and densely packed. The fusion of a vesicle is assumed to happen step by step; first adhesion of vesicles, than bursting of vesicles and finally spreading of these membrane patches to form a homogeneous layer.

In this study, two different types of lipids were used to form a bilayer. PC was employed since it has been shown that it supplies a suitable environment for the *in-vitro* expression of membrane proteins⁶. In parallel, *E.coli* Total Extract (Avanti Polar Lipids) was examined to compare the effect of a lipid on *in-vitro* expression. Total extract is composed of 57.5% Phosphatidylethanolamine, 15.1% Phosphatidylglycerol, 9.8% Cardiolipin and other lipids. The reason lies behind choosing this lipid was relevant with mimicking the nature. In nature Cyt-bo₃ is a membrane protein which is originating from *E.coli* organism. So with this approach, we tried to have a closer look to the relation in between membrane system and expression system.

For both PC and TE lipids, vesicle solution was prepared as explained before in section 2.8.6 and solution was extruded through 50 nm polycarbonate membrane before injecting to the system. At first, vesicle solutions were examined by dynamic light scattering method to see their exact sizes after extrusion. 2 ml of each vesicle solution were transferred to sample cuvettes and measured at 13 different angles (30°-150°). Data analysis was done by Contin

⁶ Robelek, R., Lemker, E., Wiltshi, B., Kirste, V., Oesterhelt, D., Sinner, E.K., (2007) *Angewandte Chemie-International Edition*, 46(4), 605.

method which yields hydrodynamic radius of PC and TE vesicles 40 and 50 nm respectively. Corresponding distributions of hydrodynamic radius has been shown in Figure 3.14.

Since the light scattering method detects not the geometrical radius but hydrodynamic radius by regarding the contribution of solvent molecules, calculated radius is often larger than the geometrical value. Accordingly PC and TE vesicles might possibly have 10-20 nm lower radii than the measured values.

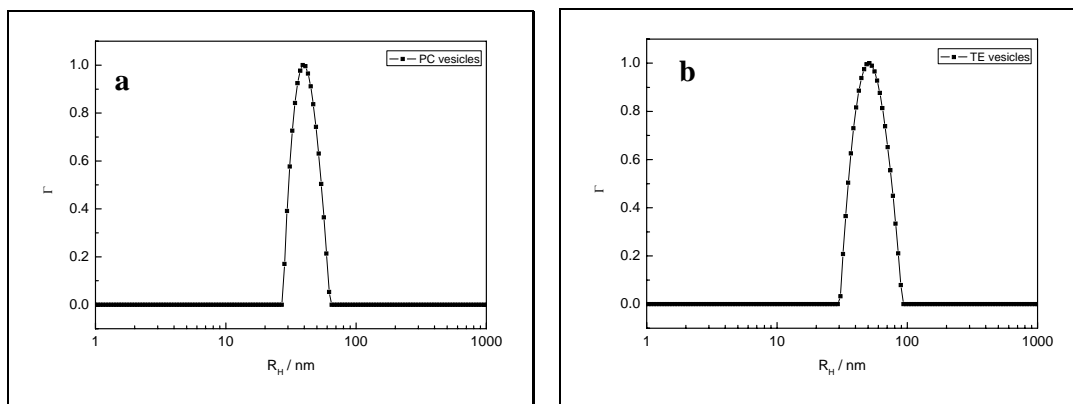


Figure 3.14 Light Scattering data of (a)PC, (b)TE vesicles

CA measurements were not sufficient enough to produce an adequate output about vesicle fusion and bilayer formation since it was not possible to obtain good or homogeneous surface. In order to obtain an idea about thickness of layers and to observe vesicle fusion SPR measurements were carried out. SPR measurement was recorded in kinetic mode to observe new layer addition and vesicle fusion. After kinetic measurements, recording was done in scan mode to obtain thickness of the new layer.

SPR scans are shown in Figure 3.15 which inset graphs represent the kinetic curve of vesicle addition. Fitting parameters for these experimental sets were listed in Table 3.1. Theoretical lengths were determined by Chem3D Ultra 7.0 software in a stretched mode of the molecules. The thickness of the monolayer which has been obtained from fitting data is quite low with respect to the real size of the molecule which indicates the low surface coverage. By the additions of vesicles, 20-22% and 30% reflectivity increases were observed for PC and TE vesicles respectively. Relative to the theoretical values, it seems like a vesicle adsorption has occurred rather than vesicle fusion. AFM results (not shown here) from the very same samples corresponds to partial vesicle adsorption as well. Such results might be attributed to the defects of layer by layer assembled membrane structure. The P19 spacer does not form a dense layer

CHAPTER III : RESULTS & DISCUSSION

on the surface, and therefore DMPE monolayer does not cover the surface completely. This has been observed as a low CA values as well. As a result of this, the monolayer was not hydrophobic enough for vesicle fusion for both PC and TE lipids. In accordance to these findings membrane components might not form completely planar membrane, but they form planar membrane patches together with the adsorbed vesicles in some extent. Obtaining such results cause a motivation to improve the monolayer system.

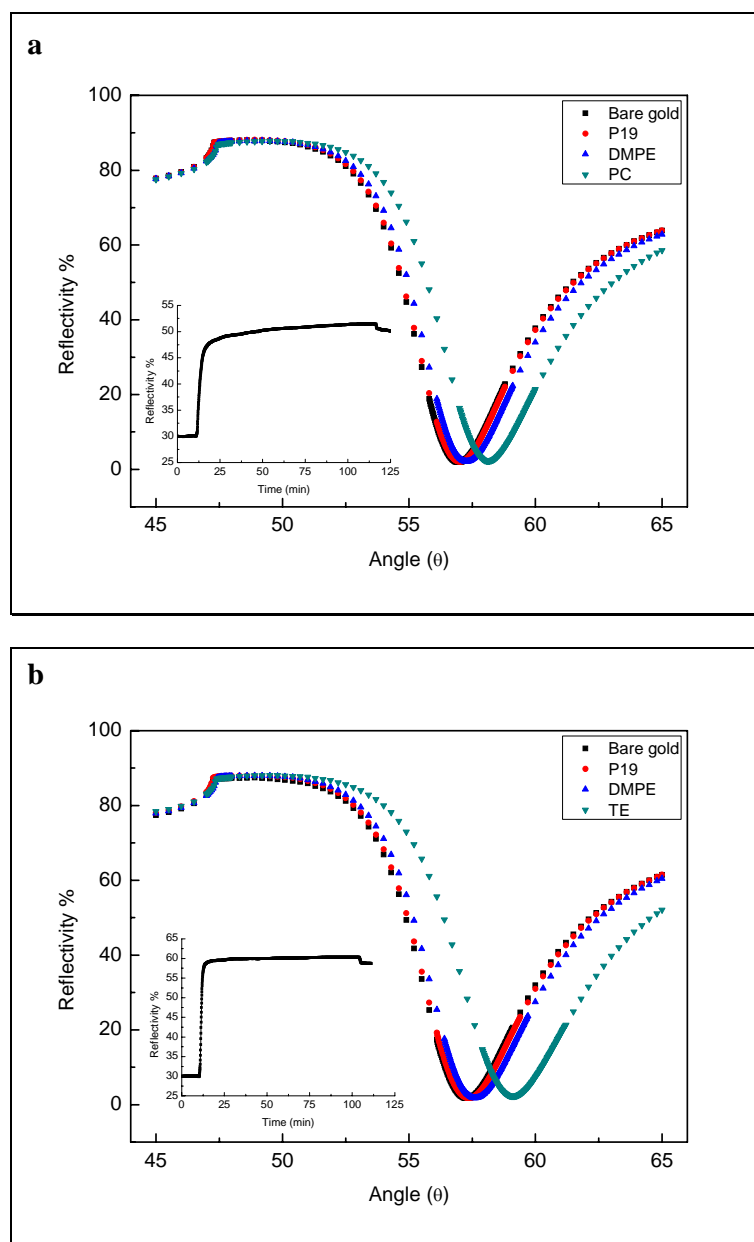
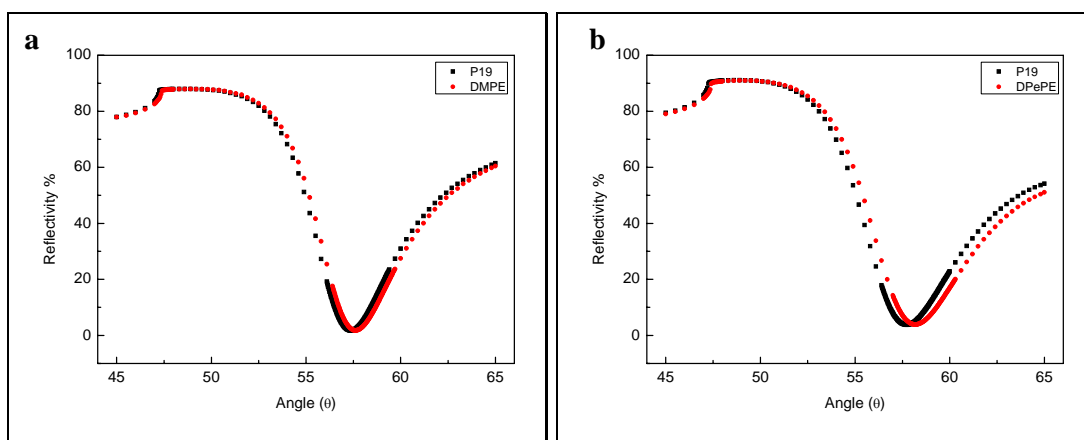


Figure 3.15 SPR data of (a)P19/DMPE/PC, (b)P19/DMPE/TE system

Table 3.1 SPR Fit Parameters

<i>Layer</i>	<i>Material</i>	<i>Refractive Index / n</i>	<i>Adsorption Coefficient</i>	<i>Theoretical thickness (nm)</i>	<i>Calculated thickness (nm)</i>
1	LaSFN9 slide	1.85	-	0 (∞)	-
2	Gold	0.2	3.4	50	48-49
3	air	1	0	0 (∞)	-
4	MilliQ/Buffer	1.3	0	0 (∞)	-
5	P19	1.4	0	1.1	1.09
6	DMPE	1.33	0.22	3.1	0.89
7	PC	1.4	0	4.1	4.18
8	TE	1.4	0	5.5	5.84

To improve the monolayer properties, different structured phospholipids were examined to increase the surface coverage and hydrophobicity of the monolayer. In Figure 3.16 the scan curves of different monolayers and corresponding P19 curves are given. They indicate better surface coverage of monolayer has obtained. Corresponding kinetic curves of these systems for PC vesicle addition are shown in Figure 3.17 and they conclude the fact that longer chains, double bonds or branched structures produce more reasonable results for vesicle fusion in comparison to DMPE layer. The kinetic curve of vesicle fusion seems more likely in the range of typical trend. PC vesicles appear to fuse and bilayer formation can be observed or at least get more oriented and ordered to produce membrane patches rather than vesicle adsorption.



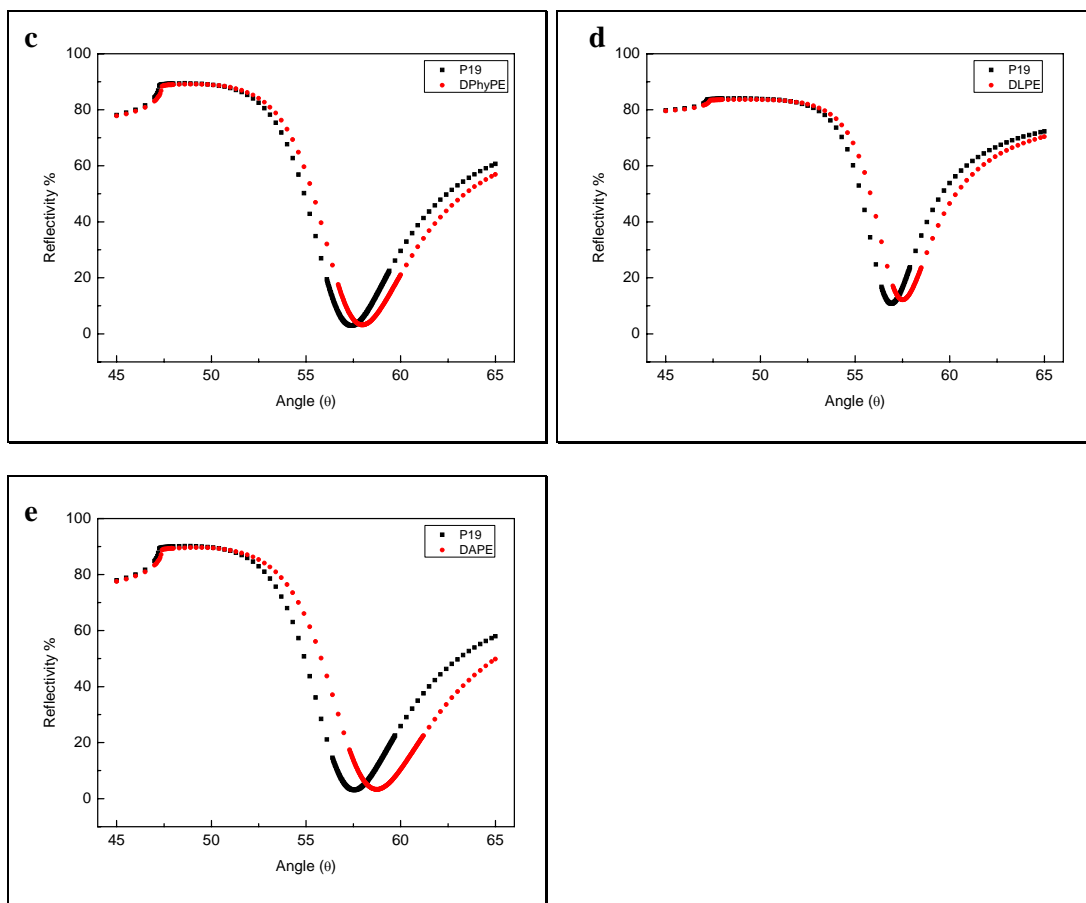


Figure 3.16 SPR data of (a)P19/DMPE, (b)P19/DPePE, (c)P19/DPhyPE, (d)P19/DAPE, (e)P19/DLPE system

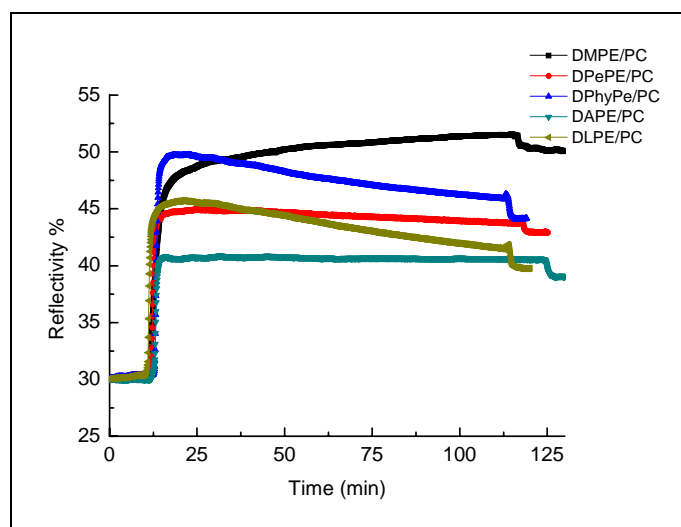


Figure 3.17 SPR kinetic curves of PC vesicle addition

Thickness of simulated monolayer and bilayer is shown in Table 3.2. All fitting values indicate the phospholipid molecules do not attach to the spacer as dense monolayers so do not provide good monolayer. By using longest lipid chain increase the surface coverage was obvious but still was not sufficient enough to have really dense monolayer.

Table 3.2 SPR Fit Parameters of Varied Monolayers

<i>Layer</i>	<i>Material</i>	<i>Refractive Index / n</i>	<i>Adsorption Coefficient</i>	<i>Theoretical thickness (nm)</i>	<i>Calculated thickness (nm)</i>	<i>Bilayer thickness (nm) PC</i>
1	DMPE	1.33	0.2	3.1	0.89	4.18
2	DPePE	1.33	0.2	3.3	0.21	5.15
3	DPhyPE	1.33	0.2	3.5	0.78	4.58
4	DLPE	1.33	0.2	3.9	0.63	5.02
5	DAPE	1.33	0.2	4.3	1.78	4.2

3.1.5 Conclusion of Membrane Construction

In this chapter a quick investigation of a membrane system was done. From the scientific point of view, it was necessary to understand the properties of different membrane systems and components. tBLM formation was investigated using different membrane components and applying different procedures. Obtained monolayers *via* self assembly, yield in quite low CA values. Dense bilayer structures could not be obtained as well, since hydrophobicity of the monolayer was quite low for vesicle fusion. None of these monolayers represent perfect monolayer properties.

These results may show that these molecules might not be the best candidate to construct perfect membrane architecture, nevertheless the right balance in between high packing and good fluidity of a membrane is a prerequisite for insertion of proteins. At the very beginning of this work a quick investigation which was not shown in here, but was done for Cyt-bo₃ and it presented that insertion of this protein does not happen when we use perfect membrane structure. However after membrane formation it is important to confirm whether this membrane is able to carry inserted protein in an active state. So this project was carried on with P19/DMPE/PC and P19/DMPE/TE systems, in the next chapters we present the insertion and *in-vitro* expression results.

3.2 Plasmid DNA Overview

The strains to be used have been summarized in Table 2.1. pJRHisA and pRCO3 were constructed by J. N. Rumbley and pETcyo was constructed by L. L. Yap. Further details of cloning procedure can be found in corresponding references. In Figure 3.18 *cyo* operon is given in detail which containing *cyoA* encoding subunit II, *cyoB* encoding subunit I, *cyoC* encoding subunit III, *cyoD* encoding subunit IV and *cyoE* encoding farnesyl transferase.

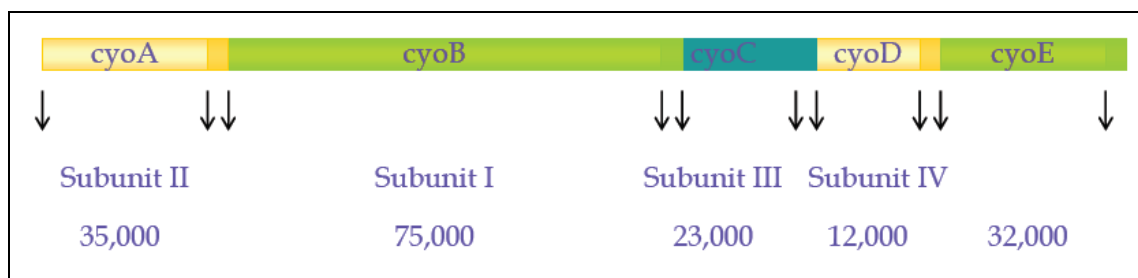


Figure 3.18 *cyo* operon containing *cyoA*, encoding subunit II, *cyoB*, encoding subunit I, *cyoC*, encoding subunit III, *cyoD*, encoding subunit IV, and *cyoE*, encoding a farnesyl transferase.

Farnesyl Transferase (FR) adds a farnesyl group to proteins carrying a four-amino acid at the carboxyl terminus (C-terminus). *cyoE* operon which encodes FR, is responsible for the conversion of HemeB to HemeO. Possible Heme structures⁷ which have been found in cytochrome derivatives are give in Figure 3.19.

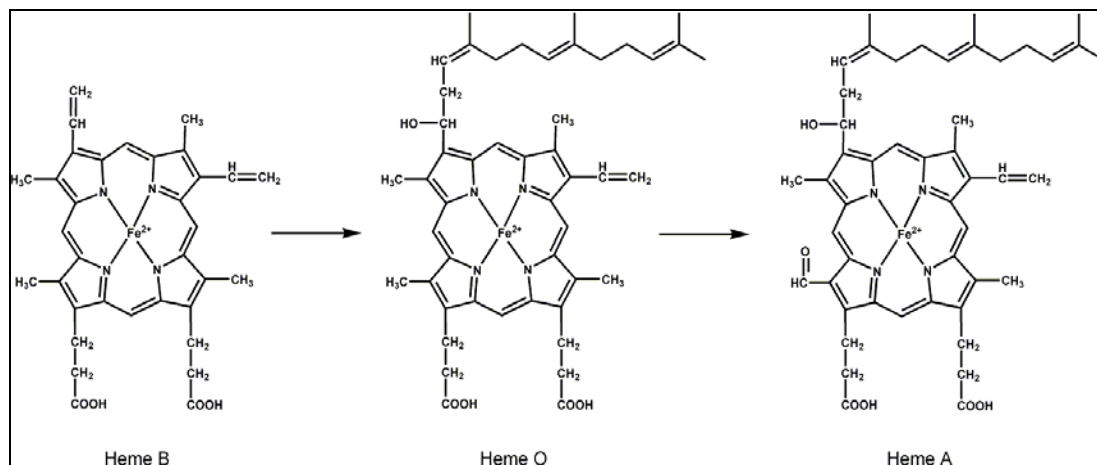


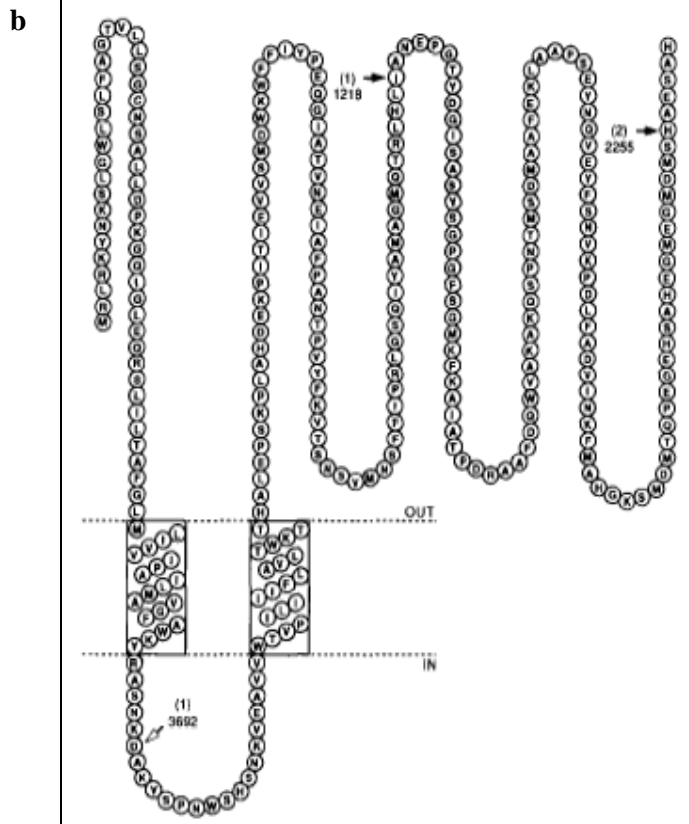
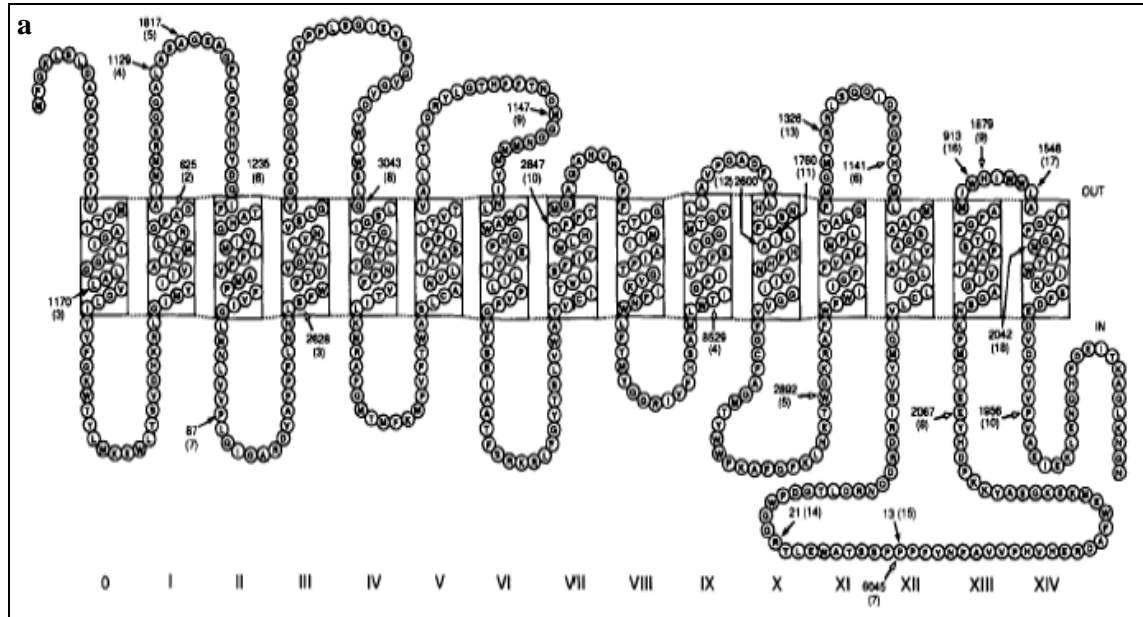
Figure 3.19 Conversion scheme for HemeB to HemeO and HemeA⁸

⁷ Tsubaki, M., Mogi, T., Hori, H., Hirota, S., Ogura, T., Kitagawa, T., Anraku, Y., (1994) J. Biol. Chem, 269, 30861.

⁸ Morrison, S.M., Cricco, J.A., Hegg, E.L., (2005) Biochemistry, 44, 12554.

CHAPTER III : RESULTS & DISCUSSION

pJRHSA plasmid which encodes the *cyoABCDE* operon express the wild type Cyt-*b*₀3 with 6xHis tag on the C-terminus of subunitII. Proposed topological models for each subunit were shown in Figure 3.20.



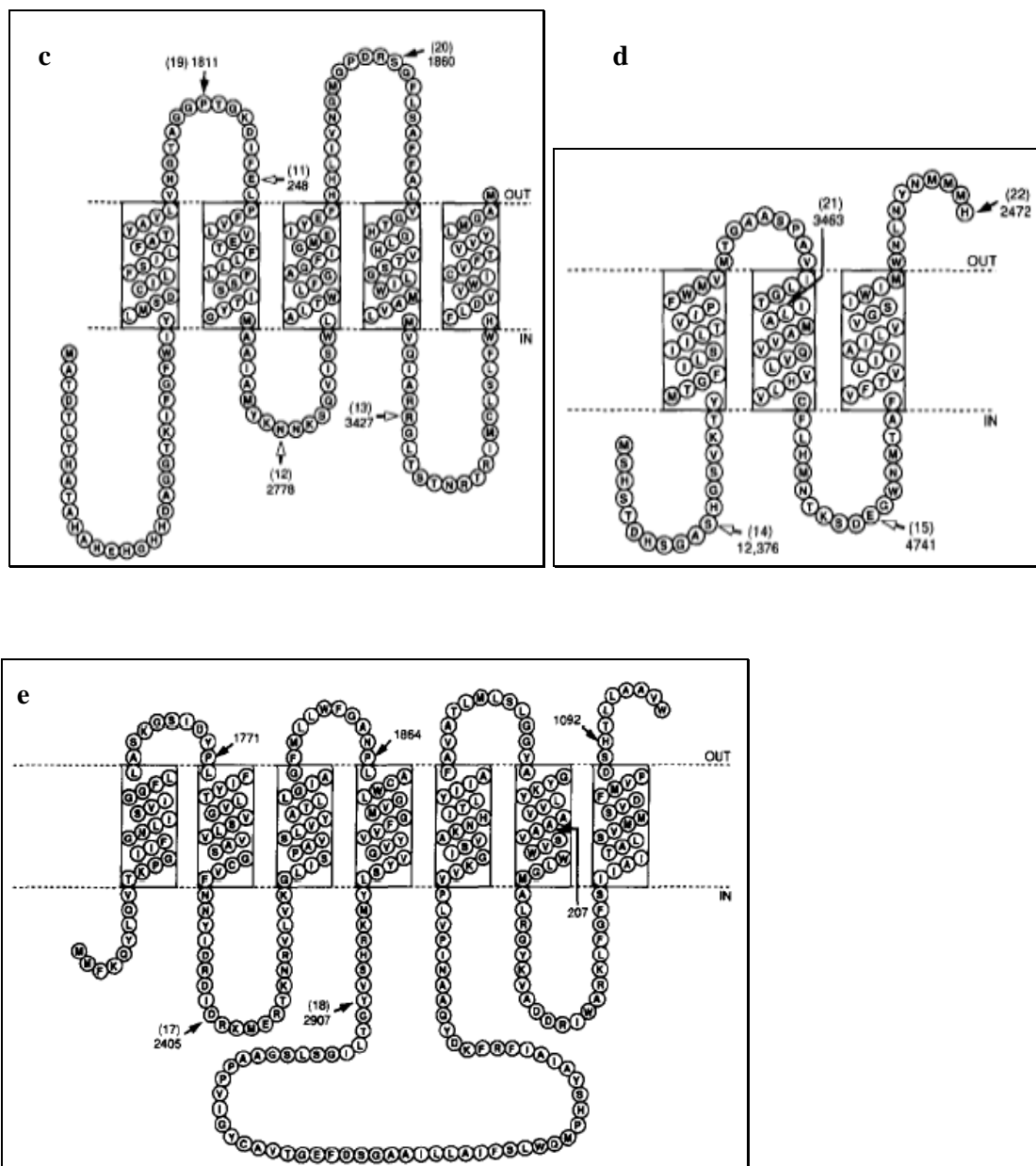


Figure 3.20 Topological models of (a)subunit I, (b)subunit II, (c)subunit III, (d)subunit IV, of *E.coli* Cyt-bo₃ and (e)cyoE encoding polypeptide⁹

⁹ Chepuri, V., Gennis, R.B., (1990) The Journal of Biological Chemistry, 265, 22, 12978.

CHAPTER III : RESULTS & DISCUSSION

Vector map of pJRHisA which has been obtained from Rumbley, J.N. and depicted cartoon is given in Figure 3.21.

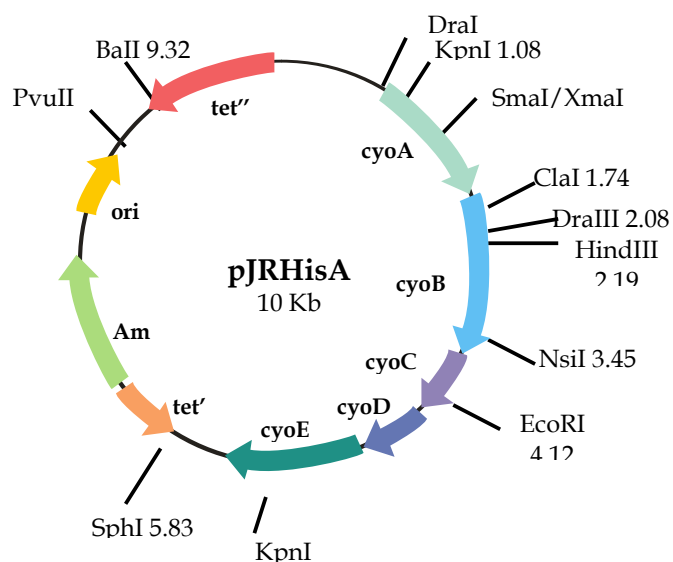
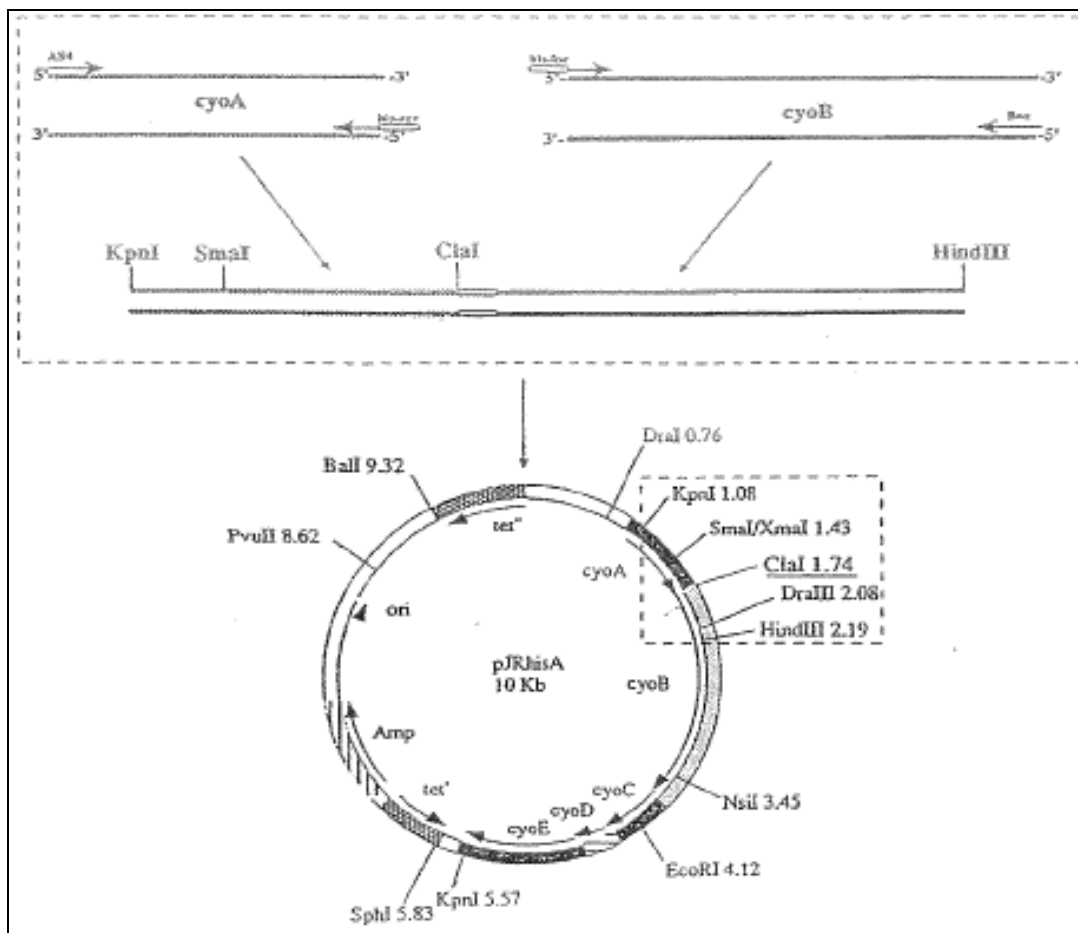


Figure 3.21 Vector map of pJRHisA plasmid

CHAPTER III : RESULTS & DISCUSSION

Another construct, pRCO₃ plasmid was used to compare the effect of different structures on *in-vitro* synthesis. This plasmid encodes *cyoA*, *cyoB* and *cyoC* respectively in a row which means there is a fusion in between *cyoA* and *cyoB* and another fusion in between *cyoB* and *cyoC*. It was shown before by Gennis Group this genetic fusion (II-I-III) resulted in an active oxidase. Vector map of pRCO₃ is given in Figure 3.22 and the proposed topological model for this oxidase was shown in .

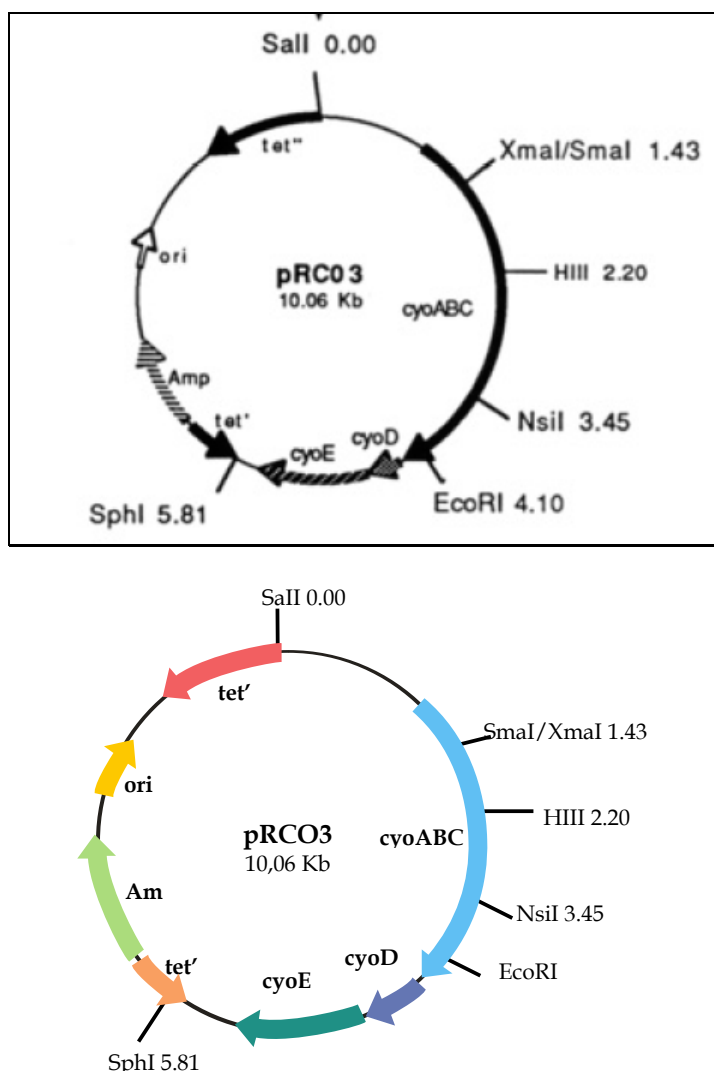


Figure 3.22 Vector map of pRCO₃ plasmid that contains fused genes

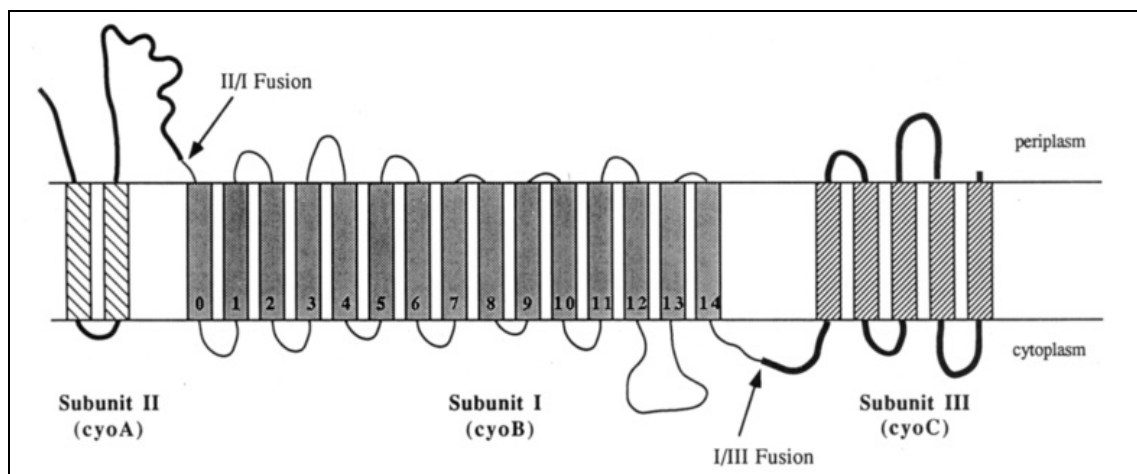


Figure 3.23 Membrane topology of fused subunits II, I, III for Cyt-bo₃

The third plasmid of this study was pETcyo plasmid which the *cyo* operon subcloned into inducible pET17b vector (Novagen). Complete *cyo* operon was cloned from pJRHSA originally which encodes the wild type Cyt-bo₃ with 6xHis affinity tag on the C-terminus of subunit II. The most important point of newly cloned plasmid is T7 promoter part which is coming from commercial pET17b vector. Vector map of pETcyo is given in Figure 3.24 and topology of the protein is supposed to be the same with Figure 3.20.

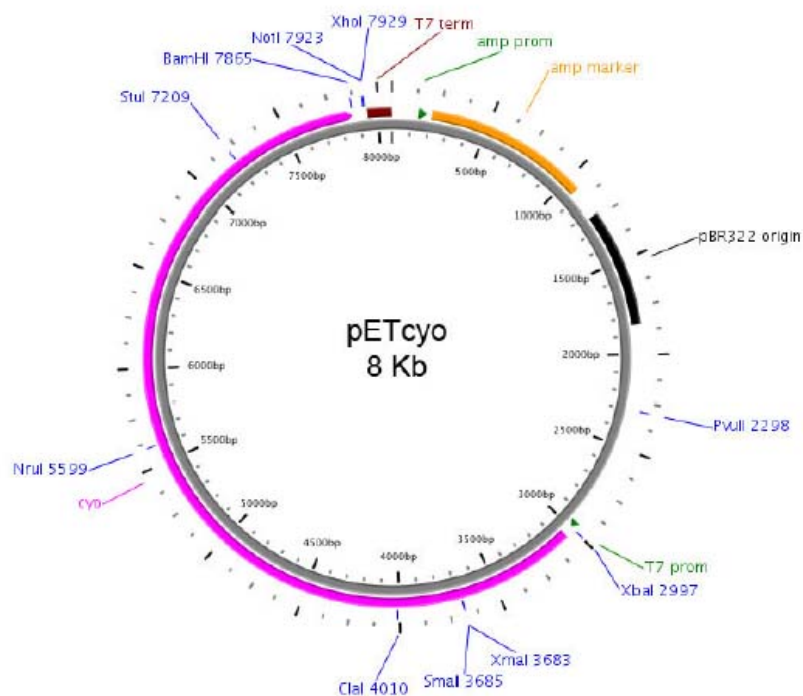


Figure 3.24 Vector map of pETcyo plasmid

CHAPTER III : RESULTS & DISCUSSION

Complete DNA sequence of *Cyt-bo₃* which is encoded by *cyo* operon was given in Figure 3.25. Starting from bp 3047-4015 (322aa), bp 4037-6028 (663aa), bp 6018-6632 (204aa), bp 6632-6961 (109aa), bp 6973-7863 (298aa) correspond to *cyoA*, *cyoB*, *cyoC*, *cyoD* and *cyoE* respectively.

1	TTCTGAAGA	CGAAAGGGCC	TCGTGATACG	CCTATTTTTA	TAGGTTAATG	TCATGATAAT
61	AATGGTTTCT	TAGACGTCAG	GTGGCACTTT	TCGGGGAAAT	GTGCGCGGAA	CCCCTATTTG
121	TTTATTTTTC	TAAATACATT	CAAATATGTA	TCCGCTCATG	AGACAATAAC	CCTGATAAAT
181	GCTTCAATAA	TATTGAAAAA	GGAAGAGTAT	GAGTATTCAA	CATTTCCTGT	TCGCCCTTAT
241	TCCCTTTTTT	GCGGCATTTT	GCCTTCCTGT	TTTTGCTCAC	CCAGAAACGC	TGGTGAAAGT
301	AAAAGATGCT	GAAGATCAGT	TGGGTGCACG	AGTGGGTTAC	ATCGAACTGG	ATCTCAACAG
361	CGGTAAGATC	CTTGAGAGTT	TTCCGCCCGA	AGAACGTTTT	CCAATGATGA	GCACTTTTAA
421	AGTTCTGCTA	TGTGGCGCGG	TATTATCCCG	TGTTGACGCC	GGGCAAGAGC	AACTCGGTCC
481	CCGCATACAC	TATTCTCAGA	ATGACTTGGT	TGAGTACTCA	CCAGTCACAG	AAAAGCATCT
541	TACGGATGGC	ATGACAGTAA	GAGAATTATG	CAGTGCTGCC	ATAACCATGA	GTGATAACAC
601	TGCGGCCAAC	TTACTTCTGA	CAACGATCGG	AGGACCGAAG	GAGCTAACCG	CTTTTTTGCA
661	CAACATGGGG	GATCATGTAA	CTCGCCTTGA	TCGTTGGGAA	CCGAGACTGA	ATGAAGCCAT
721	ACCAAACGAC	GAGCGTGACA	CCACGATGCC	TGCAGCAATG	GCAACAACGT	TGCGCAAAC
781	ATTAACGGC	GAACACTTAA	CTCTAGCTTC	CCGGCAACAA	TTAATAGACT	GGATGGAGGC
841	GGATAAAGTT	GCAGGACCAC	TTCTGCGCTC	GGCCCTTCCG	GCTGGCTGGT	TTATTGCTGA
901	TAAATCTGGA	GCCGGTGAGC	GTGGGTCTCG	CGGTATCATT	GCAGCACTGG	GGCCAGATGG
961	TAAGCCCTCC	CGTATCGTAG	TTATCTACAC	GACGGGGAGT	CAGGCAACTA	TGGATGAACG
1021	AAATAGACAG	ATCGCTGAGA	TAGGTGCCTC	ACTGATTAAG	CATTGGTAAC	TGTCAGACCA
1081	AGTTTACTCA	TATATACTTT	AGATTGATTT	AAAACCTCAT	TTTTAATTTA	AAAGGATCTA
1141	GGTGAAGATC	CTTTTTGATA	ATCTCATGAC	CAAAATCCCT	TAACGTGAGT	TTTCGTTCCA
1201	CTGAGCGTCA	GACCCCGTAG	AAAAGATCAA	AGGATCTTCT	TGAGATCCTT	TTTTTCTGCG
1261	CGTAATCTGC	TGCTTGCAAAA	CAAAAAAACC	ACCGCTACCA	GCGGTGGTTT	GTTTGCCGGA
1321	TCAAGAGCTA	CCAACCTTTT	TTCCGAAGGT	AACTGGCTTC	AGCAGAGCGC	AGATACCAAA
1381	TACTGTCCTT	CTAGTGTAGC	CGTAGTTAGG	CCACCACTTC	AAGAACTCTG	TAGCACCGCC
1441	TACATACCTC	GCTCTGCTAA	TCCTGTTACC	AGTGGCTGCT	GCCAGTGGCG	ATAAGTCGTG
1501	TCTTACCGGG	TTGGACTCAA	GACGATAGTT	ACCGGATAAG	GCGCAGCGGT	CGGGCTGAAC
1561	GGGGGGTTCC	TGCACACAGC	CCAGCTTGGG	GCGAACGACC	TACACCGAAC	TGAGATACCT
1621	ACAGCGTGAG	CTATGAGAAA	GCGCCACGCT	TCCCGAAGGG	AGAAAGGCGG	ACAGGTATCC
1681	GGTAAGCGGC	AGGGTCGGAA	CAGGAGAGCG	CACGAGGGAG	CTTCCAGGGG	GAAACGCTCG
1741	GTATCTTTAT	AGTCCTGTCG	GGTTTCGCCA	CCTCTGACTT	GAGCGTCGAT	TTTTGTGATG
1801	CTCGTCAGGG	GGGCGGAGCC	TATGAAAAAA	CGCCAGCAAC	GCGGCCTTTT	TACGGTTTCT
1861	GGCCTTTTGC	TGGCCTTTTG	CTCACATGTT	CTTTCCTGCG	TTATCCCTCG	ATTCTGTGGA
1921	TAACCGTATT	ACCGCCTTTG	AGTGAGCTGA	TACCGCTCGC	CGCAGCCGAA	CGACCGAGCC
1981	CAGCGAGTCA	GTGAGCGAGG	AAGCGGAAGA	GCGCCTGATG	CGGTATTTTC	TCCTTACGCA
2041	TCTGTGCGGT	ATTTCACACC	GCATATATGG	TGCACTCTCA	GTACAATCTG	CTCTGATGCC
2101	GCATAGTTAA	GCCAGTATAC	ACTCCGCTAT	CGCTACGTGA	CTGGGTCATG	GCTGCGCCCC
2161	GACACCCGCC	AACACCCGCT	GACGCGCCCT	GACGGGCTTG	TCTGCTCCCG	GCATCCGCTT
2221	ACAGACAAGC	TGTGACCGTC	TCCGGGAGCT	GCATGTGTCA	GAGGTTTTCA	CCGTCATCAC
2281	CGAAACGCGC	GAGGCAGCTG	CGGTAAAGCT	CATCAGCGTG	GTCGTGAAGC	GATTACAGA
2341	TGTCTGCCTG	TTCATCCGCG	TCCAGCTCGT	TGAGTTTCTC	CAGAAGCGTT	AATGTCTGGC
2401	TTCTGATAAA	GCGGGCCATG	TTAAGGGCGG	TTTTTTCCTG	TTTGGTCACT	GATGCCTCCG
2461	TGTAAGGGGG	ATTCTGTGTT	ATGGGGGTAA	TGATACCGAT	GAAACGAGAG	AGGATGCTCA
2521	CGATACGGGT	TACTGATGAT	GAACATGCC	GGTACTGGA	ACGTTGTGAG	GGTAAACAAC
2581	TGGCGGTATG	GATGCGGCGG	GACCAGAGAA	AAATCACTCA	GGGTCAATGC	CAGCGCTTCG
2641	TTAATACAGA	TGTAGGTGTT	CCACAGGGTA	GCCAGCAGCA	TCCTGCGATG	CAGATCCGGA
2701	ACATAATGGT	GCAGGGCGCT	GACTTCCGCG	TTTCCAGACT	TTACGAAACA	CGGAAACCGA
2761	AGACCATTCA	TGTTGTTGCT	CAGGTCGCAG	ACGTTTTGCA	GCAGCAGTCG	CTTACGTTTC
2821	GCTCGCGTAT	CGGTGATTCA	TTCTGCTAAC	CAGTAAGGCA	ACCCCGCCAG	CCTAGCCGGG

CHAPTER III : RESULTS & DISCUSSION

2881	TCCTCAACGA	CAGGAGCACG	ATCATGCGCA	CCCGTGGCCA	GGACCCAACG	CTGCCCGAGA
2941	TCTCGATCCC	GCGAAATTAA	TACGACTCAC	TATAGGGAGA	CCACAACGGT	TTCCCTCTAG
3001	AAATAATTTT	GTTTAACTTT	AAGAAGGAGA	TATACATATG	GCTAGCATGA	GACTCAGGAA
3061	ATACAATAAA	AGTTTGGGAT	GGTTGTCAAT	ATTTGCAGGC	ACTGTATTGC	TCAGTGGCTG
3121	TAATTCTGCG	CTGTTAGATC	CCAAAGGACA	GATTGGTCTG	GAGCAACGTT	CACTGATACT
3181	GACGGCATT	GGCCTGATGT	TGATTGTCTG	TATCCCGCA	ATCTTGATGG	CTGTTGGTTT
3241	CGCCTGGAAG	TACCGTGCGA	GCAATAAAGA	TGCTAAGTAC	AGCCCCAACT	GGTCACACTC
3301	CAATAAAGTG	GAAGCTGTGG	TCTGGACGGT	ACCTATCTTA	ATCATCATCT	TCCTTGCACT
3361	ACTGACCTGG	AAAACCACTC	ACGCTCTTGA	GCCTAGCAA	CCGCTGGCAC	ACGACGAGAA
3421	GCCCATTACC	ATCGAAGTGG	TTCCATGGA	CTGGAATGG	TTCTTCATCT	ACCCGGAACA
3481	GGGCATTGCT	ACCGTGAATG	AAATCGCTTT	CCCGGCGAAC	ACTCCGGTGT	ACTTCAAAGT
3541	GACCTCCAAC	TCCGTGATGA	ACTCCTTCTT	CATTCCGCGT	CTGGGTAGCC	AGATTTATGC
3601	CATGGCCGGT	ATGCAGACTC	GCCTGCATCT	GATCGCCAAC	GAACCCGGCA	CTTATGACGG
3661	TATCTCCGCC	AGCTACAGCG	GCCCGGGCTT	CTCAGGCATG	AAGTTCAAAG	CTATTGCAAC
3721	ACCGGATCGC	GCCGCATTCC	ACCAGTGGGT	CGCAAAAGCG	AAGCAGTCGC	CGAACACCAT
3781	GTCTGACATG	GCTGCGTTCG	AAAACTGGC	CGCGCCTAGC	GAATACAACC	AGGTGGAATA
3841	TTTCTCCAAC	GTGAAACCAG	ACTTGTTCG	CGATGTAATT	AACAAGTTTA	TGGCTCACGG
3901	TAAGAGCATG	GACATGACCC	AGCCAGAAGG	TGAGCACAGC	GCACACGAAG	GTATGGAAGG
3961	CATGGACATG	AGCCACGCGG	AATCCGCCCA	TCACCATCAC	CATCACCATC	GATAAAGGGG
4021	TTGAGGAAGA	ATAAAGATGT	TCGGAAAATT	ATCACTTGAT	GCAGTCCCGT	TCCATGAACC
4081	TATCGTCATG	GTTACGATCG	CTGGCATTAT	TTTGGGAGGT	CTGGCGCTCG	TTGGCCTGAT
4141	CACTTACTTC	GGTAAGTGG	CCTACCTGTG	GAAAGAGTGG	CTGACCTCCG	TCGACCATAA
4201	ACGCCTCGGT	ATCATGTATA	TCATCGTGGC	GATTGTGATG	TTGCTGCGTG	GTTTTGCTGA
4261	CGCCATTATG	ATGCGTAGCC	AGCAGGCTCT	TGCCTCGGCG	GGCGAAGCGG	GCTTCCTGCC
4321	ACCTCACCAC	TACGATCAGA	TCTTTACCGC	GCACGGCGTG	ATTATGATCT	TCTTCGTAGC
4381	GATGCCTTTC	GTTATCGGTC	TGATGAACCT	GGTGGTTCCG	CTGCAGATCG	GC CGCGTGA
4441	CGTTGCGTTC	CCGTTCTCA	ACAACCTAAG	CTTCTGGTTT	ACCGTTGTTG	GTGTGATTCT
4501	GGTTAACGTT	TCTCTCGGCG	TGGGCGAATT	TGCGCAGACC	GGCTGGCTGG	CCTATCCACC
4561	GCTATCGGGA	ATAGAGTACA	GTCCGGGAGT	CGGTGTCGAT	TACTGGATAT	GGAGTCTCCA
4621	GCTATCCGGT	ATAGGTACGA	CGCTTACCGG	TATCAACTTC	TTCGTTACCA	TTCTGAAGAT
4681	GCGCGCACCG	GGCATGACCA	TGTTCAAGAT	GCCAGTATTT	ACCTGGGCAT	CACTGTGCGC
4741	GAACGTAATG	ATTATTGCTT	CCTTCCCAAT	TCTGACGGTT	ACCGTCGCGT	TGTTGACCCT
4801	GGATCGCTAT	CTGGGCACCC	ATTTCTTTAC	CAACGATATG	GGTGGCAACA	TGATGATGTA
4861	CATCAACCTG	ATTTGGGCCCT	GGGGCCACCC	GGAAGTTTAC	ATCCTGATCC	TGCCTGTTTT
4921	CGGTGTGTTT	TCCGAAATTG	CGGCAACCTT	CTCGCGTAAA	CGTCTGTTTG	GTTATACCTC
4981	GCTGGTATGG	GCAACCGTCT	GTATCACCGT	GCTGTGCTTC	ATCGTTTGGC	TGCACCACTT
5041	CTTTACGATG	GGTGCGGGCG	CGAACGTAAT	CGCCTTCTTT	GGTATCACCA	CAATGATTAT
5101	CGCCATCCCG	ACCGGGGTGA	AGATCTTCAA	CTGGCTGTTT	ACCATGTATC	AGGGCCGCAT
5161	CGTGTTCAT	TCTGCGATGC	TGTGGACCAT	CGTTTTTATC	GTCACCTTCT	CGGTGGGCGG
5221	GATGACTGGC	GTGCTGCTGG	CCGTACCGGG	CGCGGACTTC	GTTCTGCATA	ACAGCCTGTT
5281	CCTGATTGCG	CACTTCCATA	ACGTGATCAT	CGCGGCGTG	GTCTTCGGCT	GCTTCGAGG
5341	GATGACCTAC	TGGTGGCCTA	AAGCGTTCGG	TTTCAAACCTG	AACGAAACCT	GGGGTAAACG
5401	CGCGTTCG	TTCTGGATCA	TCGGCTTCTT	CGTTGCCTTT	ATGCCACTGT	ATGCGCTGGG
5461	CTTCATGGGC	ATGACCCGTC	GTTTGAGCCA	GCAGATTGAC	CCGCAGTTCC	ACACCATGCT
5521	GATGATTGCA	GCCAGCGGTG	CAGTACTGAT	TGCGCTGGGT	ATTCTCTGCC	TCGTTATTCA
5581	GATGTACGTT	TCTATTGCGG	ACCGCGACCA	GAACCGTGAC	CTGACTGGCG	ACCCGTGGGG
5641	TGGCCGTACG	CTGGAGTGGG	CAACCTCTTC	CCCGCCTCCG	TTCTATAACT	TTGCCGTAGT
5701	GCCGCACGTT	CACGAACGTG	ATGCATTCTG	GGAAATGAAA	GAGAAAGGCG	AAGCGTATAA
5761	AAAGCCTGAC	CACTATGAAG	AAATTCATAT	GCCGAAAAAC	AGCGGTGCAG	GTATCGTCAT
5821	TGCAGCTTTC	TCCACCATCT	TCGGTTTCGC	CATGATCTGG	CATATCTGGT	GGCTGGCGAT
5881	TGTTGGCTTC	GCAGGCATGA	TCATCACCTG	GATCGTGAAT	AGCTTCGACG	AGGACGTGGA
5941	TACTACGTG	CCGGTGGCAG	AAATCGAAAA	ACTGGAAAAAC	CAGCATTTCC	ATGAGATTAC
6001	TAAGGCAGGG	CTGAAAAATG	GCAACTGATA	CTTTGACGCA	CGCGACTGCC	CACGCGCACG
6061	AACACGGGCA	CCACGATGCA	GGCGGAACCA	AAATCTTCGG	ATTTTGGATC	TACCTGATGA
6121	GCGACTGCAT	TCTGTTCTCT	ATCTTGTTCG	CTACCTATGC	CGTTCTGGTG	AACGGCACCG

CHAPTER III : RESULTS & DISCUSSION

6181	CAGGCGGCC	GACAGGTAAG	GACATTTTCG	AACTGCCGTT	CGTTCTGGTT	GAAACTTTCT
6241	TGCTGTTGTT	CAGCTCCATC	ACCTACGGCA	TGGCGGCTAT	CGCCATGTAC	AAAAACAACA
6301	AAAGCCAGGT	TATCTCCTGG	CTGGCGTTGA	CCTGGTTGTT	TGGTGCCGGA	TTTATCGGGA
6361	TGGAAATCTA	TGAATTCCAT	CACCTGATTG	TTAACGGCAT	GGGTCCGGAT	CGCAGCGGCT
6421	TCCTGTCAGC	GTTCTTTGCG	CTGGTCGGCA	CGCACGGTCT	GCACGTCACT	TCTGGTCTTA
6481	TCTGGATGGC	GGTGCTGATG	GTGCAAATCG	CCCGTCGCGG	CCTGACCAGC	ACTAACCCTA
6541	CCCGCATCAT	GTGCCTGAGC	CTGTTCTGGC	ACTTCCTGGA	TGTGGTTTGG	ATCTGTGTGT
6601	TCACTGTTGT	TTATCTGATG	GGGGCGATGT	AATGAGTCAT	TCTACCGATC	ACAGCGGCGC
6661	GTCCCATGGC	AGCGTAAAAA	CCTACATGAC	AGGCTTTATC	CTGTGCATCA	TTCTGACGGT
6721	GATTCCGTTT	TGGATGGTGA	TGACAGGAGC	TGCCTCTCCG	GCCGTAATTC	TGGGAACAAT
6781	CCTGGCAATG	GCAGTGGTAC	AGGTTCTGGT	GCATCTGGTG	TGCTTCTGTC	ACATGAATAC
6841	CAAATCAGAT	GAAGGCTGGA	ACATGACGGC	GTTTGTCTTC	ACCGTGCTAA	TCATCGCTAT
6901	CCTGGTTGTA	GGCTCCATCT	GGATTATGTG	GAACCTCAAC	TACAACATGA	TGATGCACTA
6961	AGAGCGGCGG	TTATGATGTT	TAAGCAATAC	CTGCAAGTAA	CGAAACCAGG	CATCATCTTT
7021	GGCAACCTGA	TCTCGGTGAT	TGGGGGATTC	CTGCTGGCCT	CAAAGGGCAG	CATTGATTAT
7081	CCCCTGTTTA	TCTACACGCT	GGTTGGGGTG	TCACTGGTTG	TGGCGTCGGG	TTGTGTGTTT
7141	AACAACATA	TCGACAGGGA	TATCGACAGA	AAGATGGAAA	GGACGAAGAA	TCGGGTGCTG
7201	GTGAAAGGCC	TGATCTCTCC	TGCTGTCTCG	CTGGTGTACG	CCACGTTGCT	GGGTATTGCT
7261	GGCTTTATGC	TGCTGTGGTT	TGGCGCGAAT	CCGCTGGCCT	GCTGGCTGGG	GGTGATGGGC
7321	TTTGTTGTTT	ATGTCGGCGT	TTATAGCCTG	TACATGAAAC	GCCACTCTGT	CTACGGCAGC
7381	TTGATTGGTT	CGCTCTCCGG	CGCTGCGCCG	CCGGTGATCG	GCTACTGTGC	GGTAACCGGT
7441	GAGTTCGATA	GCGGCGCAGC	GATCCTGCTG	GCTATCTTCA	GCCTGTGGCA	GATGCCTCAC
7501	TCCTATGCCA	TCGCCATTTT	CCGCTTTAAG	GATTACCAGG	CGGCAAACAT	TCCGGTATTG
7561	CCAGTGGTAA	AAGGCATTTT	GGTGGCGAAG	AATCACATCA	CGCTGTATAT	CATCGCCTTT
7621	GCCGTTGCCA	CGCTGATGCT	CTCTCTTGGC	GGTTACGCTG	GGTATAAATA	TCTGGTGGTC
7681	GCCGCGGCGG	TTAGCGTCTG	GTGGTTAGGT	ATGGCTCTGC	GCGGTTATAA	AGTTGCTGAT
7741	GACAGAATCT	GGGCGCGCAA	GCTGTTCCGC	TTCTCTATCA	TCGCCATCAC	TGCCCTCTCG
7801	GTGATGATGT	CCGTTGATTT	TATGGTACCG	GACTCGCATA	CGCTGCTGGC	TGCTGTGTGG
7861	TAAGGATCCA	CTAGTAACGG	CCGCCAGTGT	GCTGGAATTC	TGCAGATATC	CATCACACTG
7921	GCGGCCGCTC	GAGCAGATCC	GGCTGCTAAC	AAAGCCCGAA	AGGAAGCTGA	GTTGGCTGCT
7981	GCCACCGCTG	AGCAATAACT	AGCATAACCC	CTTGGGGCCT	CTAAACGGGT	CTTGAGGGGT
8041	TTTTTGCTGA	AAGGAGGAAC	TATATCCGGA	TAA		

Figure 3.25 Nucleotide sequence of *cyo* operon

3.3 Plasmid Extraction for *in-vitro* Expression and General Analysis

3.3.1 Cell growth for Plasmid DNA Isolation

As it has been explained in section 2.2, special media components were used for the growth of *E.coli* cells carrying pJRH_{isA}, pRCO₃ and pET_{cyo} plasmids. It was shown before pJRH_{isA} and pRCO₃ media which is supplemented with additional salts and trace metals, yields high quality enzyme in comparison to simple LB media. It was observed that cells start to form aggregates with the high salt concentration, so it is necessary to grow them in a good aerated media and never lower than 200rpm shaking rate. This aggregation behavior of the cells were detected instead the typical tumbling behavior of the cells *via* fluorescence microscope (Olympus IX70) with a 100x magnification, sampling was done directly from overnight culture. Microscope images of cells in LB media and high salt containing media

were given in Figure 3.26. For further applications; 250-500ml culture pellet was used for plasmid extraction and for His-tag protein purification *via* Ni-NTA affinity system. For the preparation of cytoplasmic membrane samples generally 6-10L culture pellet was used, since it has been reported before at a number of points cell lysis was observed during the progress and it cause to decrease in the yield.

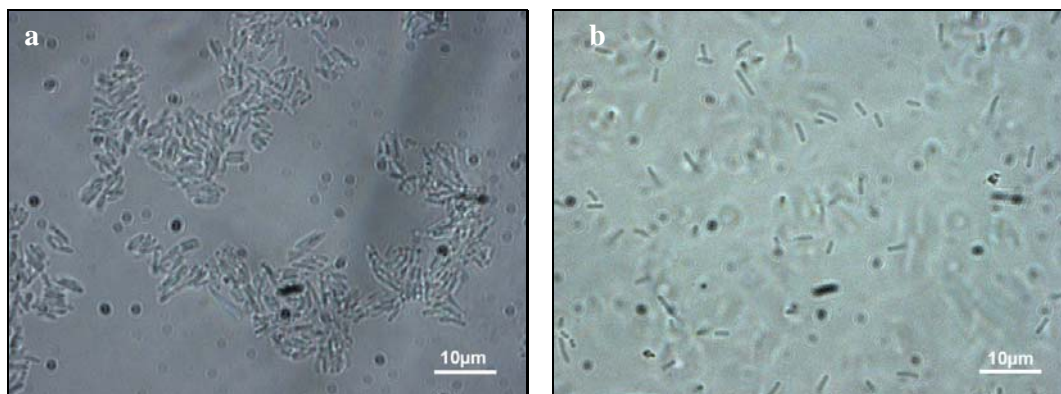


Figure 3.26 Microscope images of *E.coli* cells in (a)pJRHSA media with aggregates appearing during cultivation, (b)LB media

Regarding to the cells carrying pETcyo plasmid, as it was explained before cells were grown in M63 minimal media and over-expression of protein was done *via* IPTG induction. For the plasmid extraction cells were grown in LB media without and induction and 250-500ml of cell pellet was used for plasmid extraction. IPTG induction only done on case of protein purification and 1-2L of cell pellet was used for protein purification. Compared to the pJRHSA strain, pETcyo carrying cells produce high amount of active protein depending on IPTG induction. Result will be given in numbers in the following sections.

3.3.2 Isolation of Plasmid DNA

Plasmid extraction was done by using PureYield Plasmid Midiprep, Promega. Used maximum culture volume was 500ml. Ethanol precipitation was performed after plasmid extraction to increase the quality and the concentration of the plasmid, since concentration and purity of the plasmid DNA is a crucial point for *in-vitro* synthesis.

The DNA concentration was determined by optical density measurement at 260nm directly after plasmid extraction and ethanol precipitation (see Table 3.3). A_{260} / A_{280} ratio corresponds to protein contamination and A_{260} / A_{230} ratio corresponds to other contaminants

CHAPTER III : RESULTS & DISCUSSION

such as carbohydrates, peptides, organic compounds, etc. Theoretical values for a pure plasmid DNA solution with low organic contamination is shown in the same table as well.

Table 3.3 Plasmid DNA concentrations

<i>Sample</i>	<i>Culture volume</i>	<i>Concentration (µg/µl)</i>	A_{260} / A_{280}	A_{260} / A_{230}
Theoretical	-	-	$1.7 < A_{260} / A_{280} \leq 2.0$	$A_{260} / A_{230} > 2.0$
pJRHisA	100ml	0.220	1.42	2.30
pJRHisA (EtOH precipitated)		0.490	1.49	2.20
pRCO ₃	100ml	0.215	1.82	2.13
pETcyo	250ml	0.106	1.82	1.57
pETcyo (EtOH precipitated)		0.356	1.82	1.69

3.3.3 Gel Electrophoresis Analysis

Isolated plasmid DNA samples were tested for their content and size *via* gel electrophoresis. Plasmid DNA samples were digested with corresponding restriction enzymes (see section 2.3.4). This digestion control allows us to monitor isolation products in a linear form and to provide a convenient comparison in between experimental and theoretical data.

Isolated and digested pJRHisA plasmid samples gave positive results in comparison with literature data, shown in Figure 3.27. A 20 kb band was observed for the isolated sample which corresponds to double and engaged 10 kb circular DNA structure. After double digestion with EcoRI and ClaI 8.0 and 2.5 bands were observed which fits directly with theoretical values.

Figure 3.28 shows gel electrophoresis results for pRCO₃ plasmid DNA samples. Two different concentrations were used and a broad band was observed in between 10-20 kb region which presumably coming from engaged and circular DNA mixture. EcoRI digestion was performed for each sample and 10 kb band was observed coming from linear pRCO₃ plasmid.

Gel electrophoresis analysis was performed containing various digestion samples of pETcyo plasmid. A 20kb band was observed again for the circular plasmid and other bands clearly indicate the digestion products of the same plasmid. Different restriction enzymes were used for controlling the pETcyo plasmid. Gel electrophoresis image of pETcyo which contains

CHAPTER III : RESULTS & DISCUSSION

many samples was given in Figure 3.29. Band intensities were varied depending on the sample concentration and digestion efficiency.

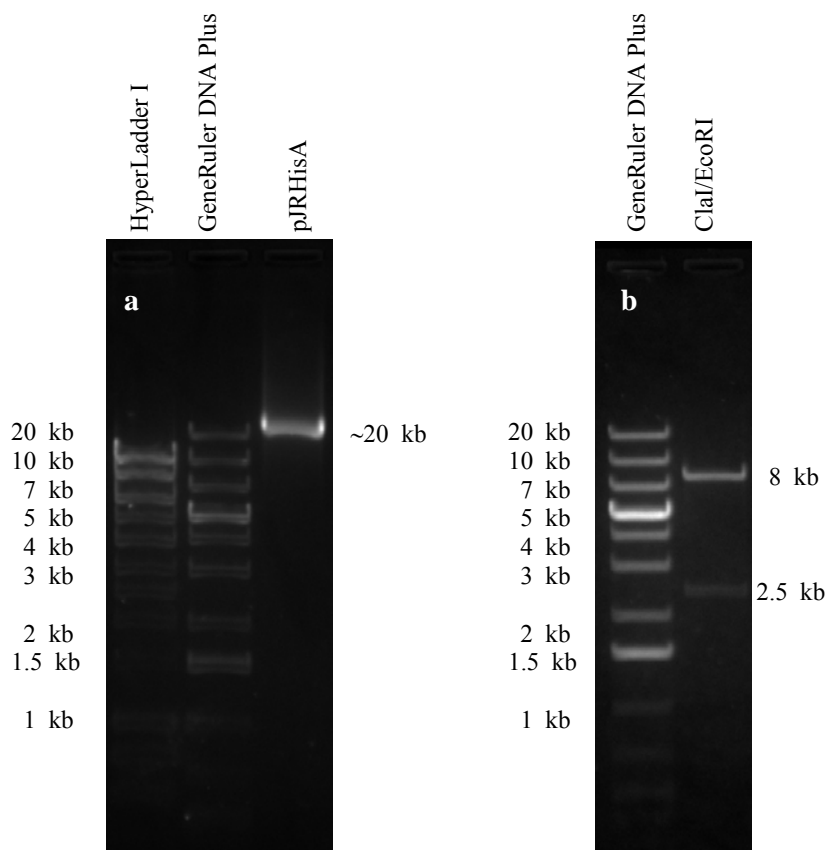


Figure 3.27 Gel electrophoresis analysis of pJRHisA plasmid (a) circular DNA, (b) double digest with ClaI/EcoRI

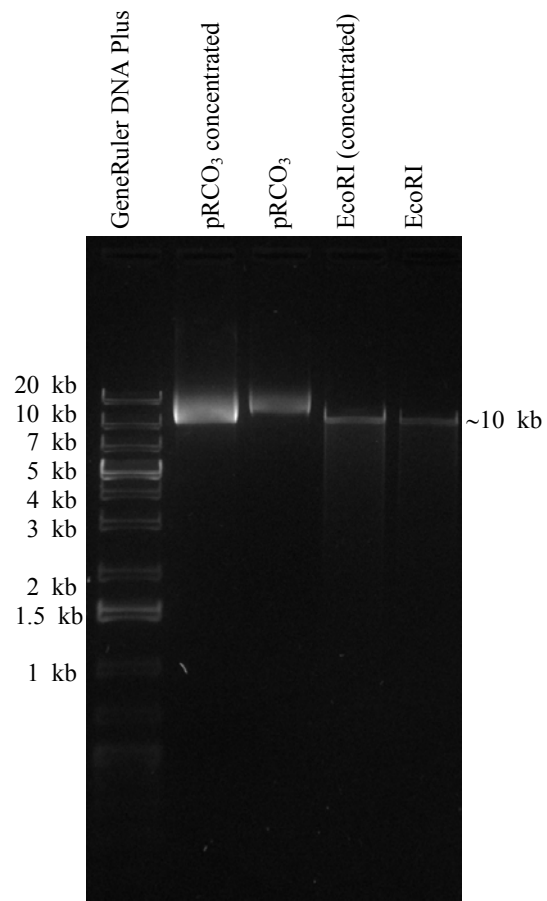


Figure 3.28 Gel electrophoresis analysis of pRCO₃ plasmid

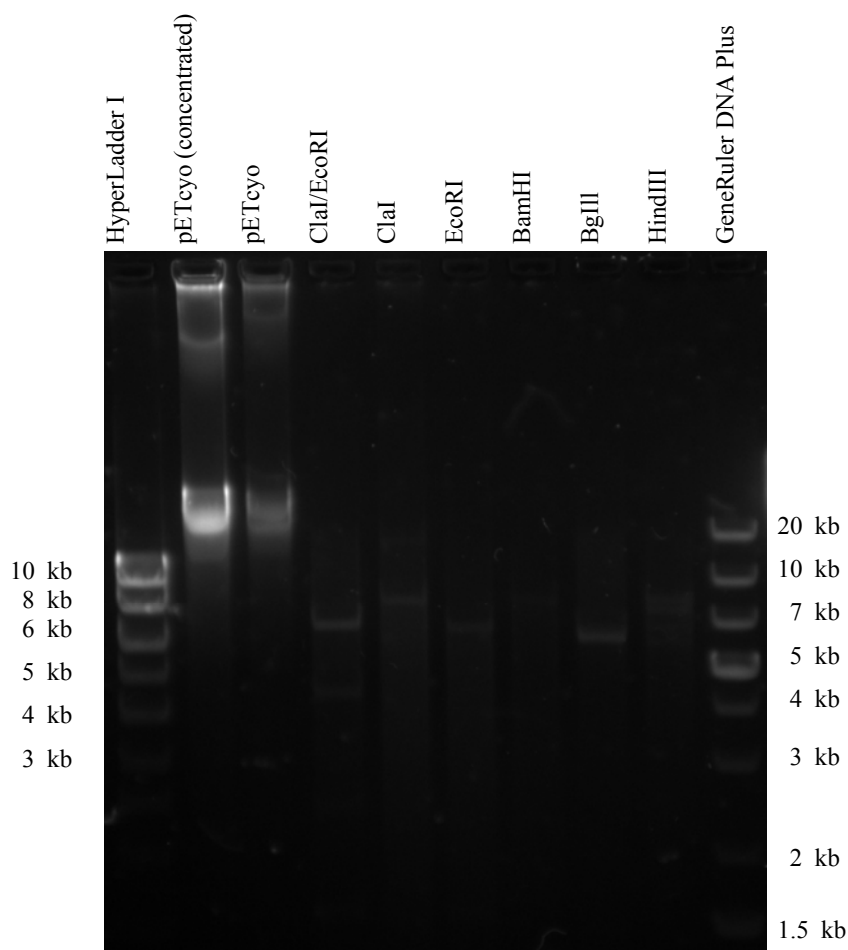


Figure 3.29 Gel electrophoresis analysis of pETcyo plasmid

3.4 Purification of Histidine Tagged Cytochrome *bo*₃ Ubiquinol Oxidase

3.4.1 Isolation of Histidine Tagged Cytochrome *bo*₃

pETcyo clone was cultured, roughly prepared and tested for the expression of Cyt-*bo*₃ by western blot analysis after IPTG induction. After IPTG induction, the expression levels were observed for different time periods and best expression time period was chosen for the purification of Cyt-*bo*₃. 1ml cell culture was collected hourly during 4 hours directly from culture media and cell pellets were treated in a same way as explained before in section 2.6, gel was run directly with these samples. Western blot and Coomassie Blue results were given in Figure 3.30, a band was observed at around 33kDa which corresponds to subunit II of Cyt-*bo*₃ and it has been clearly shown at a time period t=4 (4 hours) expression level was the highest.

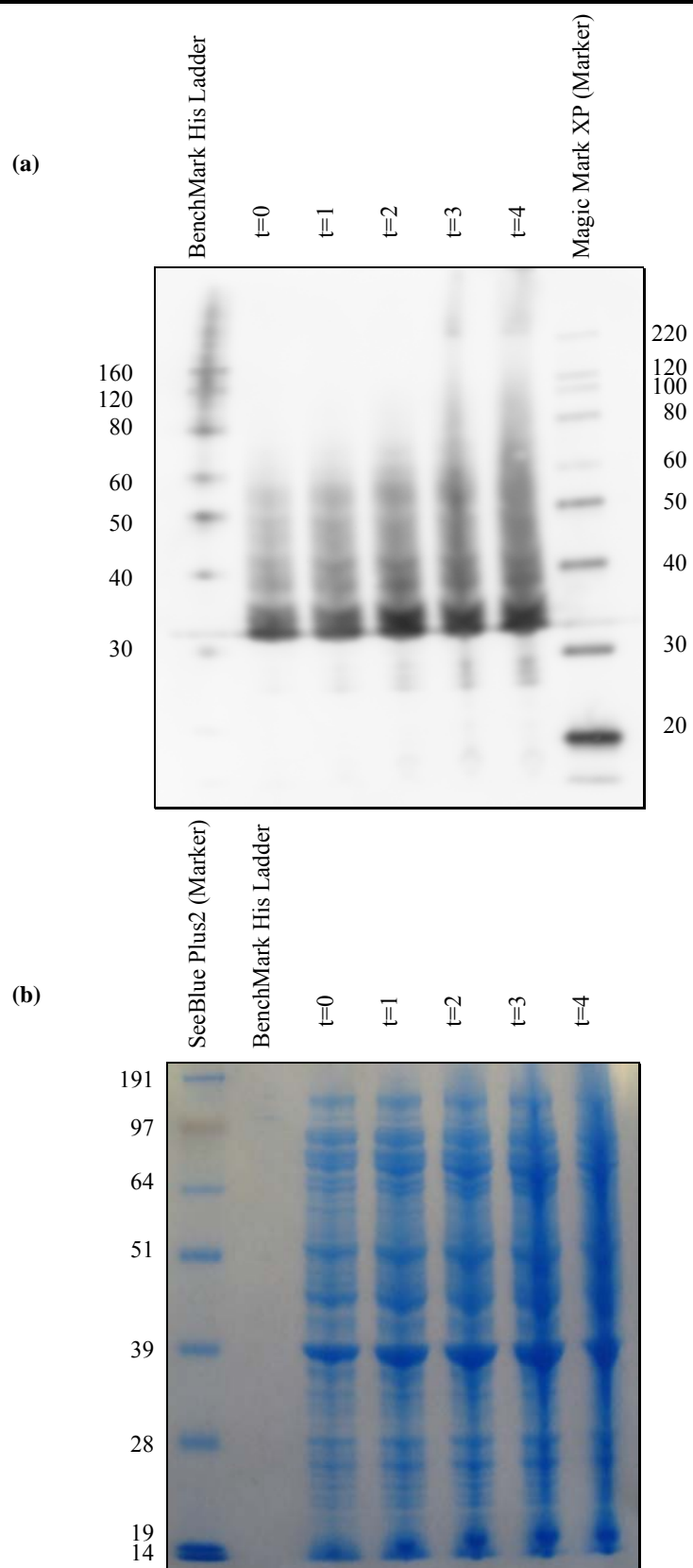


Figure 3.30 (a)Western blotting, (b)Coomassie Blue staining results of pETcyo cell pellets for IPTG induction (NuPAGE®Novex 10% Bis-Tris gel, 200V, 50 min, MOPS Buffer, PVDF membrane, WesternBreeze® Chemiluminescent Anti-mouse kit)

CHAPTER III : RESULTS & DISCUSSION

Histidine tagged Cyt-bo₃ enzyme was purified based on affinity chromatography by using Qiagen Ni-NTA kit and column. Final protein samples were characterized *via* immuno blotting technique and the protein concentration was determined *via* BCA Protein Analysis.

Native and denaturing purification protocols were performed separately as explained in the manual for each 250ml cell culture pellets carrying either pJRHSA or pETcyo strains. Protein purification steps and yield was followed by Western blot and Coomassie Blue staining. Results of purified Cyt-bo₃ were presented in Figure 3.31 and Figure 3.32 for pJRHSA carrying cells and for the pETcyo carrying cells results were given in Figure 3.33 and Figure 3.34.

Single band ~35kDa which corresponds to subunit II of Cyt-bo₃ was detected under Native conditions and double band 33-35kDa was seen for pJRHSA carrying cells under Denaturing conditions, the lower band representing the C-terminal cleavage product. This result has a good agreement with the previous reports¹⁰, subunit II of Cyt-bo₃ is a lipoprotein which means there is a signaling peptide sequence at the N-terminus of subunit II. Reported data shows that the size of subunit II is around 35kDa and without the signaling peptide part, it is around 33kDa. Therefore obtained results reveal considerable similarity with previous reports under two different preparation conditions. Under native purification conditions, signaling peptide was not chopped off, so by applying this purification protocol only a single band of Cyt-bo₃ was observed at 35kDa. On the other hand, under denaturing conditions double band was observed since pH of elution buffer was really low and it facilitates the cleavage of signaling peptide part. Although Coomassie Blue staining did not produce sharp and clearly visible bands for both native and denaturing protocols, separation of desired protein was clearly displayed in each step. In parallel to Coomassie Blue results, highest band intensity was observed at the first elution step. Protein yield was roughly measured *via* BCA Protein Assay and results were given in Table 3.4. Reduced minus oxidized spectra did not produce any meaningful result hence purified protein concentration was low to detect *via* that method as it was also not clearly seen in the Coomassie gel.

Results were quite different for the pETcyo carrying cells. Nearly same trend, cleavage of subunit II, was observed in western blot results as well. The main difference was double band feature was observed for both under Native and Denaturing conditions. Another crucial thing is third band was detected at ~27-28kDa for this clone. This corresponds to another

¹⁰ Ma, J., Katsonouri, A., Gennis, R. B., (1997) Biochemistry, 36,11298.

CHAPTER III : RESULTS & DISCUSSION

cleavage of N-terminus after cleavage of signaling peptide and chopped sequence assumed to be the outer part of the membrane protein depending on heavy proteolysis during purification treatments. Removal of signaling peptide part was speculated as a post-translational modification rather than proteolytic digestion so it was also known that this process does not affect the functionality of enzyme. But in this case this fraction of the purified enzyme might not show proper enzyme activity.

Again separation of the enzyme from the cell mixture was clearly displayed and highest intensity was observed for the first elution step. Although IPTG induction enhances the expression of protein thus resulting protein concentration of pETcyo clone was higher than pJRHisA clone, still yield was quite low for the Coomassie Blue detection and reduced minus oxidized spectra. Hence BCA protein assay was used to determine the yield of purified protein samples as well. Results were presented in Table 3.4.

Table 3.4 Cyt-bo₃ concentrations, determined *via* BCA Assay

<i>Sample</i>	<i>Culture volume (ml)</i>	<i>Concentration ($\mu\text{g}/\mu\text{l}$)</i>
pJRHisA/Native	250	1103 (± 30)
pJRHisA/Denaturing	250	147 (± 10)
pETcyo/Native	250	1600 (± 30)
pETcyo/Denaturing	250	1840 (± 40)

Ni-NTA affinity chromatography was inadequate method for the purification of pRCO₃ carrying cells because of the fact that this clone of Cyt-bo₃ does not have an affinity tag. So in this case purification¹¹ and detection¹² of the protein is quite difficult and even impossible. Meaningful results could not be obtained from pRCO₃ clone for the *in-vivo* expression and purification of Cyt-bo₃.

¹¹ Lemieux, L. J., Calhoun, M. W., Thomas, J. W., Ingledew, W. J., Gennis, R. B., (1992) The Journal of Biological Chemistry, 267, 3, 2105.

¹² Ma, J., Lemieux, L., Gennis, R. B., (1993) Biochemistry, 32, 7692.

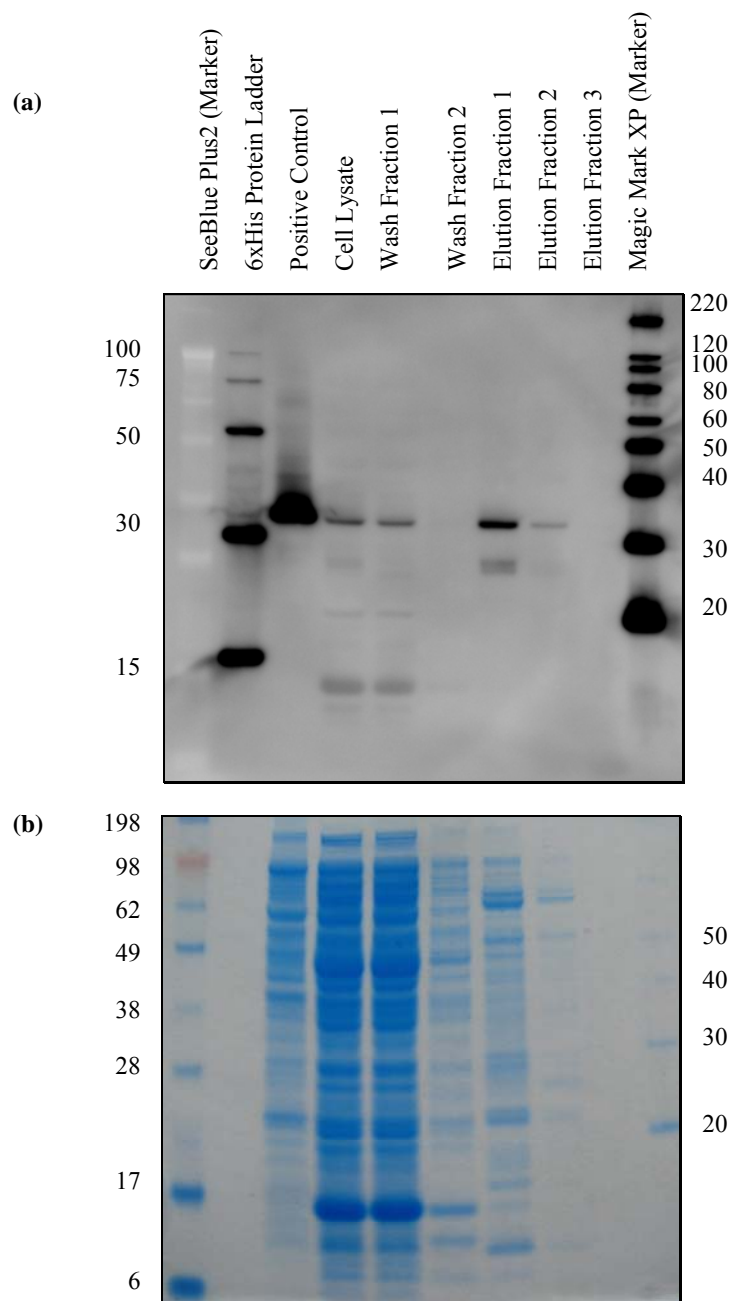


Figure 3.31 (a)Western blotting, (b)Coomassie Blue staining results of pJRHisA under Native purification conditions (NuPAGE®Novex 10% Bis-Tris gel, 200V, 35min, MES Buffer, PVDF membrane, WesternBreeze® Chemiluminescent Anti-mouse kit)

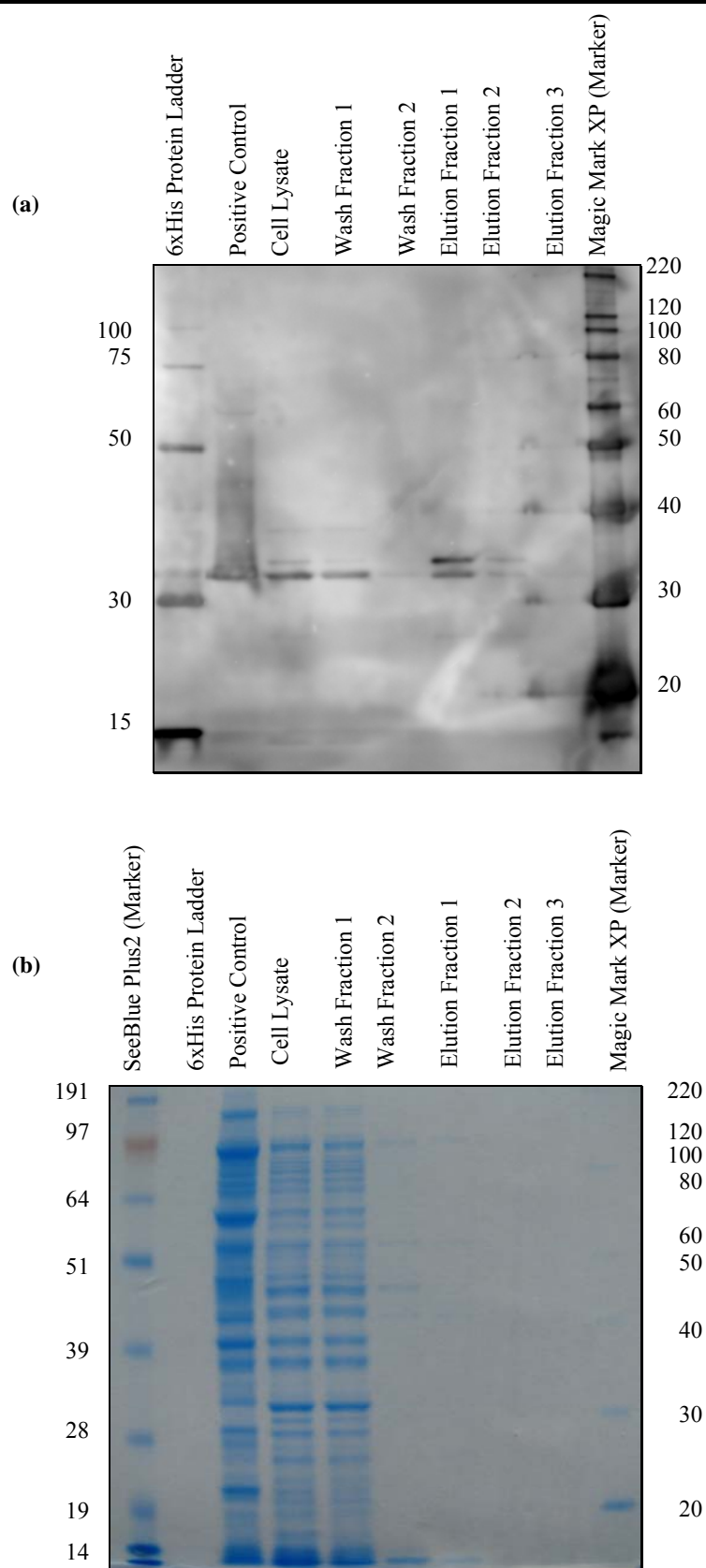


Figure 3.32 (a)Western blotting, (b)Coomassie Blue staining results of pJRHSA under Denaturing purification conditions (NuPAGE®Novex 10% Bis-Tris gel, 200V, 50 min, MOPS Buffer, PVDF membrane, WesternBreeze® Chemiluminescent Anti-mouse kit)

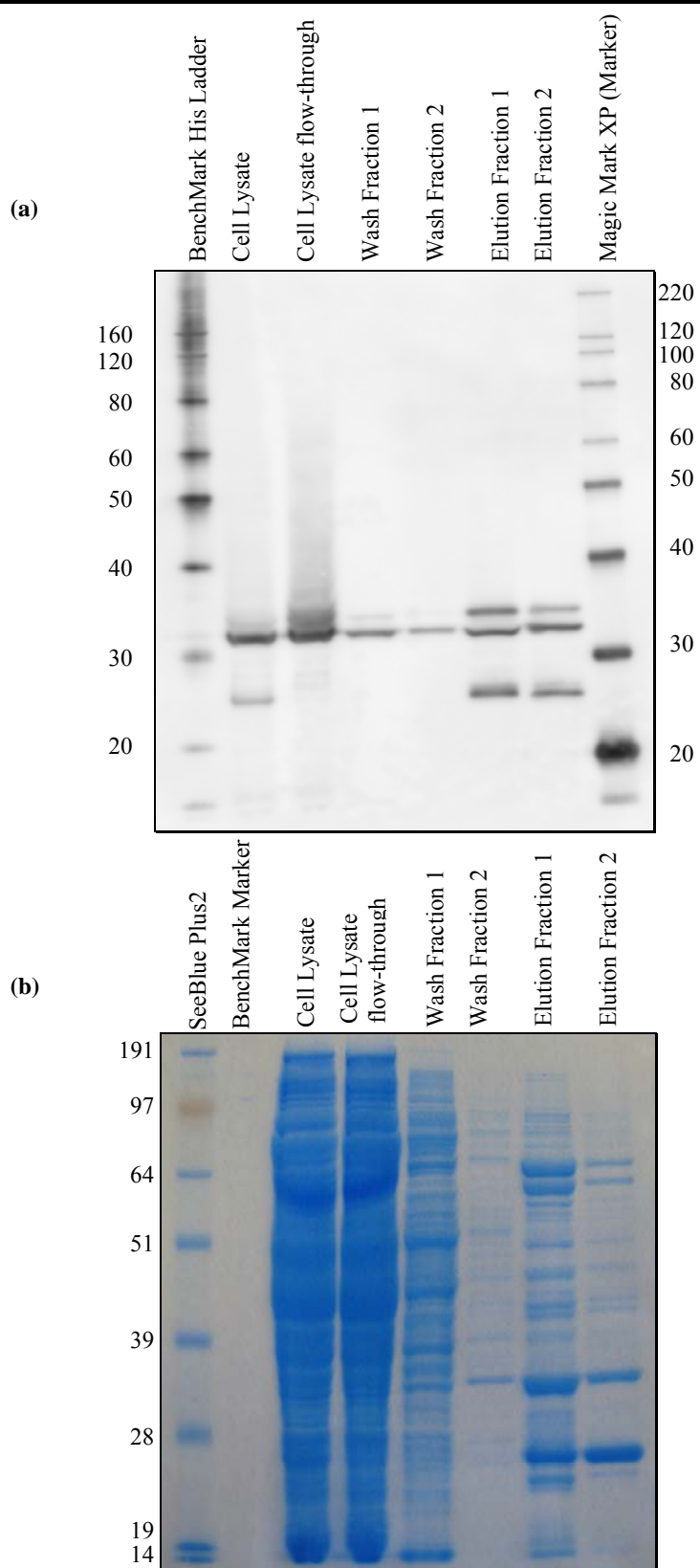


Figure 3.33 (a)Western blotting, (b)Coomassie Blue staining results of pETcyo under Native purification conditions (NuPAGE®Novex 10% Bis-Tris gel, 200V, 50 min, MOPS Buffer, PVDF membrane, WesternBreeze® Chemiluminescent Anti-mouse kit)

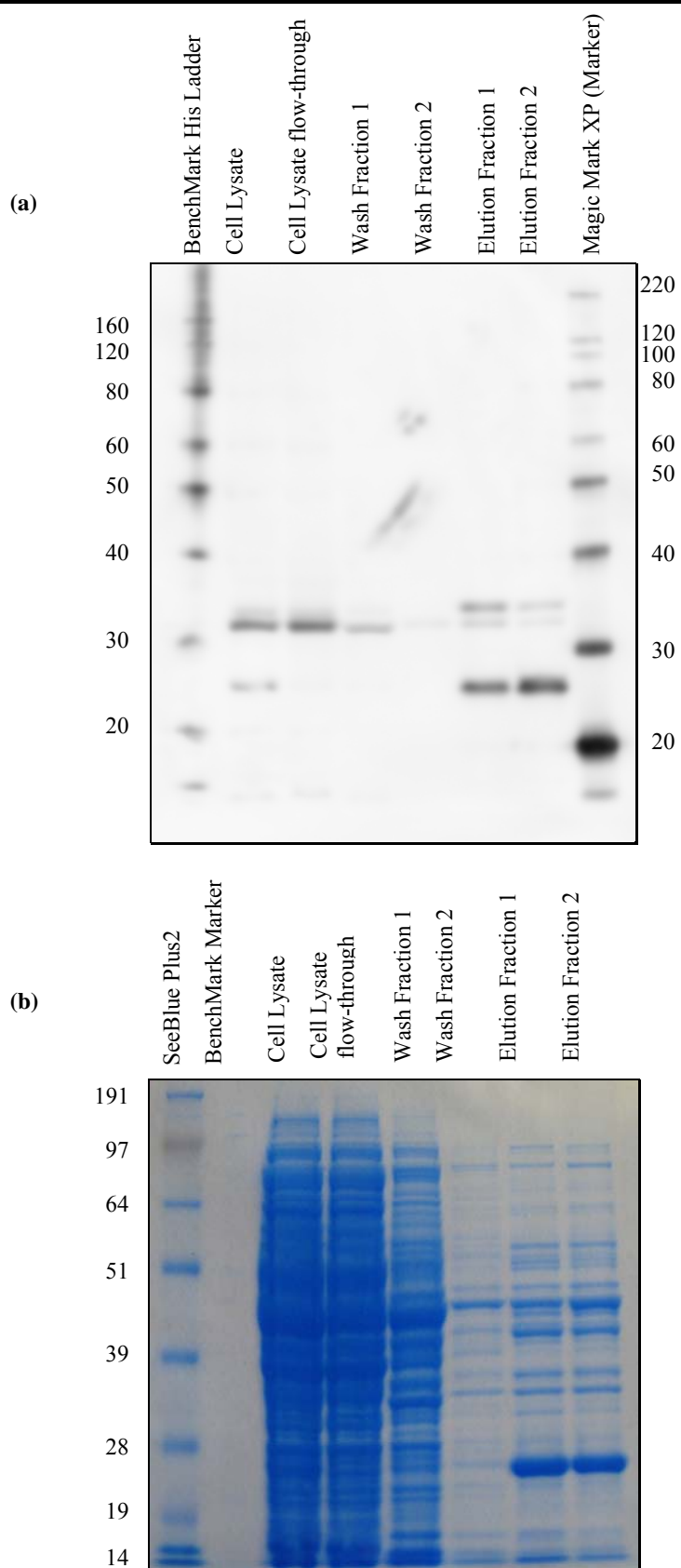


Figure 3.34 (a)Western blotting, (b)Coomassie Blue staining results of pETcyo under Denaturing purification conditions (NuPAGE®Novex 10% Bis-Tris gel, 200V, 50 min, MOPS Buffer, PVDF membrane, WesternBreeze® Chemiluminescent Anti-mouse kit)

3.4.2 Preparation of Cytoplasmic Membranes

In-vivo expressed Cyt-bo₃ samples were used just as a positive control to be compared with *in-vitro* samples, by this comparison, quality and the function of Cyt-bo₃ was determined. All of the results presented in this part were obtained on a cytoplasmic membrane state without affinity purification.

The protocol for cytoplasmic membrane preparation was described previously in section 2.4.2. Cytoplasmic membranes of Cyt-bo₃ enzyme were purified roughly and purified enzyme was characterized by western blot and the yield was determined *via* reduced minus oxidized spectroscopy instead of BCA protein assay. The spectra was taken with high concentrations of Cyt-bo₃, for this reason either 6L cell culture of pJRHSA clone or 2L cell culture of pETcyo clone was used separately for the protein purification. Reduced minus oxidized spectra results will be presented separately in the following sections.

Immuno blotting results of membrane samples for each pJRHSA and pETcyo clones are given in Figure 3.35 and Figure 3.36 respectively. Results clearly demonstrate and confirm the expression of Cyt-bo₃ for each clone. This time, ~35kDa single band was observed for pJRHSA clone which shows there is no degradation or cleavage product after purification. Among the four purification steps, it is clearly demonstrated that enzyme was not lost during purification process.

Western blot analysis of pETcyo clone shows a little cleavage product (Figure 3.36, lane 2), nevertheless the biggest proportion still represent the uncleaved product. Concerning to purification steps, significant loss of enzyme was not observed at each step. The most obvious difference than the other results is complete separation of degradation product from the uncleaved and “good” enzyme was observed after wash step. Only single band was obtained from final solubilized enzyme solution and the band coming from the degradation product ~28kDa was disappeared. So after concentration of this sample *via* concentration tube, enzyme activity and spectrophotometric measurements were done by using this enzyme.

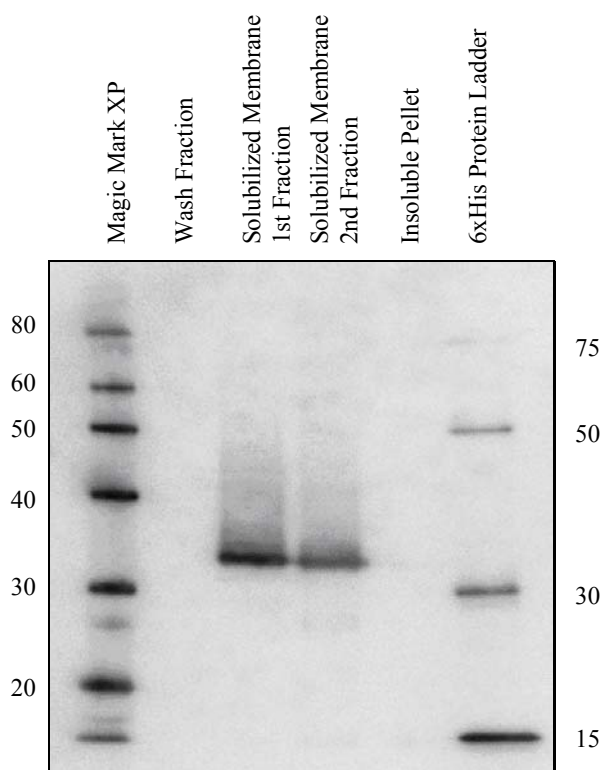


Figure 3.35 Western blot analysis of Cyt-bo₃ expressed by pJRHSA strain (NuPAGE®Novex 10% Bis-Tris gel, 200V, 50 min, MOPS Buffer, PVDF membrane, WesternBreeze® Chemiluminescent Anti-mouse kit)

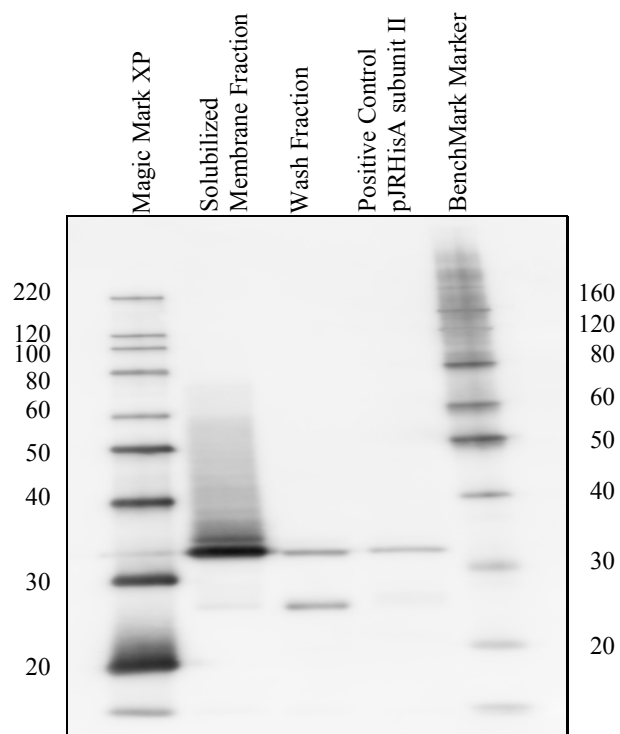


Figure 3.36 Western blot analysis of Cyt-bo₃ expressed by pETcyo strain (NuPAGE®Novex 10% Bis-Tris gel, 200V, 50 min, MOPS Buffer, PVDF membrane, WesternBreeze® Chemiluminescent Anti-mouse kit)

3.4.3 Conclusion of Cyt-bo₃ Purification

In the current chapter isolation and purification results of histidine tagged Cyt-bo₃ were presented. It is obvious that insertion of His-tag at the C-terminus of subunit II facilitates purification and isolation of the enzyme. Present results show that subunit II his-tagged enzyme can be isolated easily *via* using Ni-NTA affinity chromatography. Addition of his-tag eliminates the tedious and time consuming separation steps which were pointed out for pRCO₃ clone. Also, using affinity chromatography simplifies the separation of inactive Cyt-bo₃ mutants. One limiting factor is obtaining higher concentrations of enzyme sample can increase the required time. For this reason two different routes were concerned; first another construct, pETcyo, was used which carries an induction part and second option was using cytoplasmic membranes instead of highly pure enzyme. Since purified enzyme samples was only used as a positive control for *in-vitro* expressed enzyme samples, the quality of cytoplasmic membranes were good enough for the comparison.

3.5 *In-vitro* Expression of Histidine Tagged Cytochrome bo₃ Ubiquinol Oxidase and Western Blot Analysis

3.5.1 Expression of Cytochrome bo₃ *via* Promega E.coli Kit

In-vitro expression of Cyt-bo₃ was performed by using *E.coli* T7 S30 Extract System, details were given in section 2.5.1. There are several reasons for choosing this system, the very first one is the conformity of the expression system to the natural counterpart. Since bacterial Cyt-bo₃ was naturally expressed by *E.coli* organism, this expression system is supposed to be the best candidate for the *in-vitro* expression of the aimed protein and its functionality. The next reason is the characteristics of the system that simplifies the transcription and translation of cloned genetic information and its compatibility of the system with the most common labeling methods and other applications. Last but not least, *E.coli* T7 S30 Extract fulfils the requirement for a system that works under the control of either T7 or any other good *E.coli* promoters.

In-vitro expression of Cyt-bo₃ was performed as described in section 2.5 and as well as in the manual of the kit. Standard protocol was followed without radioactive labeling. It must be noted that ethanol precipitation was always done for the plasmids to get the highest concentration and the purity, so ethanol precipitated plasmid samples were used for the *in-vitro* expression reactions. Mainly western blot analysis was used to detect the translation products. After *in-vitro* synthesis, acetone precipitation was carried out for each sample to remove PEG

CHAPTER III : RESULTS & DISCUSSION

and other lipids from the extract to avoid background staining. Otherwise resulting blot produced bands with a zigzag shape.

Results of *in-vitro* expressed pJRHSA Cyt-bo₃ were presented in Figure 3.37. Plasmid DNA concentrations were 4μg, 2μg and 1μg for the samples 1, 2 and 3 respectively. These results provide information about best plasmid DNA concentration, so looking at the intensity of the bands, highest expression yield was observed for the highest plasmid concentration. Concentration of plasmid DNA was kept at maximum 4μg as suggested by producer (Promega), an increased amount of DNA can result in another side effect. Negative control which is a same expression mixture contains no plasmid DNA, was done as well to check if there is a background effect caused by expression mixture or not. As a positive control previously expressed and purified *in-vivo* Cyt-bo₃ was used. Three different preparations produced double band ~33-35kDa which corresponds to uncleaved and cleaved form of subunit II Cyt-bo₃. Little proteolysis was observed which is not bad hence it was the same trend observed for *in-vivo* expression product.

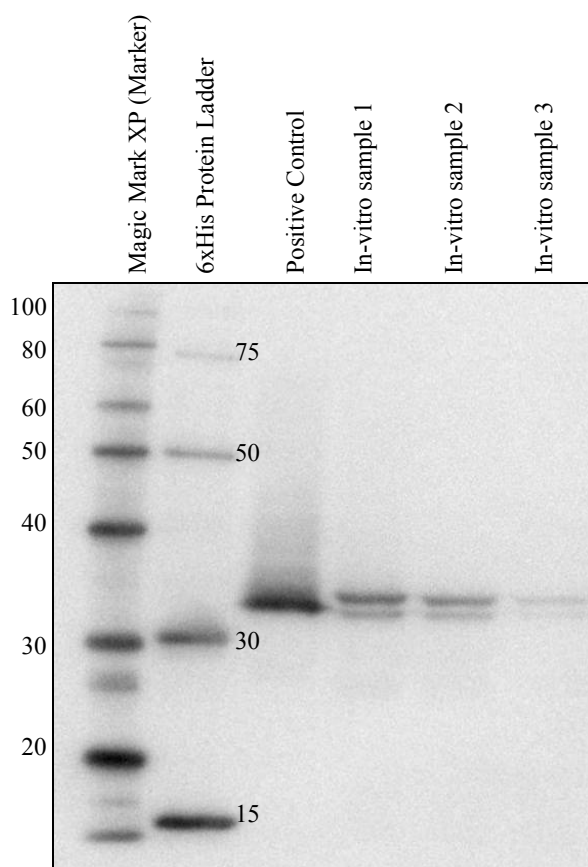


Figure 3.37 Western blot analysis of *in-vitro* expressed Cyt-bo₃ by pJRHSA strain (NuPAGE®Novex 10% Bis-Tris gel, 200V, 50 min, MOPS Buffer, PVDF membrane, WesternBreeze® Chemiluminescent Anti-mouse kit)

CHAPTER III : RESULTS & DISCUSSION

Figure 3.38 indicates the western blotting results of *in-vitro* expressed Cyt-bo₃ for pETcyo plasmid. Resulting bands of *in-vitro* expressed protein introduces once more both cleaved and uncleaved subunit II Cyt-bo₃. Sample 1 and 2 represents the expression mixture containing 4μg and 2μg plasmid DNA respectively. It appears to be there is no significant difference in between both samples and even a little amount of plasmid produces quite high yield *in-vitro* products. Again no band was obtained for negative control as expected and as a positive control *in-vivo* expressed and purified Cyt-bo₃ pETcyo clone was used.

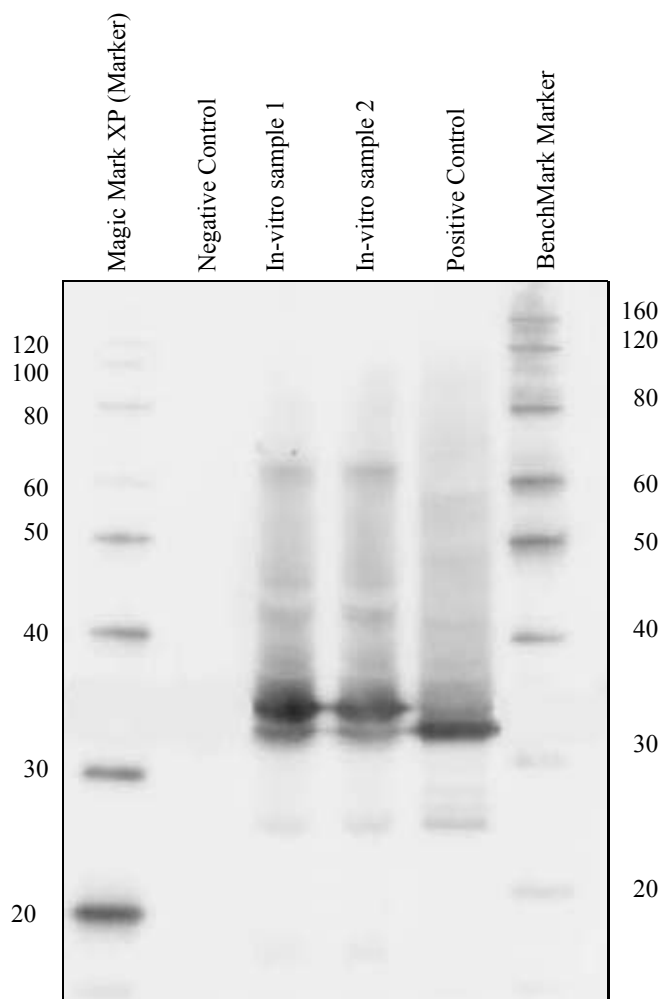


Figure 3.38 Western blot analysis of *in-vitro* expressed Cyt-bo₃ by pETcyo strain (NuPAGE®Novex 10% Bis-Tris gel, 200V, 50 min, MOPS Buffer, PVDF membrane, WesternBreeze® Chemiluminescent Anti-mouse kit)

Comparing results of expression products for two different plasmids it was obvious that type of promoter has a big impact on the *in-vitro* synthesis of Cyt-bo₃. As it was pointed out before, *E.coli* T7 S30 system works efficiently under the control of T7 or any other good *E.coli* promoter such as lambda P_R, lambda P_L, *tac*, *trc* and *lacUV5*. But anyway expression from T7

promoter is higher than other promoters by using this extract. According to the literature^{13,14} and cloning information, pJRHSA does not encode any of these good *E.coli* promoters mentioned above. As far as it is known pJRHSA has a “natural” promoter which originates from natural genetic code and works with *E.coli* mixture. Although pJRHSA plasmid does not have a good promoter Cyt-bo₃ expression *via* this system resulted in a meaningful achievement.

3.5.2 Expression of Cytochrome bo₃ *via* Qiagen Insect Kit

Another challenging part was to observe the effect of expression system on the efficiency of *in-vitro* synthesis. EasyXpress Insect Expression Kit (Qiagen) was chosen because it provides the possibility to synthesize eukaryotic proteins or complex proteins with posttranslational modifications and it has a wide range of applications. Not different than *E.coli* extract this system contains all necessary components for transcription and translation reactions. Reaction details were given in section 2.5.2 in detail.

Afterwards *in-vitro* synthesis, products were directly analyzed by western blot method without any other purification steps. Results were presented in Figure 3.39 for both plasmids. No band was observed for any of two plasmids which indicate *in-vitro* synthesis was disrupted by some other factors. Since *in-vitro* synthesis of Cyt-bo₃ was successfully done *via E.coli* extract previously, expression of target protein is not possible using EasyXpress extract based on the present findings. At this point failure of Cyt-bo₃ expression for pJRHSA plasmid was expected result due to the lack of T7 promoter, nevertheless using pETcyo plasmid which contains T7 promoter did not produce any expression product either. Consequently it was very well understood that employing T7 promoter and *E.coli* system are equally important in terms of expression of the Cyt-bo₃.

¹³ Rumbley, J. N., Analysis of Heme-Copper Ligation, Quinol Activity and Ligand Binding Kinetics of Cytochrome bo₃ Quinol Oxidase from *E.coli*, Dissertation Thesis (1995), University of Illinois at Urbana-Champaign.

¹⁴ van der Oost, J., Lappalainen, P., Musacchio, A., Warne, A., Lemieux, L., Rumbley, J., Gennis, R.B., Aasa, R., Pascher, T., Malmstrom, B.G., and Saraste, M., (1992) EMBO J., 11, 3209.

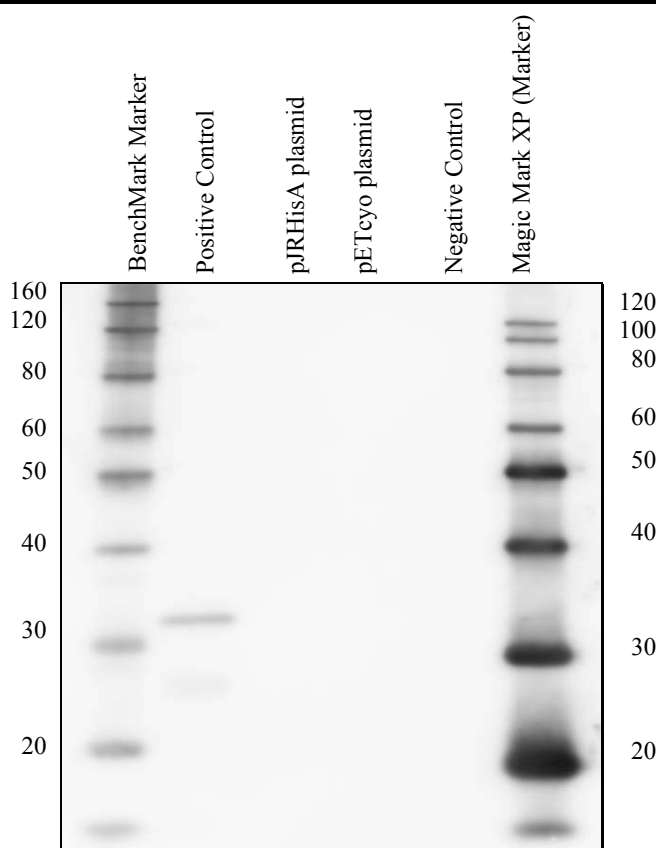


Figure 3.39 Western blot analysis of *in-vitro* expressed Cyt-bo₃ by using Insect Kit for pJRHSA(lane3) and pETcyo(lane4) strain (NuPAGE®Novex 10% Bis-Tris gel, 200V, 50 min, MOPS Buffer, PVDF membrane, WesternBreeze® Chemiluminescent Anti-mouse kit)

3.5.3 Expression and Characterization of Non-Histidine Tagged Cytochrome bo₃ via BODIPY-FL Labelling

Based on the previous discussions, absence of affinity tag is the most important feature of pRCO₃ plasmid. FluoroTect™ Green_{Lys} *in-vitro* Translation Labeling System enables the fluorescent labeling of *in-vitro* products by using modified lysine transfer RNA which is labeled with the fluorophore BODIPY-FL (Figure 3.40). Labelled lysine residues are integrated into the final *in-vitro* product during translation step. This system offers several advantages such as; fast detection, convenient results based on SDS-gel, non-radioactive labeling, high sensitivity and compatibility with either eukaryotic or prokaryotic *in-vitro* expression systems.

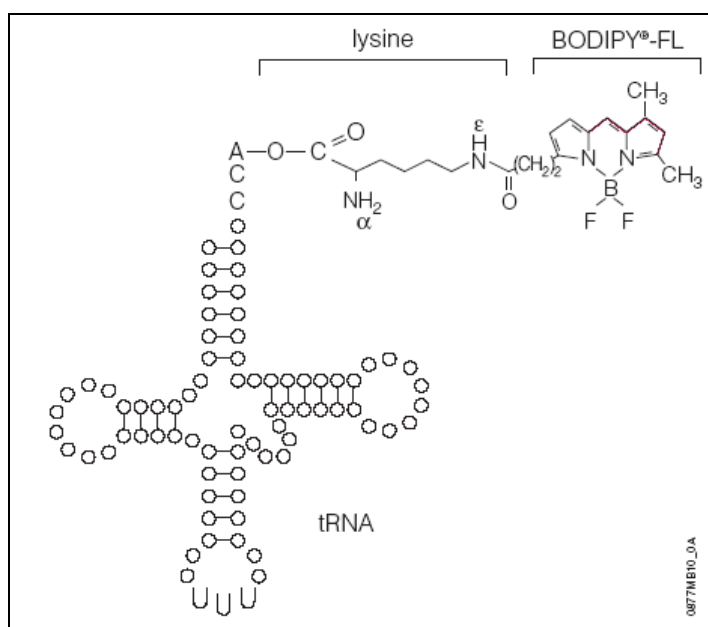


Figure 3.40 Structure of FluoroTect™ Green_{Lys} tRNA¹⁵

In this work, FluoroTect™ Green_{Lys} labeling system was used while performing *in-vitro* synthesis for pRCO₃ plasmid DNA. Reaction details were given previously in section 2.5.4.

Once expression of the target protein was complete, SDS-gel electrophoresis performed directly for the expression product without any additional treatment. Immediately after running SDS-gel, image was taken from the gel (Figure 3.41). LAS 3000 Imaging System (Fuji) system was used for the determination of fluorescent labeling, blue light and corresponding filters were chosen since system itself does not have a green laser, so it must be taken into account exposure efficiency was not maximum. Although background signals were quite high for this product because it was nearly impossible to remove unconsumed tRNA from the expression mixture, a single band was observed for the *in-vitro* expression product. To be sure about the synthesis two different amount of tRNA solution, 1µl and 5µl additions were tested. As logically expected, stronger band intensity was observed for the concentrated sample.

The most significant disadvantage of this system is its strong background effect. Even though labeling of the *in-vitro* product was efficient and resulting protein was easily monitored, it was not possible to use this labeling system for SPFS detection. Background signal completely overlapped with the signal of the protein, so this system was good candidate to detect labeled proteins *via* western blot but not good enough for SPFS detection method.

¹⁵ FluoroTect™ Green_{Lys} in vitro Translation Labelling System, (2007) Technical Bulletin, Promega.

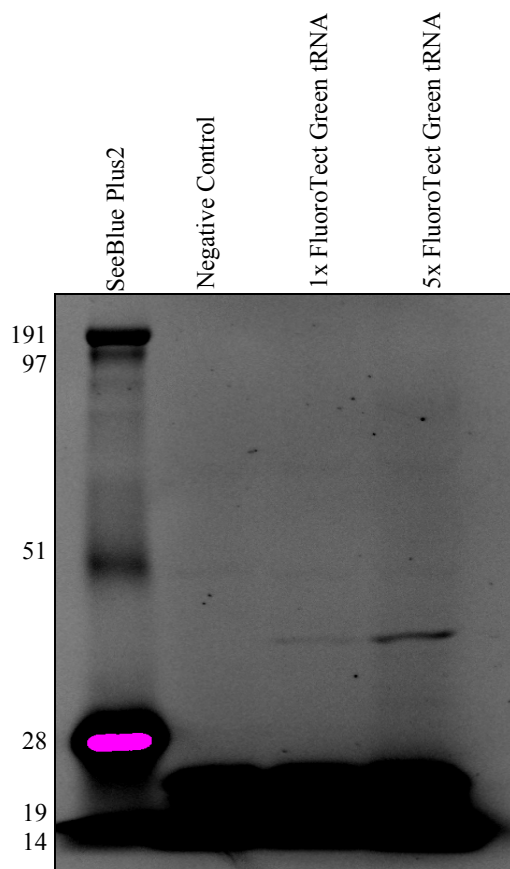


Figure 3.41 FluoroTect™ Green_{Lys} labeling result of *in-vitro* expressed Cyt-bo₃ for pRCO₃ plasmid (NuPAGE®Novex 10% Bis-Tris gel, 200V, 50 min, MOPS Buffer, PVDF membrane, WesternBreeze® Chemiluminescent Anti-mouse kit)

3.5.4 Conclusion of *In-vitro* Expression of Cyt-bo₃

In conclusion, a complete *in-vitro* expression overview of cytochrome bo₃ ubiquinol oxidase has been presented in this part. As indicated above cell-free expression of Cyt-bo₃ was successfully achieved for each pJRHSA, pETcyo and pRCO₃ plasmids. Both expression mixture and plasmid type were examined and their effect on *in-vitro* synthesis was observed. Importantly it was shown that although Cyt-bo₃ is a huge four-subunit membrane protein, combining suitable facts all together results in success. Suitable facts refer to the *in-vitro* extract and cloning details such as T7 promoter. As a consequence, best expression yield was produced by using T7 promoter and *E.coli* extract. On the other hand, heading towards completely different system than target protein's nature, namely insect extract didn't produce any result at all. This finding was somewhat surprising but not unpredicted.

3.6 Observation of Histidine Tagged Cytochrome bo_3 Expression in Artificial Membranes by Surface Plasmon Enhanced Fluorescent Spectroscopy

For the detection of *in-vitro* expression products, SPFS method was chosen to enhance the detection limit of optical sensors which is based on evanescent wave techniques such as SPR. Fluorescence detection was done based on the presence of bound fluorophores in the evanescent field.

Here two different approaches were followed to detect *in-vitro* expression of Cyt- bo_3 via antibody-protein interaction. First of all “Sandwich assay” which utilizes the primary (1° Ab) and secondary (2° Ab) antibodies were used to detect the target protein. The 1° Ab (PentaHis Ab, Mouse monoclonal IgG, Qiagen) was directed against target protein Cyt- bo_3 and labeled 2° Ab(Cy5-Conjugated Secondary Antibody, Goat-Antimouse IgG, Chemicon) was directed against 1° Ab. As a second route, only labeled 1° Ab (PentaHis Alexa Fluor 647 Conjugate, Qiagen) was used directly against Cyt- bo_3 . In the following sections results will be presented according to these approaches.

All experiments carried out in this work varies in chemicals but the following experimental steps were used for each sample to measure absorption, desorption or binding process on the surface.

- Background scan was measured to determine the thickness of film or other layer and to determine the fluorescence background before sample addition.
- Kinetic run was performed until having a stable baseline to monitor the absorption or binding process. Subsequently the system was rinsed with pure buffer to remove unbound, excess material from the sample surface.
- Sample scan was done to determine thickness and refractive index change which has been stated before and to measure fluorescence signal from the target molecule. For all scan curves, background correction was performed by subtracting corresponding background signal from each scan curve.
- All results have been obtained from at least 3-5 independent experiments and average result was presented here.

3.6.1 Kinetic Mode Measurements

The fluorophores which has been used for SPFS detection were Cy5 and Alexa Fluor 647. They were excited by using red laser (632nm) in SPR setup. Characteristic absorption and fluorescence emission spectra were given in Figure 3.42 for both Cy5 and Alexa Fluor 647.

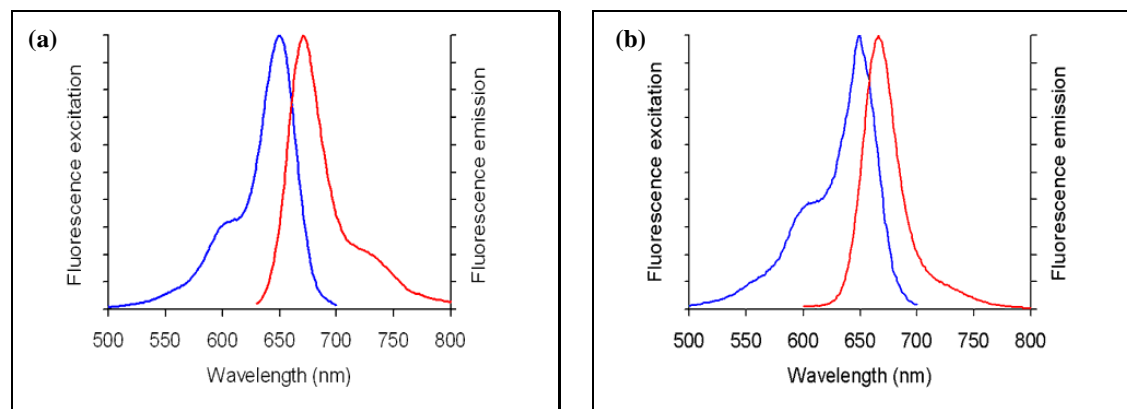


Figure 3.42 Absorption and Fluorescence emission spectra of (a)Alexa Fluor 647, (b)Cy5 conjugated antibody¹⁶

Comparison in between two fluorophores was done for each SPR measurement. Alexa Fluor 647 was preferred to compare with Cy5, since it was very well known that Alexa dyes are more stable, brighter and less sensitive to pH changes than any other cyanine dyes. Another reason for choosing Alexa Fluor 647 labeled 1°Ab was to prevent misinterpretation coming from amplification of the signal caused by multiple binding of 2°Ab.

tBLM construction and *in-vitro* synthesis was done as explained in section 2.8.6. The kinetic of the antibody binding was monitored for each Cy5 and Alexa Fluor conjugated antibodies. Stability and photobleaching of fluorophores was detected *via* simultaneous recording during 45-75 min. As shown in Figure 3.43 and Figure 3.44, although illumination was blocked by the shutter, fluorescent intensity of Cy5 decreased 5% within the 40min. On the other side, intensity of Alexa Fluor 647 conjugated antibody remained constant for 45min and decreased 2% within the 70min. As expected, observed results showed the photo stability of Alexa Fluor 647 is higher than Cy5 fluorophore.

These results have given another feed back; that *via* using Alexa Fluor 647 labelled antibody, the incubation time can be shortened and optimized with very small amount of loss in intensity.

¹⁶ Molecular Probes, Invitrogen, Online Datasheet.

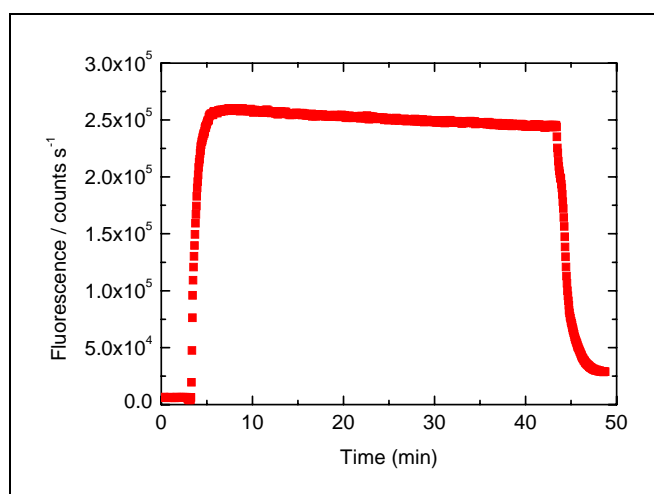


Figure 3.43 Fluorescence kinetic of Cy5 conjugated antibody binding

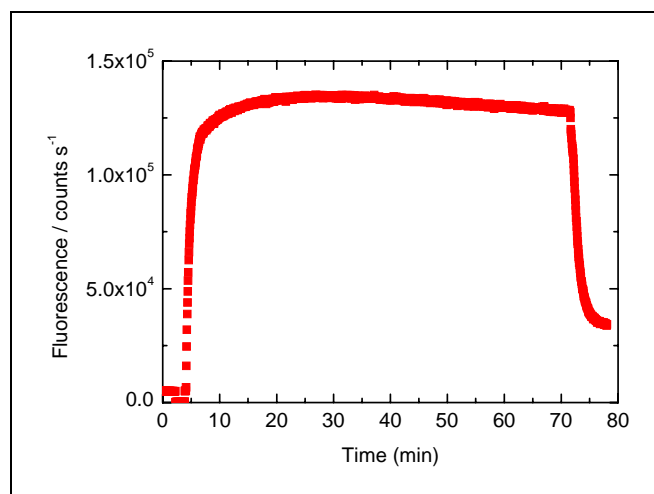


Figure 3.44 Fluorescence kinetic of Alexa Fluor 647 conjugated antibody binding

3.6.2 Membrane-Antibody Interaction

Membranes have strong tendency to bind protein structures and the most important issue while detecting interactions in between protein structures and membrane system is unspecific interactions, such as unspecific adsorption of antibodies to the membrane since antibody is a protein itself. In order to identify if there is any interaction in between antibody and the tBLM structure, antibody solutions were directly applied to the tBLM construct. Same procedure was followed as explained before with omitting *in-vitro* expression part.

SPFS scan curves as measured after applying antibody solutions on a membrane surface are presented in Figure 3.45 and Figure 3.46 for both Cy5 and Alexa Fluor 647 labelled antibodies. These scan curves are resulting data after subtraction of background curves. A relatively strong signal was observed near the resonance minimum after addition of labeled antibodies for both Cy5 and Alexa Fluor 647 conjugates. As a consequence, employed antibodies show a strong affinity to the P19/DMPE/PC membrane structure which can cause to background signal while detecting the signal of real sample. In this case, background can be interpreted as a false positive signal. Therefore the “blocking” method was chosen to overcome this background problem.

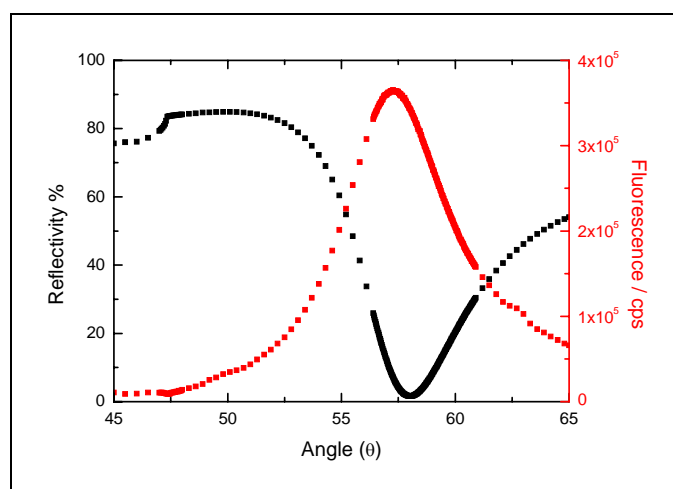


Figure 3.45 SPFS scan of the system P19/DMPE/PC/PentaHis 1°Ab/Cy5 conjugated 2°Ab

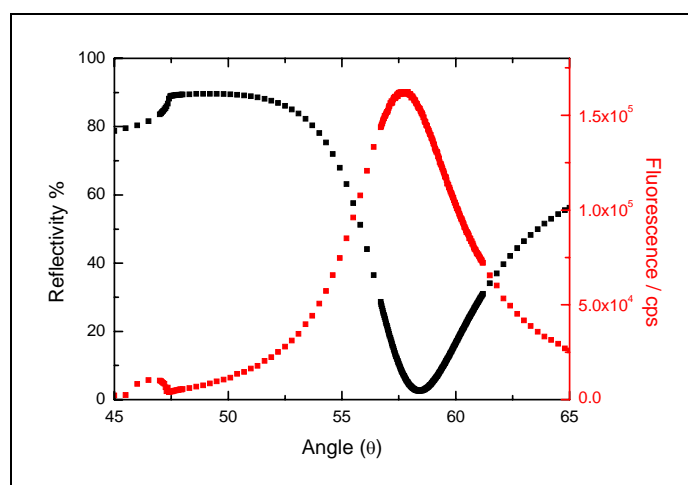


Figure 3.46 SPFS scan of the system P19/DMPE/PC/Alexa Fluor 647 conjugated 1°Ab

Blocking strategy is a well known concept for immuno blotting applications. Blocking of unspecific binding is generally achieved by applying a dilute solution of small proteins such as BSA (Bovine Serum Albumine) or non-fat dry milk solution to the membrane surface. The protein in this dilute solution attaches to the unoccupied places of membrane, so there will be no empty place on the membrane surface for antibody adsorption.

Same strategy was applied for this system which produces satisfying results for each antibody system, given in Figure 3.47. After construction of membrane structure surface was covered with optimized amount of Western blocking solution (Roche) and rinsed of after 1hour incubation time. Than labeled antibody solutions were applied separately to this blocked membrane surface which produces no false positive signal coming from the interaction of antibody and the membrane itself. Similar strategy was used for all measurements which will be discussed on the following parts and it will be named as “blank”.

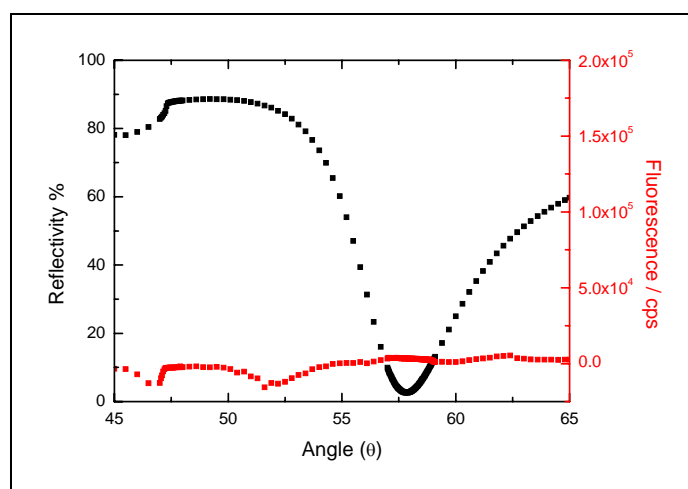


Figure 3.47 SPFS scan of the system P19/DMPE/PC/Blocking Solution/Cy5 conjugated 2°Ab or P19/DMPE/PC/Blocking Solution/Alexa Fluor 647 conjugated 1°Ab

3.6.3 Incorporation of Isolated Enzyme

To have a brief idea about this membrane system and Cyt-bo₃ incorporation, *in-vitro* synthesized or *in-vivo* synthesized and purified protein was used as a model. Since the main idea of this study is to prove that *in-vitro* expression of a membrane protein is much more favorable inside the membrane in a way to preserve its functionality and correct folding. It is important to have insight about the behavior of the very same protein in our model membrane system. In this part we describe the interaction in between artificial membrane and Cyt-bo₃

which was synthesized outside of the membrane and insertion of Cyt-bo₃ quantified by SPFS technique.

Insertion process for both *in-vitro* and *in-vivo* expressed protein was observed. Either 100µl of *in-vitro* expression product or 100µl of purified and concentrated *in-vivo* product was pumped to the membrane surface and allowed to interact during 1hour incubation time. This experiment was done with and without blocking solution to be aware of the background signal. SPFS curves of *in-vitro* expressed Cyt-bo₃ insertion for both Cy5 and Alexa Fluor 647 conjugated antibodies were given in Figure 3.48 and Figure 3.49. SPFS signal was detected after applying *in-vitro* expressed product to the system without using any blocking solution. Afterwards, same experiment was performed in the presence of blocking solution and signal was completely disappeared. This result indicates clearly observed signal again comes from the antibody adsorption without using blocking solution. Another important output of these results, Cyt-bo₃ was not inserted into the membrane structure hence it is really complex and big membrane protein this result was not unpredicted. Most probably large subunits and different interactions coming from hydrophilic and hydrophobic domains of the membrane protein prevent this integration process. To clarify this situation completely, *in-vivo* protein sample which is more concentrated and has a high purity than *in-vitro* samples was used and same protocol was applied. Resulting SPFS scans were presented in Figure 3.50.

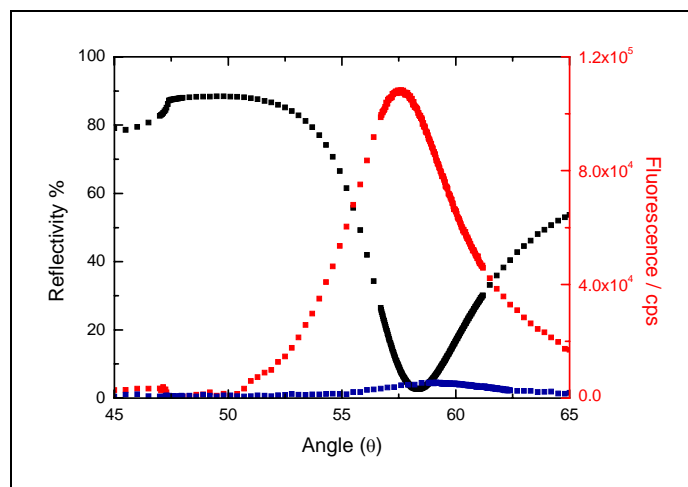


Figure 3.48 SPFS scan of the system (■) P19/DMPE/PC/*in-vitro* Cyt-bo₃/PentaHis 1°Ab/Cy5-conjugated 2°Ab and (■) P19/DMPE/PC/*in-vitro* Cyt-bo₃/Blocking Solution/PentaHis 1°Ab/Cy5-conjugated 2°Ab

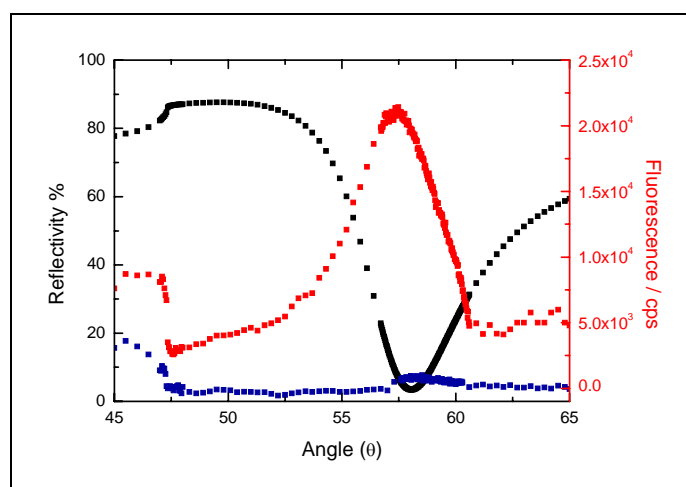


Figure 3.49 SPFS scan of the system (■) P19/DMPE/PC/*in-vitro* Cyt-bo₃/Alexa Fluor 647 conjugated 2°Ab and (■) P19/DMPE/PC/*in-vitro* Cyt-bo₃/Blocking Solution/Alexa Fluor 647 conjugated 2°Ab

In parallel to results of the *in-vitro* samples positive signal was observed for insertion of *in-vivo* sample without blocking solution, when the blocking solution was used signal was not disappeared completely but it was relatively too small signal. Even though a small signal was detected it is not possible to claim that is coming from the inserted protein since it is very low and close to the background level. So, all findings indicate that integration of this membrane protein into this artificial membrane is not possible after construction of the membrane under these conditions. Moreover these results support our theory and show that while expressing membrane proteins they need membranes for integration and folding.

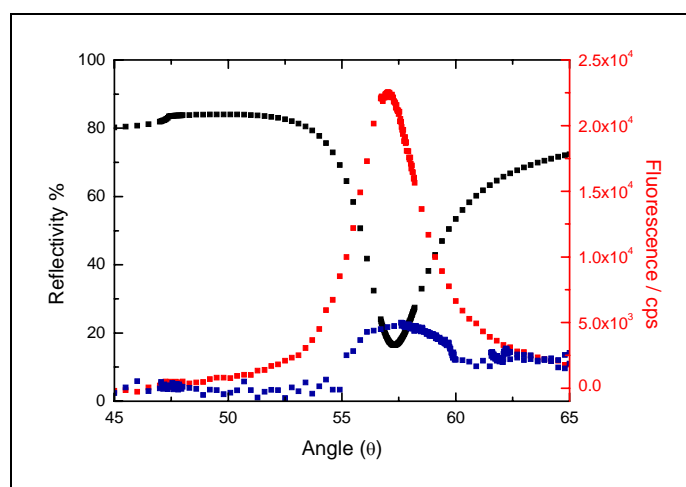


Figure 3.50 SPFS scan of the system (■) P19/DMPE/PC/*in-vivo* Cyt-bo₃/PentaHis 1°Ab/Cy5-conjugated 2°Ab and (■) P19/DMPE/PC/*in-vivo* Cyt-bo₃/Blocking Solution/PentaHis 1°Ab/Cy5-conjugated 2°Ab

3.6.4 Detection of *in-vitro* Expression of the Cytochrome bo_3 in Real Time

To have a better understanding about *in-vitro* expression of Cyt- bo_3 and all interactions in the system such as insertion mechanism and parameters, limitations for insertion and expression, unspecific interactions, were examined *via* using different combinations for the system. As it was explained previously for several times, various membrane components and various plasmid DNAs were used to get the best expression result and functionality.

Here two main routes were investigated; first effect of different plasmid DNA pJRHisA and pETcyo, was checked *via* SPFS, then two different membrane systems P19/DMPE/PC and P19/DMPE/TE were analyzed to observe their influence on *in-vitro* expression product.

3.6.4.1 *In-vitro* Expression of Cyt- bo_3 for pJRHisA plasmid

As outlined before, the main idea of this work is to focus on *in-vitro* expression of membrane proteins directly inside the artificial membrane structure. Hence, in this part we discuss *in-vitro* expression of Cyt- bo_3 in a P19/DMPE/PC membrane construct in detail. Once again two different antibody systems, PentaHis 1°Ab/Cy5-conjugated 2°Ab and Alexa Fluor 647 conjugated 1°Ab were used to compare differences and to clarify if there is any amplification of signal coming from 1°Ab/2°Ab sandwich structure.

After construction of tBLM, *in-vitro* mix was prepared freshly and pumped to the system immediately and allowed to develop or complete during 2 hours. Excess material was rinsed off after incubation time and immuno labeling protocol was carried on in the same way as explained before in section 2.8.6. Since it was very well known that employed antibodies have a high affinity to bind membrane surface, blocking strategy was applied every time after *in-vitro* expression of the target protein. On the other hand, to be sure about the expression of target protein and to be sure that observed signal is directly coming from the expressed and integrated membrane protein, negative control was preformed which means same protocol was applied without any DNA in the *in-vitro* mixture during incubation time. In the figures, positive signal which is coming directly from *in-vitro* expression product was shown in red square legends and negative control is given as a blue square legends.

Expression of Cyt- bo_3 was observed easily *via* SPFS method. A typical angular fluorescent scan curves were presented in Figure 3.51 and Figure 3.52 for the *in-vitro* mix containing pJRHisA plasmid DNA. Two different labeling systems produced nearly same results. Fluorescent maxima of both systems were in the same range and same order of magnitude, $2.5 - 3.5 \times 10^4$ cps. Therefore it shows there is not much effect coming from signal

amplification *via* multiple binding of Cy5 conjugated 2°Ab. Another important point it was shown with the help of negative control, absolutely positive signal is coming from *in-vitro* synthesized product.

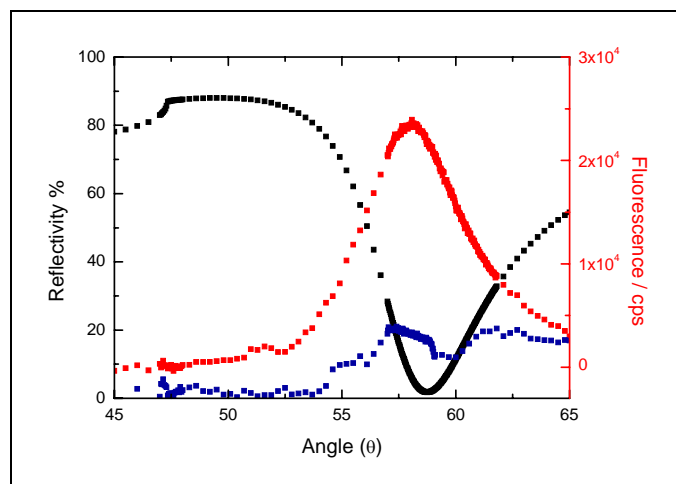


Figure 3.51 SPFS scan of (■) P19/DMPE/PC/*in-vitro* Cyt-bo₃ pJRHsA plasmid/Blocking Solution/PentaHis 1°Ab/Cy5-conjugated 2°Ab and (■) P19/DMPE/PC/*in-vitro* extract without DNA/Blocking Solution/ PentaHis 1°Ab/Cy5-conjugated 2°Ab

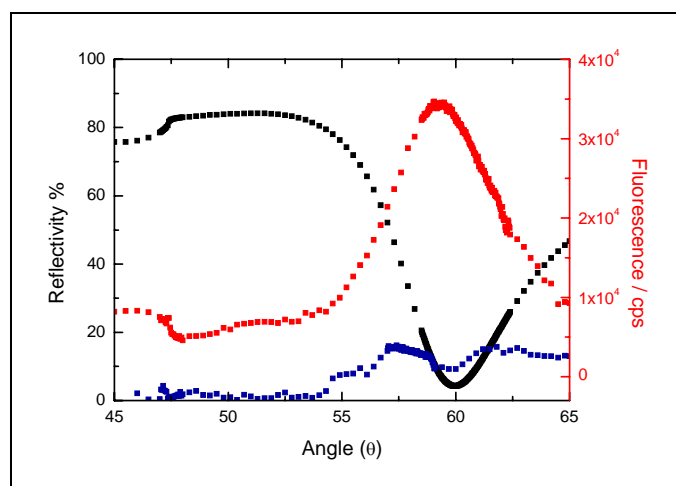


Figure 3.52 SPFS scan of (■) P19/DMPE/PC/*in-vitro* Cyt-bo₃ pJRHsA plasmid/Blocking Solution/ Alexa Fluor 647 conjugated 2°Ab and (■) P19/DMPE/PC/*in-vitro* extract without DNA/Blocking Solution/ Alexa Fluor 647 conjugated 2°Ab

3.6.4.2 *In-vitro* Expression of Cyt-bo₃ for pETcyo plasmid

As explained and discussed beforehand, presence of T7 promoter makes a significant difference in the expression level and efficiency. Although it was certified *via* western blotting,

in-vitro synthesis efficiency of pETcyo plasmid was compared and characterized through SPFS method. All steps were as carried out in the same parallel like pJRHSA plasmid. Resulting fluorescence maxima of angular scan curves were ten-fold higher than the signal detected with pJRHSA plasmid. Detected values for fluorescent maxima of each system were around 5 - 6.5×10^5 cps. There is a slight difference in between Cy5 labeled and Alexa Fluor 647 labeled antibodies which is in acceptable range and also shows every *in-vitro* expression reaction produces nearly same amount of product. Even that much variation of the signal may be effect of different batches of gold evaporation events or different batches of expression mixture.

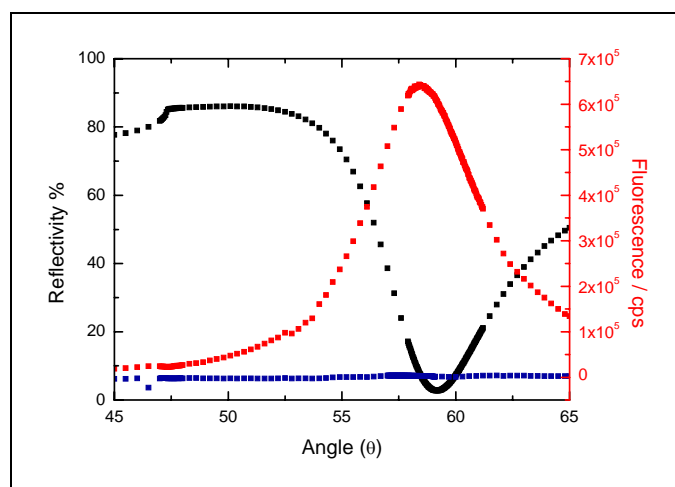


Figure 3.53 SPFS scan of (■) P19/DMPE/PC/*in-vitro* Cyt-bo₃ pETcyo plasmid/Blocking Solution/PentaHis 1°Ab/Cy5-conjugated 2°Ab and (■) P19/DMPE/PC/*in-vitro* extract without DNA/Blocking Solution/ PentaHis 1°Ab/Cy5-conjugated 2°Ab

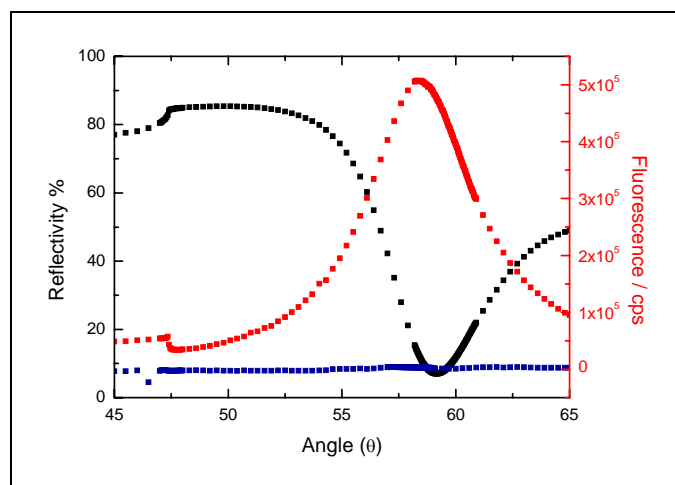


Figure 3.54 SPFS scan of (■) P19/DMPE/PC/*in-vitro* Cyt-bo₃ pETcyo plasmid/Blocking Solution/ Alexa Fluor 647 conjugated 2°Ab and (■) P19/DMPE/PC/*in-vitro* extract without DNA/Blocking Solution/ Alexa Fluor 647 conjugated 2°Ab

Additionally, effect of lipids on expression of target protein was observed by using pETcyo plasmid as well. Same protocol and preparation steps were followed instead of using PC bilayer TE lipids were examined in here. Resulting angular fluorescent scan curve was presented in Figure 3.55. Observed fluorescent maximum was 4×10^5 cps. Although the reason lies behind this approach was to create a closer model to the native environment of target protein, as expected and predicted TE lipids did not show a strong impact on increasing the expression yield.

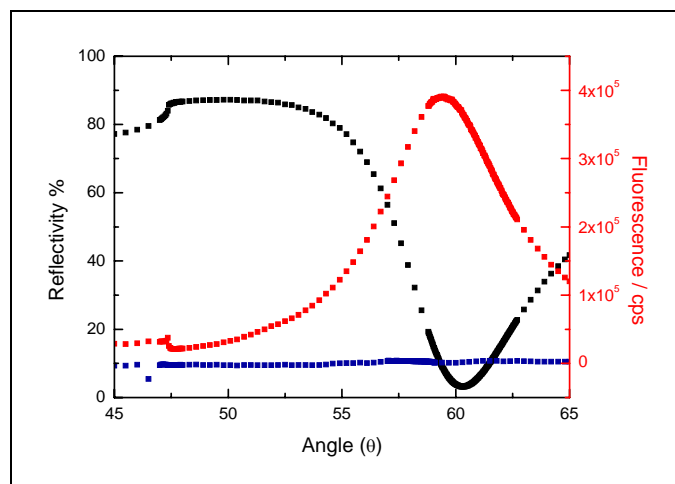


Figure 3.55 SPFS scan of (■) P19/DMPE/TE/*in-vitro* Cyt-bo₃ pETcyo plasmid/Blocking Solution/ Alexa Fluor 647 conjugated 2°Ab and (■) P19/DMPE/TE/*in-vitro* extract without DNA/Blocking Solution/ Alexa Fluor 647 conjugated 2°Ab

3.6.5 Western Blot Analysis of SPFS

After completion of *in-vitro* expression of Cyt-bo₃ in artificial tBLM system, *in-vitro* extract was collected from the reaction media for western blot analysis. This application could provide information about expression product in bulk solution but not about the integrated protein. Another challenging point is to observe the expression product which is integrated into the membrane. Since this membrane/expression system has many of components and SPR only provides an increase in optical mass, hence no specificity is involved; detection of insertion is not possible by using SPR or SPFS. To detect inserted protein all components, artificial membrane and its content, were treated with LDS buffer for at least 2 hours. LDS buffer is a buffer solution which is used for preparations of samples for western blotting procedure. Since LDS buffer contains strong detergents and reducing agents, resulting solution should contain the *in-vitro* expressed protein which is integrated in artificial membrane.

CHAPTER III : RESULTS & DISCUSSION

Western blot results of corresponding samples which has been mentioned and discussed above were presented in Figure 3.56 for pJRHisA plasmid and in Figure 3.57 for pETcyo plasmid. In Figure 3.56, it has been named SPR bulk for the collected expression mixture afterwards expression reaction and solubilized membrane sample was named as SPR membrane. Corresponding bands of Cyt-bo₃ was observed for each case at the right molecular weight which supports the expression of the protein, weak bands were detected for the sample collected from membrane which is the proof of insertion. Expression yield and amount of inserted product can be seen and observed roughly from the intensity of the bands. Similarly to the previous immuno blotting results, same double band trend was detected which means cleaved and uncleaved product was produced during expression.

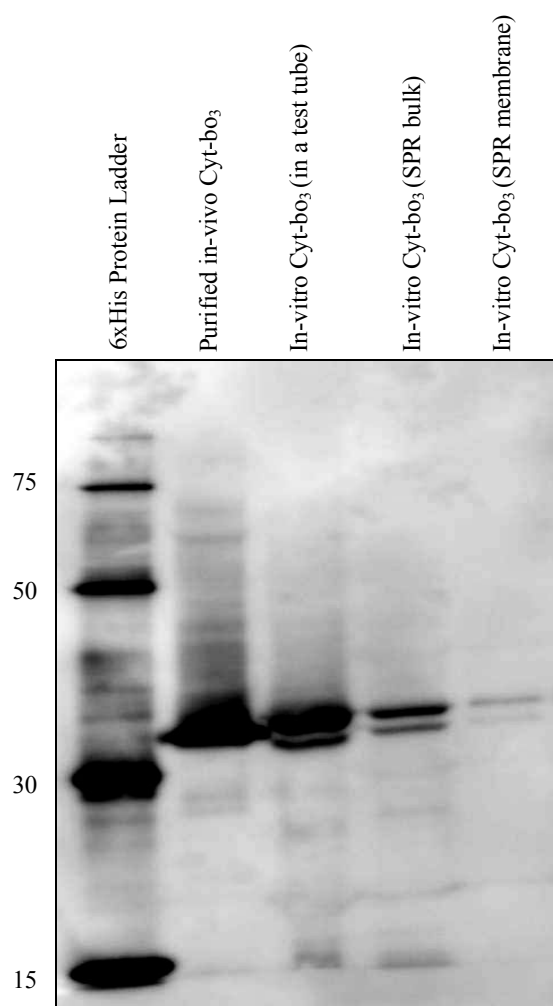


Figure 3.56 Western blot analysis of SPFS samples, *in-vitro* expressed Cyt-bo₃ pJRHisA plasmid (NuPAGE®Novex 10% Bis-Tris gel, 200V, 50 min, MOPS Buffer, PVDF membrane, WesternBreeze® Chemiluminescent Anti-mouse kit)

In Figure 3.57, western blot results of SPFS measurements for pETcyo plasmid were shown. Characteristic bands of Cyt-bo₃ ~33 kDa were detected here as well. Most promising result is the of course improved band intensity of membrane solubilized product which means higher expression and integration yield. Another interesting point is the missing band of membrane product at very low molecular weight region which was observed previously and shown in bulk product as well and supposed to correspond to a degradation product.

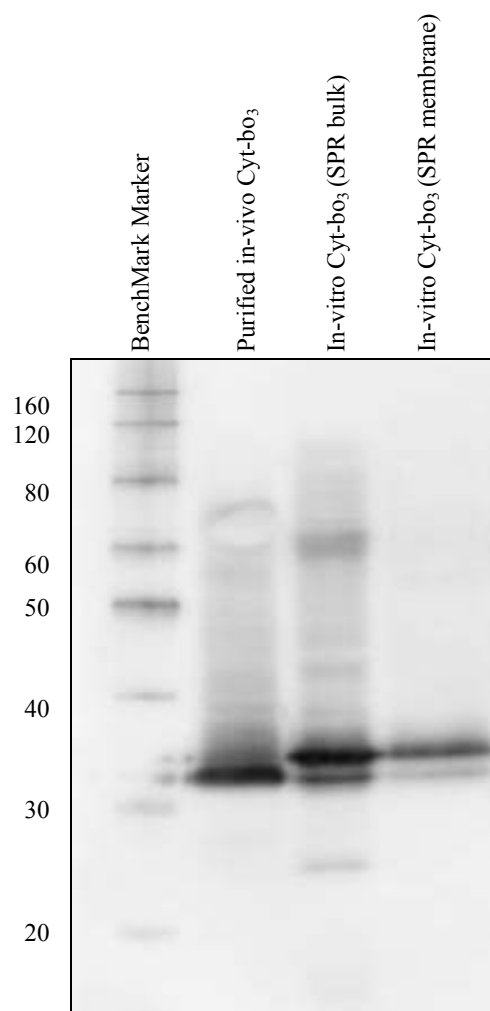


Figure 3.57 Western blot analysis of SPFS samples, *in-vitro* expressed Cyt-bo₃ pETcyo plasmid (NuPAGE®Novex 10% Bis-Tris gel, 200V, 50 min, MOPS Buffer, PVDF membrane, WesternBreeze® Chemiluminescent Anti-mouse kit)

3.6.6 Conclusion of SPFS detection of Cyt-bo₃ in Artificial Membranes

SPFS measurements of both pJRHisA and pETcyo plasmids showed that expression of Cyt-bo₃ *via* using *E.coli* extract produces effective results. Western blot results further

supported the expression and insertion of Cyt-bo₃. In a good agreement with previous findings, production yield of the protein was higher with pETcyo plasmid and detected clearly *via* SPFS.

Complementary to this work, integration behavior of *in-vivo* expression products and *in-vitro* expression products which was done in a test tube, was examined as well. Importantly, it was shown that insertion of readily expressed protein does not happen. Insertion was favored in the presence of artificial membrane and most probably integration process is a kind of stimuli which starts directly on the membrane surface in parallel with expression of the target protein.

3.7 Spectroscopic Features of Cytochrome bo₃

As stated previously in section 3.2, *E.coli* Cyt-bo₃ contains heme *b* and heme *o*. Normally their ration is 1:1 but it has been reported^{17, 18} that from some of the multicopy plasmids heme *o* is integrated into low spin site to produce oo₃ type enzyme instead of bo₃.

Heme *b* is the “low spin” heme which assists the electron transfer from quinol compounds to the binuclear metallic center. Heme *o* is the “high spin” heme molecule which places in binuclear metallic center with Cu_B and serving as an acceptor. All of the optical properties of Cyt-bo₃ arise from contributions of heme *b* and heme *o*. Generally spectra of these two heme molecules overlap for Cyt-bo₃ protein, so the most common method to obtain separate spectra of hemes is reduce minus oxidized spectra.

Oxidases containing heme *b* and heme *o* generally appears in red color because of the heme groups. They have soret maxima around 428 nm and α -band near 607 nm for reduced minus oxidized spectra. Soret band is a strong absorption band in the blue region of the optical absorption of a heme protein.

3.7.1 Spectrophotometric Analysis of Isolated Cytoplasmic Membranes

In this section, spectroscopic properties of his-tagged Cyt-bo₃ are described. General spectroscopic techniques such as difference spectra were applied on pure protein samples. Difference spectra were generally recorded on 4-5 μ M membrane samples. To eliminate light scattering the membrane samples were often suspended in 50mM K₂HPO₄ buffer (pH: 7.0) containing 1% TritonX-100 and 1% Octyl glucoside. Principally solubilized Cyt-bo₃ is in oxidized form. Oxidized spectra were taken directly from solubilized membrane samples

¹⁷ Puustinen, A., Wikstrom, M., (1991) Proc. Natl. Acad. Sci., 88, 6122.

¹⁸ Puustinen, A., Morgan, J. E., Verkhovsky, M., Thomas, J. W., Gennis, R. B., Wikstrom, M., (1992) Biochem., 31, 10363.

without any treatment. Reduced spectra were followed by adding a few grains of sodium hydrosulfite (dithionite or DTT) to the oxidized sample. Oxidized sample was reduced *via* addition of DTT within 1-2 min, but it must be noted that high amount of DTT cause to precipitation of enzyme.

Real method to obtain the ideal reduced minus oxidized spectra is reducing sample with addition of DTT in the presence of cyanide. After addition of DTT, “high spin” heme remains still oxidized form in the presence of cyanide. So, spectra of high spin heme and low spin heme can easily be observed by subtracting these two spectra. The most important fact in here, cytoplasmic membrane samples were used instead of pure Cyt- bo_3 , which decreases the probability getting sharp bands depending on heterogeneity of the samples and low enzyme concentration. On the other hand, cyanide has a big contribution on the background which could easily cause to loss of very weak bands. For that reason cyanide addition was not done since cytoplasmic membrane samples were used instead of pure protein.

The reduced minus oxidized spectra of *in-vivo* Cyt- bo_3 was given in Figure 3.58 for pJRHisA clone and in Figure 3.59 for pETcyo clone. In Figure 3.58 reduced, oxidized and reduced minus oxidized spectra was presented separately. In the oxidized form of the enzyme solution, the Soret maximum appears to range from 405-406 nm. The reduced minus oxidized spectra shows a Soret peak at 428 nm and a broad absorbance peak at 562-563 nm region coming from α -band. It is well known from literature data that pure protein has a Soret maximum at 407-408nm. Heterogeneity of the sample and insufficient reducing process cause that shift in Soret region and appearance of the shoulder at around 405 nm.

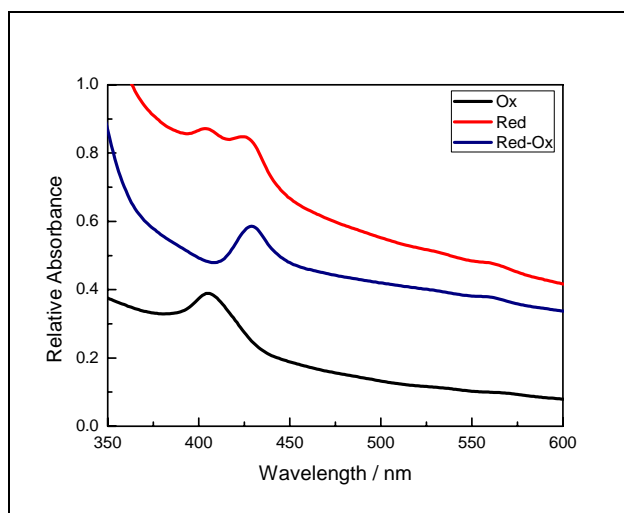


Figure 3.58 Reduced minus Oxidized spectra of Cyt- bo_3 pJRHisA clone

Optical spectra of pETcyo Cyt-bo₃ shown in Figure 3.59 displayed a Soret peak at 409nm for oxidized enzyme sample. Reduced minus oxidized spectra shows a Soret maxima at 429-430 nm region and a broad peak in the α -band region at 561 nm. The spectral properties of histidine tagged enzymes showed nearly identical optical behavior with small differences which might be related with preparation differences. In comparison to literature data, obtained results were in a good agreement with identical clones and the wild type enzyme despite the variation of preparations.

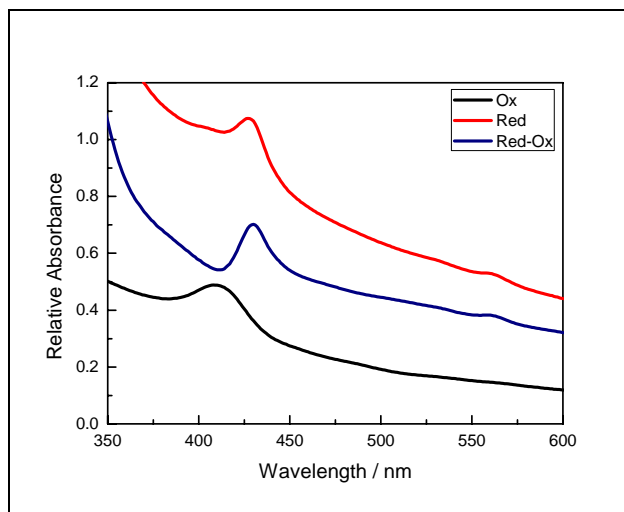


Figure 3.59 Reduced minus Oxidized spectra of Cyt-bo₃ pETcyo clone

3.7.2 Spectrophotometric Analysis of *in-vitro* Expressed Cytochrome bo₃

It is complicated and mostly not possible to detect the proteins which are expressed *via in-vitro* synthesis due to the low yield. The main limitation of the *in-vitro* expression system in this study is the amount of the synthesized product. According to this observation, it is not possible to detect *in-vitro* expressed Cyt-bo₃ *via* reduced minus oxidized spectra since concentration of protein and the heme content is another limitation for the spectrophotometric analysis. Therefore only simple absorption behavior of proteins was investigated at around 280 nm which corresponds to amino acids and peptide bonds in protein structure.

Sample preparation was done as described previously in section 2.7.4. For both pJRHisA and pETcyo plasmids, 350-400 μ l *in-vitro* expression mixture was used and purified as explained. Optical measurements were performed for 20 μ l of each solubilized sample and results were given in Figure 3.60. Absorption maxima was observed at 262-263 nm for both pETcyo and pJRHisA *in-vitro* products and the effect of *in-vitro* mixture was observed as well

since *in-vitro* extract is a protein mixture itself. It is clearly observed that there is a significant difference in between negative (blank) and positive samples coming from expressed target protein. Another substantial output regarding the absorbance values is as expected pET_{cyo} plasmid yields more concentrated sample than pJRH_{isA} plasmid. Although specific absorbance wavelength was ~280 nm for protein structures, this shift might be caused by the purification process of the protein or caused by heterogeneity of the sample. Sample concentrations were analyzed roughly by using western blot technique and found out that each sample is in “ng” amount. Detailed results will be represented in the following section together with enzyme activity results.

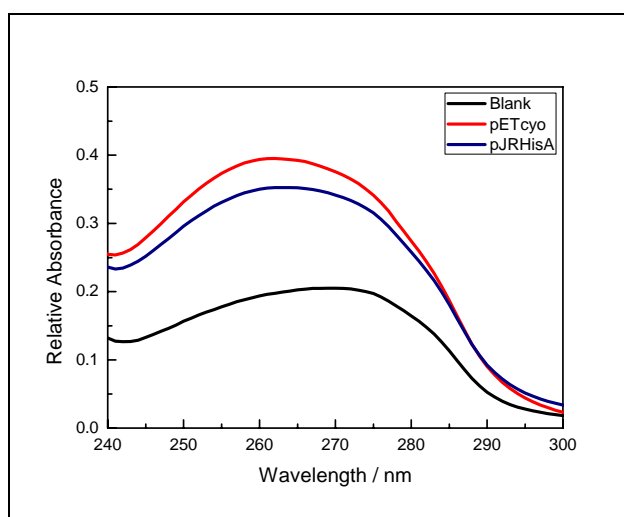


Figure 3.60 Spectrophotometric properties of *in-vitro* expressed Cyt-bo₃

3.8 Enzymatic Properties of Cytochrome bo₃

As stated previously, Cytochrome bo₃ Ubiquinol Oxidase accepts electron from quinol on the plasmic side of the membrane and as it can be understood easily from its name it oxidizes quinol compound to quinone during enzymatic activity cycle. Enzymatic activity assay was carried out either by monitoring the oxidation of UQH₂ at 278nm or by measuring oxygen consumption which is the evidence of UQH₂ consumption as well.

Quinol is the main substrate of the enzymatic reaction carried by Cyt-bo₃. Quinol is a two electron carrier which cycles between other complexes of respiratory chain such as dehydrogenases, and Cyt-bo₃ and becomes reduced and oxidized respectively. Additionally, quinol carries two protons and releases them into the periplasm during oxidation process.

Oxidation/reduction equilibrium and also chemical structures of UQ/ UQH₂ couple were given in Figure 3.61.

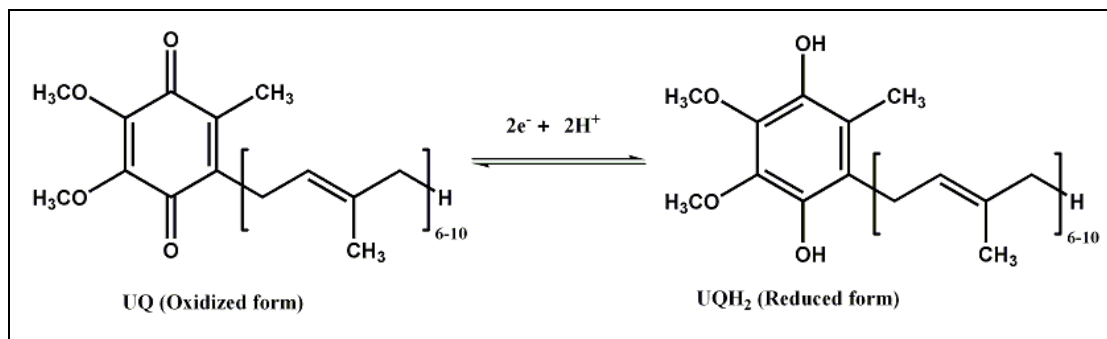


Figure 3.61 Ubiquinone-Ubiquinol conversion

3.8.1 Ubiquinol/Ubiquinone Quantification

Activity assay of enzyme was done using Ubiquinone-1 (UQ). UQ was reduced to Ubiquinol-1 (UQH₂) as described before in section 2.7.1. Quantification of the substrate before and after reducing process was done *via* optical absorption results. Oxidation of UQH₂ was detected spectroscopically at 278 nm by using $\Delta E = 12.25 \text{ mM}^{-1} \text{ cm}^{-1}$. DMSO solubilized UQH₂ was diluted in 50mM K₂HPO₄ buffer (pH: 7.0) and then spectrum of the sample was determined in the range of 240-320 nm (Figure 3.62). Afterwards concentrated Cyt-b_o3 sample was added to the same solution and oxidation of UQH₂ and conversion to UQ was observed immediately in the same range. To be able to separate these two species oxidizing/reducing cycle was performed once more, *via* addition of 1.0M DTT oxidized sample was reduced back to UQH₂ form nearly in 1 min and spectrum is redetermined. Besides DTT is not a strong reducing agent and there could be still some inactivated enzyme in the solution UQ was not completely reduced back to its beginning level. The presence or oxidation of UQ was indicated by specific absorption with maxima at 278nm. As it was also reported¹⁹ before absorption maxima of UQH₂ shifted to higher wavelength and produced this characteristic peak. Considerable amount of absorption increase in the 240-265nm region for the UQH₂ (2nd cycle) sample was originating from DTT addition.

¹⁹ Redfeam, E. R., (1967) Methods in Enzymology, 10, 381.

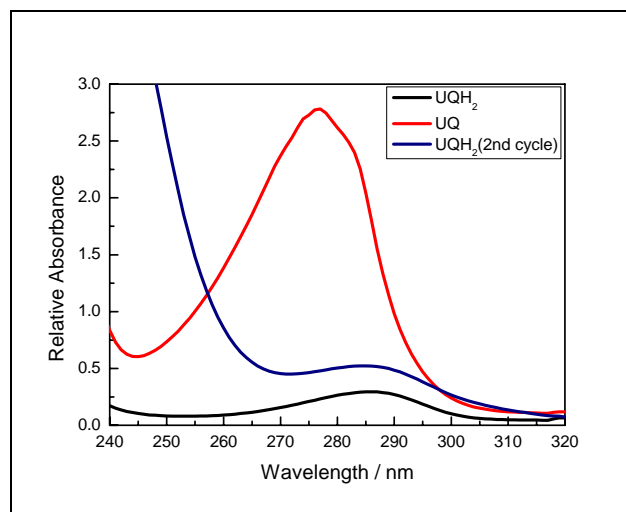


Figure 3.62 Oxidation/Reduction cycle of Ubiquinol-1/Ubiquinone-1 couple

The method described in here has been used successfully for the determination of oxidation/reduction state of UQ and this method has also been used for a quick enzyme activity test.

3.8.2 Enzyme Activity Assay of Isolated Cytoplasmic Membranes

Two different routes were followed to observe activity of the *in-vivo* expressed enzyme. The first and main method was spectroscopic analysis. The spectrophotometric activity assay was done by measuring the oxidation rate of UQH₂ at 278nm. All measurements were carried out at RT in 50mM K₂HPO₄ buffer (pH: 7.0) since it was reported before the optimum pH value is 7.0-7.4 for maximum Cyt-bo₃ enzyme activity.

Calibration curve of UQ which is shown in Figure 3.63, was obtained at 278 nm ($\Delta E=12.25 \text{ mM}^{-1}\text{cm}^{-1}$) by using UQ solutions in a range 5 μM – 1mM. Enzymatic activity, K_M and V_{max} calculations were done by using the slope of calibration curve which has been obtained *via* linear fitting.

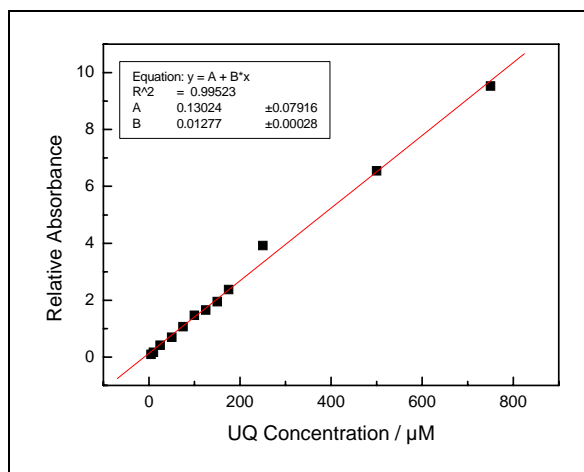


Figure 3.63 UQ Calibration curve

Conversion of UQH₂ to UQ was monitored with addition of 50nM of Cyt-bo₃ into the substrate solution with varied concentrations from 50μM to 250μM. First observation was the complete consumption of substrate molecule in maximum 2-3 minutes depending on the enzyme concentration (Figure 3.64). After 2 or 3 minutes, absorbance values reached to plateau which means there is no more substrate molecule in the solution that enzyme can consume. So, 2 minute measurement period was used with collecting data in each 2 sec time interval. To investigate enzyme kinetics, non-linear part of the curve which corresponds to 2 min time interval was used. Enzyme activity was calculated through the Lineweaver-Burk plot and Michaelis-Menten equation.

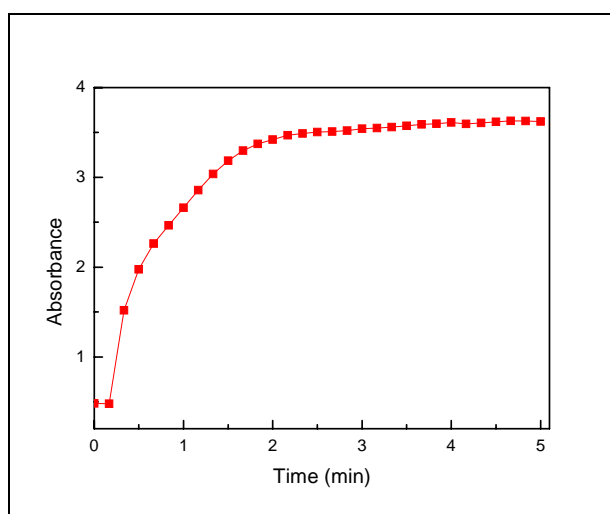


Figure 3.64 UQH₂ Consumption Curve of pETcyo Cyt-bo₃ (200μM UQH₂, 0.65μM, 30μl Cyt-bo₃)

Non-linear part of the curves was presented in Figure 3.65 for the *in-vivo* expressed pJRHSA Cyt-bo₃ by varying the amount of UQH₂ from 50μM to 250μM. Specific enzyme activities was calculated through these data with the help of calibration curve and then they were used to plot Lineweaver-Burk graph where x-axis is reciprocal substrate concentration in μM⁻¹ and y-axis is reciprocal enzyme activity in sec.mol Cyt-bo₃/μmolUQH₂, which gives K_M and V_{max} kinetic parameters. Lineweaver-Burk plot of this sample was given in Figure 3.66 and kinetic parameters were presented in Table 3.5. Data was obtained from six independent measurements.

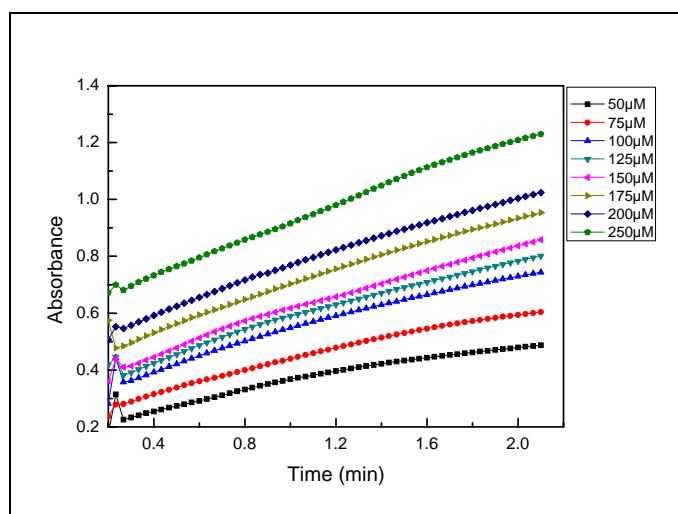


Figure 3.65 pJRHSA Cyt-bo₃ UQH₂ Consumption/Enzyme Activity Curves (50nM, 30μl Cyt-bo₃)

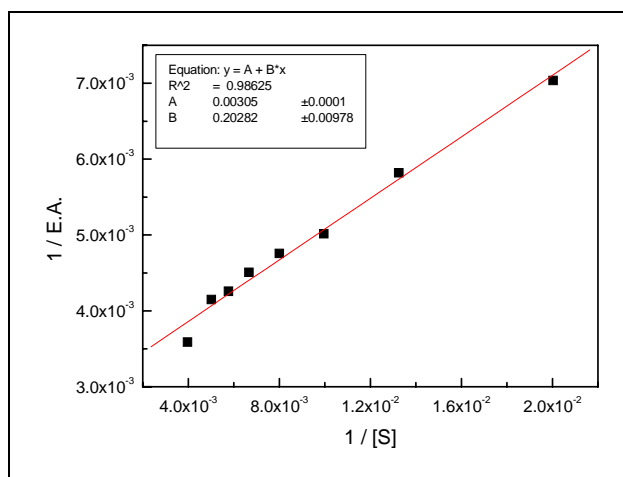


Figure 3.66 Lineweaver-Burk plot of pJRHSA Cyt-bo₃

Same procedure was applied to determine the activity of pETcyo Cyt-bo₃ and all concentrations were kept fixed to compare with the pJRHSA counterpart. UQH₂ consumption was monitored *via* absorption change at 278nm and non-linear parts of UQH₂ consumption plots were presented in Figure 3.67. Once again, Lineweaver-Burk plot was obtained from UQH₂ consumption output. K_M and V_{max} kinetic parameters were calculated directly from Lineweaver-Burk plot (Figure 3.68) and represented in Table 3.5. Calculations were performed by using six independent measurements under the same conditions.

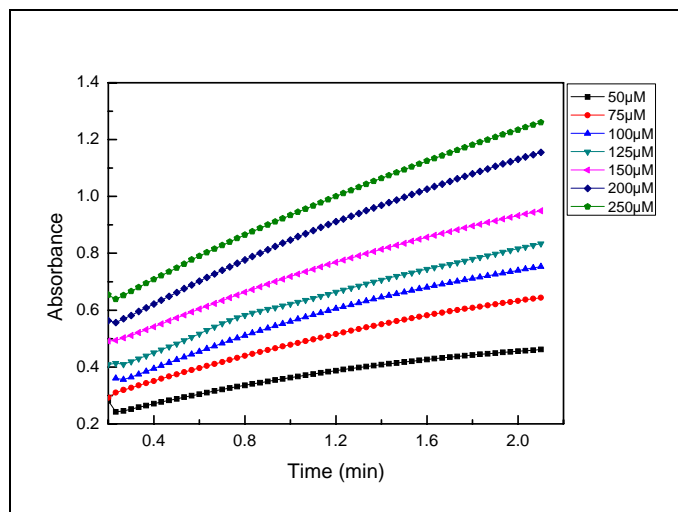


Figure 3.67 pETcyo Cyt-bo₃ UQH₂ Consumption/Enzyme Activity Curves (50nM, 30μl Cyt-bo₃)

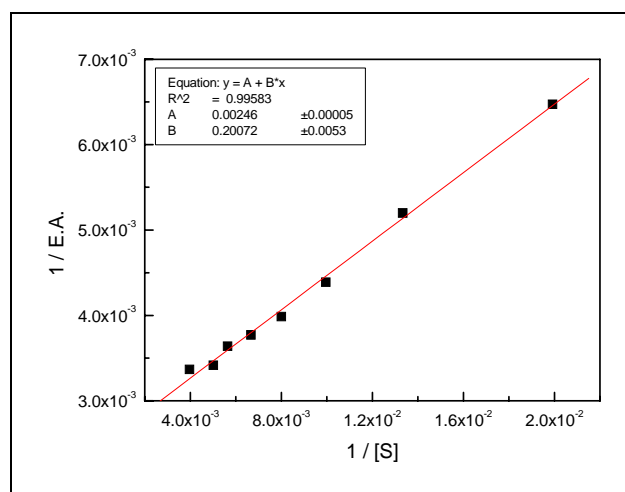


Figure 3.68 Lineweaver-Burk plot of pETcyo Cyt-bo₃

CHAPTER III : RESULTS & DISCUSSION

According to K_M and V_{max} kinetic parameters (Table 3.5) which was observed for both pJRHisA Cyt-bo₃ and pETcyo Cyt-bo₃, two proteins have nearly identical Ubiquinol activities. It is also in a good agreement with the literature data²⁰ which simply indicates expression and purification process was performed successfully. It must be taken into account that enzyme kinetics were calculated from cytoplasmic membranes and presence of cleaved subunit II cause to drop, approximately 80-90%, in the activity of the enzyme.

Table 3.5 Enzyme Kinetic Parameters observed *via* Spectrophotometric Assay

<i>Sample</i>	K_M (μM)	V_{Max} ($\mu mol UQH_2/sec.mol Cyt-bo_3$)
pJRHisA Cyt-bo ₃ (<i>in-vivo</i>)	85.0	354.4
pETcyo Cyt-bo ₃ (<i>in-vivo</i>)	95.5	388.1

Besides spectrophotometric measurements, activity of Cyt-bo₃ was measured with respect to oxygen consumption. The rate of oxygen consumption was measured by using YSI Oxygen Electrode System with a micro chamber which has a 600 μ l volume in total. For 100% air-saturated solution was used which is equivalent to 240 μ M O₂. For 0% oxygen level, excess amount of DTT was added to remove all solubilized oxygen from the solution. Activity assay was performed in a varied substrate concentrations 50-500 μ M which contains DTT to maintain the UQH₂ in reduced form. Oxygen consumption curves were shown in Figure 3.69 with the corresponding UQH₂ concentrations. As it was already reported the most important and limiting parameter is the concentration and the stability of UQH₂ while performing enzyme activity assay *via* oxygen electrode. UQH₂ is not an adequate substitute for this method since it is difficult to keep it in reduced form during activity assay and another point is UQH₂ can not be solubilized completely in buffer and can easily precipitates sometimes at higher concentrations. Considering this limitations initial rates and kinetic parameters were calculated from the slope of Lineweaver-Burk plot which is shown in Figure 3.70. Calculated enzyme activity was 135.5 mole⁻¹/sec/mol Cyt-bo₃ at 25°C for solubilized membrane samples of pETcyo Cyt-bo₃ which is nearly 5-fold less than the Ni-NTA purified ones regarding to literature data again. Affinity value, K_M , for UQH₂ is 209.7 μ M, given in Table 3.6. As pointed out previously, UQH₂ suffers from low solubility problem which can easily affect the kinetic parameters. In addition it must be noted that solubilized membrane samples namely

²⁰ Rumbley, J. N., Analysis of Heme-Copper Ligation, Quinol Activity and Ligand Binding Kinetics of Cytochrome bo₃ Quinol Oxidase from *E.coli*, Dissertation Thesis (1995), University of Illinois at Urbana-Champaign.

CHAPTER III : RESULTS & DISCUSSION

cytoplasmic membranes does not supposed to show the similar enzyme activity as purified enzyme does due to the fact environmental differences in the solution. None the less, comparing to the literature data enzyme activities and affinities were monitored quite accurately. Since concentration of pJRHisA Cyt- b_3 samples was quite low it did not produce significant and meaningful results, so it could not be evaluated at this point.

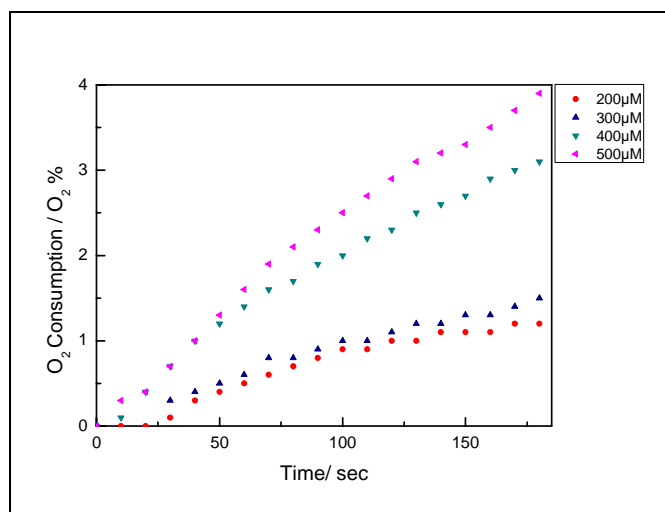


Figure 3.69 pETcyo Cyt- b_3 Oxygen Consumption Curves (200-500 μ M UQH $_2$, 4 μ M, 3 μ l Cyt- b_3)

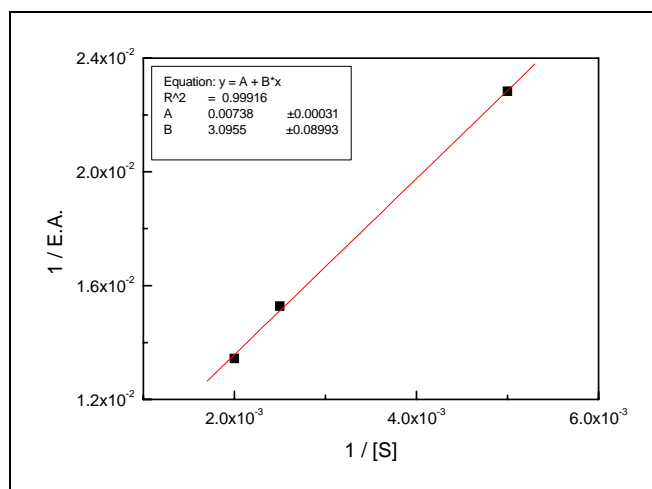


Figure 3.70 Lineweaver-Burk plot of pETcyo Cyt- b_3 obtained from Oxygen electrode

Table 3.6 Enzyme Kinetic Parameters observed *via* Oxygen Electrode

Sample	K_M (μ M)	V_{Max} ($mol\ e^-/sec.mol\ Cyt-b_3$)
pETcyo Cyt- b_3 (<i>in-vivo</i>)	209.7	135.5

3.8.3 Enzyme Activity Assay of *in-vitro* Expressed Cytochrome bo₃

While cell-free expression of protein is a significant achievement itself, maybe the most challenging improvement is to observe the activity of artificially synthesized biomolecule. Here it must be emphasized once more although it has been outlined previously for several times that observation of the enzyme activity for *in-vitro* synthesized Cyt-bo₃ is the key point of this study.

UQH₂ oxidation rate or relative enzyme activity regarding to spectrophotometric measurements could not be observed due to the limitations of the method. Since *in-vitro* expression system is a protein mixture itself, broad absorption band was observed at 278nm which is the specific wavelength for monitoring UQH₂ oxidation. Because of this overlapping problem, spectroscopic method was not used for the detection of *in-vitro* product. Even though there are another limitations for it, activity of *in-vitro* Cyt-bo₃ was measured with respect to oxygen consumption by using oxygen electrode system. *In-vitro* synthesized and purified enzyme samples were used at a fixed substrate concentration, 500μM. Lower substrate concentrations than 500μM, did not produce meaningful results due to the solubility problem of UQH₂ and very low enzyme concentration. *In-vitro* expressed enzyme concentrations were calculated from the intensities of western blot bands by using Aida Image Analyzer software. Western blot analysis evaluation (Table 3.7) showed that the amount of *in-vitro* expressed protein was in ng level for each plasmid; however expression yield of pETcyo is always higher than pJRHisA plasmid.

Table 3.7 *In-vitro* expressed Cyt-bo₃ concentrations for pJRHisA and pETcyo plasmid

<i>In-vitro product</i>	<i>Expression volume(μl)</i>	<i>Enzyme amount (ng Cyt-bo₃/μl)</i>
pJRHisA Cyt-bo ₃	350	9.1
pETcyo Cyt-bo ₃	400	79.0

5μl of each purified protein was loaded to the gel and concentration analysis results were given in Figure 3.71. 6xHis protein ladder (Qiagen) was used as a positive control for the calculation of the total enzyme amount by means of his-tagged product. In the western blot figure inner rectangle represents the mean signal coming from the protein and outer rectangle represents the error part which could be caused by randomly diffused sample. The first line represents the 6xHis protein ladder and intensity of 30kDa band (number 1) corresponds to

CHAPTER III : RESULTS & DISCUSSION

100ng his-tagged protein per 5 μ l sample. Regarding the *in-vitro* expression products, second line represents the pETcyo expression product and third line belongs to pJRHisA product. The band labeled as a number 2 is the uncleaved his-tagged subunit II which is exactly 63.1 ng Cyt-bo₃/ μ l and number 3 is the cleaved his-tagged subunit II which corresponds to 15.9 ng Cyt-bo₃/ μ l. Here it was shown in detail, that the concentration of the uncleaved protein is always higher than cleaved one. The amount of pJRHisA product, shown as number 4 was 9.1 ng Cyt-bo₃/ μ l. Molarity calculations were done *via* using a virtual web software²¹ (MPI Molecular Genetics) for converting the weight in molar quantity.

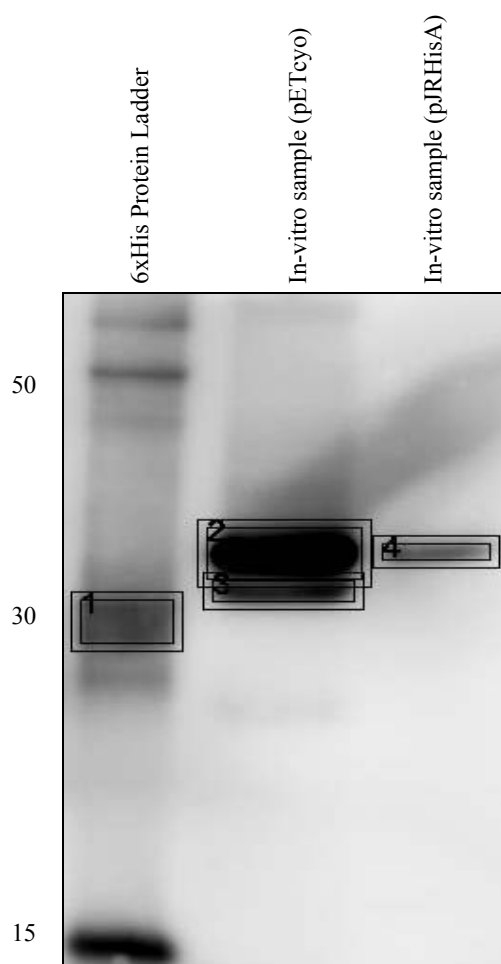


Figure 3.71 Western blot analysis of *in-vitro* expressed pJRHisA and pETcyo Cyt-bo₃ for concentration determination (NuPAGE®Novex 10% Bis-Tris gel, 200V, 50 min, MOPS Buffer, PVDF membrane, WesternBreeze® Chemiluminescent Anti-mouse kit)

²¹ <http://www.molgen.mpg.de/~soldatov/protocols/scripts/index.html>

Observation of enzyme activity was done through purified Cyt-bo₃ *in-vitro* samples and raw Cyt-bo₃ *in-vitro* mixture in parallel. Data were collected from at least two independent measurements and oxygen consumption graph of purified Cyt-bo₃ *in-vitro* samples for 400 and 500 μ M UQH₂ was given in Figure 3.72.

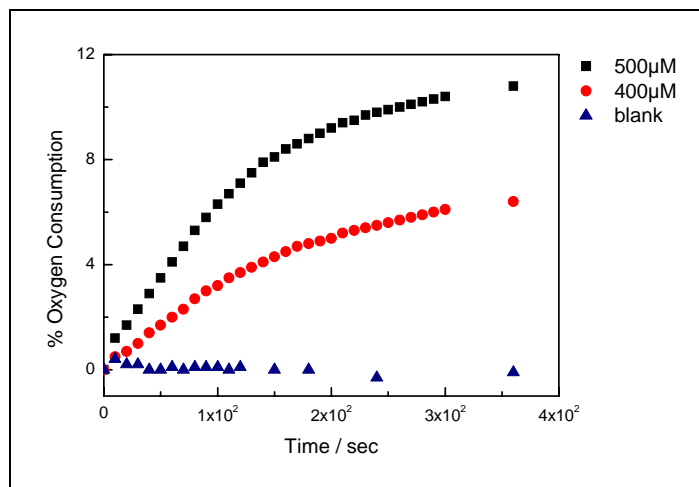


Figure 3.72 *In-vitro* expressed and purified pETcyo Cyt-bo₃ Oxygen Consumption Curves (400-500 μ M UQH₂, 6.1 μ mol, 10 μ l Cyt-bo₃)

Typical values observed for purified pETcyo Cyt-bo₃ are 121.4 μ mole⁻/sec/mol Cyt-bo₃ at 25°C by using 400 μ M UQH₂ and 146.6 μ mole⁻/sec/mol Cyt-bo₃ at 25°C by using 500 μ M UQH₂. Raw expression mixture without any purification has enzyme activity 7.7 μ mole⁻/sec/mol Cyt-bo₃ at 25°C by using 500 μ M UQH₂. This indicates although there might be a significant loss of enzyme and the activity itself during purification process, it produces meaningful results regarding to the non-purified one which can be possibly related with the enzyme concentration and decreased affinity because of the difficult reaction of enzyme and substrate molecules in the *in-vitro* expression environment.

Unfortunately it was not possible to observe any enzyme activity for purified pJRHisA Cyt-bo₃ since the calculated concentration of this sample was only 349fmol and thus, below the detection limit.

3.8.4 Conclusion Enzymatic Activity of *in-vitro* Expressed Cyt-bo₃

Spectroscopic analysis and oxygen consumption analysis showed acceptable results for *in-vivo* expressed pJRHisA and pETcyo Cyt-bo₃ samples. In comparison with the literature which must be noted only solubilized membrane samples were characterized in here, results

were in a good agreement regarding to UQH₂ oxidation rate. Despite the fact the efficiency difference in between pJRHsA plasmid and pETcyo plasmid, it did not affect the enzyme activity.

The activity of *in-vitro* synthesized pETcyo Cyt-bo₃ was apparently quite less than the *in-vivo* expressed counterpart. This was not an unexpected result since the amount of enzyme which is obtained from *in-vitro* system, is quite low comparing to *in-vivo* product. Disregarding all limitations of the expression system and activity assay methods, promising results were produced to verify the activity of *in-vitro* expressed Cyt-bo₃ which correlates well with western blot and SPFS characterization results.

4 General Conclusion & Outlook

Components of the membrane system and the procedure were optimized for the assembly of tethered bilayer lipid membranes (tBLM). The *in-vitro* synthesis and incorporation of membrane proteins were investigated and furthermore their biosensing capabilities were investigated in this artificial membrane system.

P19 spacer was self-assembled on gold surface and then EDC-NHS coupling was performed to assemble phospholipid monolayer. Eight different phospholipids were investigated to observe their influence on tBLM architecture and it was investigated by means of CA and SPR. Membrane structures showed slight differences concerning their packing density and fluidity, none of these model membranes represented the perfect planar membrane structure. Nevertheless with this work it has been shown that proposed model membrane architecture creates a quasi-natural environment for the incorporation of the aimed membrane protein and for the activity observation. With the optimization of the platform, we had valuable information not only about the insertion mechanism of the protein, but also minimum requirements of the system to observe its functionality. With this approach, *in-vitro* synthesis of the Cyt-bo₃ and observation of its functionality was successfully achieved. Further improvements and optimizations of the artificial membrane platform might be necessary to increase incorporation efficiency and functionality.

Culture conditions were optimized to obtain high efficiency of purification. Isolation and purification was done for the histidine tagged Cyt-bo₃. Purified enzyme samples were used for controlling protein insertion and functionality. For this reason, the quality of the cytoplasmic membranes was sufficient enough to compare with the *in-vitro* counterparts. So, further purification steps were not performed *via* using Ni-NTA affinity chromatography.

In-vitro expression of cytochrome bo₃ ubiquinol oxidase was successfully achieved for each pJRHisA, pETcyo and pRCO₃ plasmids. Influence of expression mixture and promoter type were examined and shown that *E.coli* extract is the best candidate for increased expression efficiency. Besides, presence of T7 promoter increased the probability of the expression and the best expression yield was produced by using T7 promoter which was cloned in pETcyo plasmid. In parallel to these findings, SPFS results also confirmed the *in-vitro* expression of Cyt-bo₃ efficiently for both pJRHisA and pETcyo plasmids. Furthermore expression and insertion was supported by western blot results of Cyt-bo₃.

Additionally, insertion behavior for both *in-vivo* and *in-vitro* expressed Cyt-bo₃ and antibody adsorption effect was observed. As proposed, it was shown that insertion of a membrane protein was favored in the presence of biomimetic membrane and insertion of readily expressed protein does not happen. Another important finding was non-specific interaction in between antibodies and the artificial membrane structure which cause to the background effect or false positive signal in SPFS measurements. To prevent this non-specific interaction, blocking solution was used and unoccupied places on the membrane surface were covered with that.

Functionality of the *in-vitro* expression product was analysed by means of UQH₂ oxidation rate and oxygen consumption. Enzyme activity was monitored for both *in-vivo* and *in-vitro* expressed pJRHSA and pETcyo Cyt-bo₃ samples. In a good agreement with SPFS results, pETcyo expression product showed higher enzyme activity than pJRHSA product depending on the presence of T7 promoter.

List of Tables

Table 2.1	Bacterial strains and plasmids
Table 2.2	Growth media for pJRHisA plasmid
Table 2.3	Growth media for pRCO3 plasmid
Table 2.4	M63 Minimal media / Growth media for pETcyo plasmid
Table 2.5	Volumes of solutions required to create lysate
Table 2.6	Sample preparation for agarose gel
Table 2.7	Restriction digest scheme
Table 2.8	Volumes of Solutions Required for His-tag protein purification
Table 2.9	<i>In-vitro</i> expression pipetting scheme (Promega Kit)
Table 2.10	Transcription reaction pipetting scheme (Qiagen Kit)
Table 2.11	Translation reaction pipetting scheme (Qiagen Kit)
Table 2.12	Volumes of components for <i>in-vitro</i> expression by using FluoroTect Labeling
Table 2.13	Sample preparation for SDS-Page gel
Table 2.14	Running conditions for SDS-Page gel
Table 2.15	Exposure conditions for Western Blotting
Table 2.16	Chemical structures of Lipid Monolayer Components
Table 3.1	SPR Fit Parameters
Table 3.2	SPR Fit Parameters of Varied Monolayers
Table 3.3	Plasmid DNA concentrations
Table 3.4	Cyt-bo ₃ concentrations, determined via BCA Assay
Table 3.5	Enzyme Kinetic Parameters observed via Spectrophotometric Assay
Table 3.6	Enzyme Kinetic Parameters observed via Oxygen Electrode
Table 3.7	<i>In-vitro</i> expressed Cyt-bo ₃ concentrations for pJRHisA and pETcyo plasmid

List of Figures

- Figure 1.1 Simplified view of mitochondrial respiratory chain
- Figure 1.2 Aerobic respiratory chains of mitochondria and *E.coli*
- Figure 1.3 Overall structure of ubiquinol oxidase from *E.coli*
- Figure 1.4 Schematic representation of electron and proton transfer in ubiquinol oxidase
- Figure 1.5 Schematic representation of a cell membrane
- Figure 1.6 Reflection at the glass/dielectric interface
- Figure 1.7 Dispersion relation of free photons and surface plasmons
- Figure 1.8 Total internal reflection (a) at a glass prism in contact with a dielectric, (b) at a metal film
- Figure 1.9 Major decay channels for fluorophores in close proximity to metal film
- Figure 1.10 Jablonski energy level diagram
- Figure 1.11 Contact angles of hydrophilic and hydrophobic surfaces
- Figure 2.1 Schematic representation of SPR/SPFS setup
- Figure 2.2 Alignment of SPR/SPFS setup
- Figure 2.3 A photograph of SPR/SPFS setup
- Figure 2.4 Assembly of flow cell
- Figure 2.5 Scan curve and Kinetic curve
- Figure 2.6 Fluorescence Scan curve and Kinetic curve
- Figure 3.1 Contact angles of P19 for different incubation times
- Figure 3.2 CCD images of (a) bare gold, (b) 20min, (c) 45min, (d) 120min, (e) overnight incubation period of 0.01mg/ml P19
- Figure 3.3 Contact angles of P19 for different concentrations
- Figure 3.4 CCD images of (a) bare gold, (b) 0.1mg/ml, (c) 0.01mg/ml, (d) 0.001mg/ml, (e) 0.0001mg/ml P19
- Figure 3.5 Kinetic SPR curve of P19 assembly
- Figure 3.6 Membrane formation steps
- Figure 3.7 Reaction Mechanism for EDC-NHS coupling
- Figure 3.8 Angles of different DMPE:TritonX mixing ratio
- Figure 3.9 CCD images of (a) 2 mg/ml, DMPE:TritonX 10:1, (b) 2 mg/ml, DMPE:TritonX 5:1, (c) 2 mg/ml, DMPE:TritonX 2:1, (d) 0.2 mg/ml, DMPE:TritonX 10:1, (e) 0.2 mg/ml, DMPE:TritonX 5:1, (f) 0.2 mg/ml, DMPE:TritonX 2:1
- Figure 3.10 Contact Angles of (1)DMPE, (2)DPePE, (3)DPPE, (4)DPalPE, (5)DPHyPE for EDC-NHS coupled samples before assembly

- Figure 3.11 CCD images of (a)DMPE, (b)DPePE, (c)DPPE, (d)DPalPE, (e)DPhyPE monolayer for EDC-NHS coupled samples before assembly
- Figure 3.12 Contact Angles of (1)DMPE, (2)DPePE, (3)DPPE, (4)DPalPE, (5)DPhyPE, (6)DLPE, (7)DAPE, (8)DDPE monolayer via self assembly
- Figure 3.13 CCD images of (a)DMPE, (b)DPePE, (c)DPPE, (d)DPalPE, (e)DPhyPE, (f)DLPE, (g)DAPE, (h)DDPE monolayer via self assembly
- Figure 3.14 Light Scattering data of (a)PC, (b)TE vesicles
- Figure 3.15 SPR data of (a)P19/DMPE/PC, (b)P19/DMPE/TE system
- Figure 3.16 SPR data of (a)P19/DMPE, (b)P19/DPePE, (c)P19/DPhyPE, (d)P19/DAPE, (e)P19/DLPE system
- Figure 3.17 SPR kinetic curves of PC vesicle addition
- Figure 3.18 *cyo* operon containing *cyoA*, encoding subunit II, *cyoB*, encoding subunit I, *cyoC*, encoding subunit III, *cyoD*, encoding subunit IV, and *cyoE*, encoding a farnesyl transferase
- Figure 3.19 Conversion scheme for HemeB to HemeO and HemeA
- Figure 3.20 Topological models of (a)subunit I, (b)subunit II, (c)subunit III, (d)subunit IV, of *E.coli* Cyt-bo₃ and (e)*cyoE* encoding polypeptide
- Figure 3.21 Vector map of pJRHisA plasmid
- Figure 3.22 Vector map of pRCO₃ plasmid that contains fused genes
- Figure 3.23 Membrane topology of fused subunits II, I, III for Cyt-bo₃
- Figure 3.24 Vector map of pETcyo plasmid
- Figure 3.25 Nucleotide sequence of *cyo* operon
- Figure 3.26 Microscope images of *E.coli* cells in (a) pJRHisA media with aggregates appearing during cultivation, (b)LB media
- Figure 3.27 Gel electrophoresis analysis of pJRHisA plasmid (a) circular DNA, (b) double digest with ClaI/EcoRI
- Figure 3.28 Gel electrophoresis analysis of pRCO₃ plasmid
- Figure 3.29 Gel electrophoresis analysis of pETcyo plasmid
- Figure 3.30 (a)Western blotting, (b)Coomassie Blue staining results of pETcyo cell pellets for IPTG induction (NuPAGE®Novex 10% Bis-Tris gel, 200V, 50 min, MOPS Buffer, PVDF membrane, WesternBreeze® Chemiluminescent Anti-mouse kit)
- Figure 3.31 (a)Western blotting, (b)Coomassie Blue staining results of pJRHisA under Native purification conditions (NuPAGE®Novex 10% Bis-Tris gel, 200V, 35min, MES Buffer, PVDF membrane, WesternBreeze® Chemiluminescent Anti-mouse kit)

- Figure 3.32 (a)Western blotting, (b)Coomassie Blue staining results of pJRHisA under Denaturing purification conditions (NuPAGE®Novex 10% Bis-Tris gel, 200V, 50 min, MOPS Buffer, PVDF membrane, WesternBreeze® Chemiluminescent Anti-mouse kit)
- Figure 3.33 (a)Western blotting, (b)Coomassie Blue staining results of pETcyo under Native purification conditions (NuPAGE®Novex 10% Bis-Tris gel, 200V, 50 min, MOPS Buffer, PVDF membrane, WesternBreeze® Chemiluminescent Anti-mouse kit)
- Figure 3.34 (a)Western blotting, (b)Coomassie Blue staining results of pETcyo under Denaturing purification conditions (NuPAGE®Novex 10% Bis-Tris gel, 200V, 50 min, MOPS Buffer, PVDF membrane, WesternBreeze® Chemiluminescent Anti-mouse kit)
- Figure 3.35 Western blot analysis of Cyt-bo₃ expressed by pJRHisA strain (NuPAGE®Novex 10% Bis-Tris gel, 200V, 50 min, MOPS Buffer, PVDF membrane, WesternBreeze® Chemiluminescent Anti-mouse kit)
- Figure 3.36 Western blot analysis of Cyt-bo₃ expressed by pETcyo strain (NuPAGE®Novex 10% Bis-Tris gel, 200V, 50 min, MOPS Buffer, PVDF membrane, WesternBreeze® Chemiluminescent Anti-mouse kit)
- Figure 3.37 Western blot analysis of *in-vitro* expressed Cyt-bo₃ by pJRHisA strain (NuPAGE®Novex 10% Bis-Tris gel, 200V, 50 min, MOPS Buffer, PVDF membrane, WesternBreeze® Chemiluminescent Anti-mouse kit)
- Figure 3.38 Western blot analysis of *in-vitro* expressed Cyt-bo₃ by pETcyo strain (NuPAGE®Novex 10% Bis-Tris gel, 200V, 50 min, MOPS Buffer, PVDF membrane, WesternBreeze® Chemiluminescent Anti-mouse kit)
- Figure 3.39 Western blot analysis of *in-vitro* expressed Cyt-bo₃ by using Insect Kit for pJRHisA(lane3) and pETcyo(lane4) strain (NuPAGE®Novex 10% Bis-Tris gel, 200V, 50 min, MOPS Buffer, PVDF membrane, WesternBreeze® Chemiluminescent Anti-mouse kit)
- Figure 3.40 Structure of FluoroTect™ Green_{Lys} tRNA
- Figure 3.41 FluoroTect™ Green_{Lys} labeling result of *in-vitro* expressed Cyt-bo₃ for pRCO₃ plasmid (NuPAGE®Novex 10% Bis-Tris gel, 200V, 50 min, MOPS Buffer, PVDF membrane, WesternBreeze® Chemiluminescent Anti-mouse kit)
- Figure 3.42 Absorption and Fluorescence emission spectra of (a)Alexa Fluor647, (b)Cy5 conjugated antibody
- Figure 3.43 Fluorescence kinetic of Cy5 conjugated antibody binding
- Figure 3.44 Fluorescence kinetic of Alexa Fluor 647 conjugated antibody binding
- Figure 3.45 SPFS scan of the system P19/DMPE/PC/PentaHis 1°Ab/Cy5 conjugated 2°Ab
- Figure 3.46 SPFS scan of the system P19/DMPE/PC/Alexa Fluor 647 conjugated 1°Ab

- Figure 3.47 SPFS scan of the system P19/DMPE/PC/Blocking Solution/Cy5 conjugated 2°Ab or P19/DMPE/PC/Blocking Solution/Alexa Fluor 647 conjugated 1°Ab
- Figure 3.48 SPFS scan of the system (■) P19/DMPE/PC/*in-vitro* Cyt-bo₃/PentaHis 1°Ab/Cy5-conjugated 2°Ab and (■) P19/DMPE/PC/*in-vitro* Cyt-bo₃/Blocking Solution/ PentaHis 1°Ab/Cy5-conjugated 2°Ab
- Figure 3.49 SPFS scan of the system (■) P19/DMPE/PC/*in-vitro* Cyt-bo₃/Alexa Fluor 647 conjugated 2°Ab and (■) P19/DMPE/PC/*in-vitro* Cyt-bo₃/Blocking Solution/Alexa Fluor 647 conjugated 2°Ab
- Figure 3.50 SPFS scan of the system (■) P19/DMPE/PC/*in-vivo* Cyt-bo₃/PentaHis 1°Ab/Cy5-conjugated 2°Ab and (■) P19/DMPE/PC/*in-vivo* Cyt-bo₃/Blocking Solution/ PentaHis 1°Ab/Cy5-conjugated 2°Ab
- Figure 3.51 SPFS scan of (■) P19/DMPE/PC/*in-vitro* Cyt-bo₃ pJRHSA plasmid/Blocking Solution/PentaHis 1°Ab/Cy5-conjugated 2°Ab and (■) P19/DMPE/PC/*in-vitro* extract without DNA/Blocking Solution/ PentaHis 1°Ab/Cy5-conjugated 2°Ab
- Figure 3.52 SPFS scan of (■) P19/DMPE/PC/*in-vitro* Cyt-bo₃ pJRHSA plasmid/Blocking Solution/ Alexa Fluor 647 conjugated 2°Ab and (■) P19/DMPE/PC/*in-vitro* extract without DNA/Blocking Solution/ Alexa Fluor 647 conjugated 2°Ab
- Figure 3.53 SPFS scan of (■) P19/DMPE/PC/*in-vitro* Cyt-bo₃ pETcyo plasmid/Blocking Solution/PentaHis 1°Ab/Cy5-conjugated 2°Ab and (■) P19/DMPE/PC/*in-vitro* extract without DNA/Blocking Solution/ PentaHis 1°Ab/Cy5-conjugated 2°Ab
- Figure 3.54 SPFS scan of (■) P19/DMPE/PC/*in-vitro* Cyt-bo₃ pETcyo plasmid/Blocking Solution/ Alexa Fluor 647 conjugated 2°Ab and (■) P19/DMPE/PC/*in-vitro* extract without DNA/Blocking Solution/ Alexa Fluor 647 conjugated 2°Ab
- Figure 3.55 SPFS scan of (■) P19/DMPE/TE/*in-vitro* Cyt-bo₃ pETcyo plasmid/Blocking Solution/ Alexa Fluor 647 conjugated 2°Ab and (■) P19/DMPE/TE/*in-vitro* extract without DNA/Blocking Solution/ Alexa Fluor 647 conjugated 2°Ab
- Figure 3.56 Western blot analysis of SPFS samples, *in-vitro* expressed Cyt-bo₃ pJRHSA plasmid (NuPAGE®Novex 10% Bis-Tris gel, 200V, 50 min, MOPS Buffer, PVDF membrane, WesternBreeze® Chemiluminescent Anti-mouse kit)
- Figure 3.57 Western blot analysis of SPFS samples, *in-vitro* expressed Cyt-bo₃ pETcyo plasmid (NuPAGE®Novex 10% Bis-Tris gel, 200V, 50 min, MOPS Buffer, PVDF membrane, WesternBreeze® Chemiluminescent Anti-mouse kit)
- Figure 3.58 Reduced minus Oxidized spectra of Cyt-bo₃ pJRHSA clone
- Figure 3.59 Reduced minus Oxidized spectra of Cyt-bo₃ pETcyo clone
- Figure 3.60 Spectrophotometric properties of *in-vitro* expressed Cyt-bo₃
- Figure 3.61 Ubiquinone-Ubiquinol conversion
- Figure 3.62 Oxidation/Reduction cycle of Ubiquinol-1/Ubiquinone-1 couple

- Figure 3.63 UQ Calibration curve
- Figure 3.64 UQH₂ Consumption Curve of pETcyo Cyt-bo₃ (200μM UQH₂, 0.65μM, 30μl Cyt-bo₃)
- Figure 3.65 pJRHisA Cyt-bo₃ UQH₂ Consumption/Enzyme Activity Curves (50nM, 30μl Cyt-bo₃)
- Figure 3.66 Lineweaver-Burk plot of pJRHisA Cyt-bo₃
- Figure 3.67 pETcyo Cyt-bo₃ UQH₂ Consumption/Enzyme Activity Curves (50nM, 30μl Cyt-bo₃)
- Figure 3.68 Lineweaver-Burk plot of pETcyo Cyt-bo₃
- Figure 3.69 pETcyo Cyt-bo₃ Oxygen Consumption Curves (200-500μM UQH₂, 4μM, 3μl Cyt-bo₃)
- Figure 3.70 Lineweaver-Burk plot of pETcyo Cyt-bo₃ obtained from Oxygen electrode
- Figure 3.71 Western blot analysis of *in-vitro* expressed pJRHisA and pETcyo Cyt-bo₃ for concentration determination (NuPAGE®Novex 10% Bis-Tris gel, 200V, 50 min, MOPS Buffer, PVDF membrane, WesternBreeze® Chemiluminescent Anti-mouse kit)
- Figure 3.72 *In-vitro* expressed and purified pETcyo Cyt-bo₃ Oxygen Consumption Curves (400-500μM UQH₂, 6.1pmol, 10μl Cyt-bo₃)

References

- Abramson, J., Riistama, S., Larsson, G., Jasaitis, A., Svensson-Ek, M., Laakkonen, L., Puustinen, A., Iwata, S., Wikström, M., (2000) *Nature Structural Biology*, 7, 10, 910
- Atanasov, V., Atanasov, P., Vockenroth, I., Knorr, N., Köper, I., (2006) *Bioconjugated Chem.*, 17, 631
- Attridge, J. W., Daniels, P. B., Deakon, J. K., Robins, G. A., Davidson, G. P., (1991) *Biosensors & Bioelectronics*, 6, 201
- Austin, S., Friedman, S., Ludtke, D., (1986) *Journal of Bacteriology*, 168-2, 1010
- Babcock, G. T., Wikström, M., (1992) *Nature*, 356, 301
- Benecke, R., Strümper, P., Weiss, H., (1993) *Brain*, 116, 6, 1451
- Berg, J. M., Tymoczko, J. L., Stryer, L., (2002) *Biochemistry*, 5th Edt., W. H. Freeman Co., NewYork.
- Bowie, J. U., (2001) *Curr. Op. Struct. Biol.*, 11, 397
- Bowie, J. U., (2005) *Nature*, 438, 581
- Brandt, U. (1997) *Biochim. Biophys. Acta*, 1318, 79
- Chan, Y. H. M., Boxer, S. G., (2007) *Current Opinion in Chemical Biology*, 11, 6, 581
- Chepuri, V., Gennis, R.B., (1990) *The Journal of Biological Chemistry*, 265, 22, 12978
- De Gennes, P., (1985) *Reviews of Modern Physics*, 57, 827
- Edwards, D. A., Schneck, F., Zhang, I., Davis, A. M. J., Chen, H., Langer, R., (1996) *Biophys. J.*, 71, 1208
- Ferguson-Miller, S., Babcock, G. T., (1996) *Chem. Rev.*, 96, 2889
- FluoroTectTM Green_{Lys} in vitro Translation Labelling System, (2007) Technical Bulletin, Promega
- Förch, R., Schönherr, H., Jenkins, A. T. A., (2009) *Surface Design: Applications in Bioscience and Nanotechnology*, WILEY-VCH Verlag GmbH & Co.
- Frericks, H. L., Zhou, D. H., Yap, L. L., Gennis, R. B., (2006) *Journal of Biomolecular NMR*, 36, 55
- Garcia-Horsman, J. A., Barquera, B., Rumbley, J., Ma, J., Gennis, R. B., (1994) *J. Bacteriol.*, 176, 18, 5587
- Gardner, A., Boles, R. G., (2005) *Curr. Psych. Reviews*, 1, 3, 255
- Gennis, R. B., (1991) *Biochimica Biophysica Acta*, 1058, 21
- Giess, F., Friedrich, M. G., Heberle, J., Naumann, R., (2004) *Biophysical Journal*, 87, 5, 3213
- Haas, R. H., Nasirian, F., Nakano, K., Ward, D., Pay, M., (1995) *Ann. Neurol.*, 37, 714
- Helm, C. A., Israelachvili, J. N., (1993) *Methods in Enzymology*, 220, 130

Hendler, R. W., Pardhasaradhi, K., Reynafarje, B., Ludwig, B., (1991) *Bioophys. J.*, 60, 415

Henze, K., Martin, W., (2003) *Nature*, 426, 6963, 127

Heyse, S., Stora, T., Schmid, E., Lakey, J. H., Vogel, H., (1998) *Biochimica Biophysica Acta*, 88507, 319

Israelachvili, J. N., Marcelja, S., Horn, R. G., (1980) *Quarterly Reviews of Biophysics*, 13, 121

Kasianowicz, J. J., Brandin, E., Branton, D., Deamer, D. W., (1996) *Proc. Natl. Acad. Sci.*, 102, 12377

Katzen, F., Chang, G., Kudlicki, W., (2005) *Trends in Biotechnology*, 23, 3, 150

Knobloch, H., Brunner, A., Leitner, A., Aussenegg, F., Knoll, W., (1993) *Journal of Chemical Physics*, 98, 10093

Knoll, W., (1998) *Annual Reviews of Physics and Chemistry*, 49, 569

Knoll, W., Frank, C. W., Heibel, C., Naumann, R., Offenhauser, A., R uhe, J., Schmidt, E. K., Shen, W. W., Sinner, A., (2000) *Reviews in Molecular Biotechnology*, 74, 137

Knoll, W., K oper, I., Naumann, R., Sinner, E. K., (2008) *Electrochimica Acta*, 53, 23, 6680

K oper, I., (2007) *Molecular BioSystems*, 3, 10, 651

Kretschmann, E., Raether, H., (1968) *Z. Naturforsch. A.*, 23, 2135

Kretschmann, E., (1971) *Zeitschrift f ur Physik*, 241, 313

Lakowicz, J. R., (1999) *Principles of Fluorescence Spectroscopy*, 2nd Edt., Kluwer Academic/Plenum, NewYork.

Lemieux, L. J., Calhoun, M. W., Thomas, J. W., Ingledeu, W. J., Gennis, R. B., (1992) *The Journal of Biological Chemistry*, 267-3, 2105

Liebermann, T., Knoll, W., (2000) *Colloids and Surfaces*, 171, 115

Lodish, H., Berk, A., Zipursky, S. L., Matsudaira, P., Baltimore, D., Darnell, J., (2000) *Molecular Cell Biology*, 4th Edt., W. H. Freeman Co., NewYork.

Ma, J., Lemieux, L., Gennis, R. B., (1993) *Biochemistry*, 32, 7692

Ma, J., Katsonouri, A., Gennis, R. B., (1997) *Biochemistry*, 36,11298

McBride, H. M., Neuspiel, M., Wasiak, S., (2006) *Curr. Biol.*, 16, 14, 551

Mitchell, P., (1961) *Nature*, 191, 144

Mitchell, P., (1976) *J. Theor. Biol.*, 62, 327

Molecular Probes, Invitrogen, Online Datasheet

Morrison, S.M., Cricco, J.A., Hegg, E.L., (2005) *Biochemistry*, 44, 12554

Munro, J. C., Frank, C. W., (2004) *Langmuir*, 20, 10567

- Nelson, D. L., Cox, M. M., (2005) *Lehninger Principles of Biochemistry*, 4th Edt., W. H. Freeman Co, NewYork.
- Neumann, T., (2001) *Strategies for Detecting DNA Hybridisation Using Surface Plasmon Fluorescence Spectroscopy*, Dissertation Thesis, Johannes Gutenberg University
- Nirenberg, M. W., Matthaei, J. H., (1961) *Proc. Natl. Acad. Sci.*, 47, 1588
- Ottava, A., Tvarozek, V., Racek, J., Sabo, J., Ziegler, V., Hianik, T., Tien, H., (1997) *Supramolecular Science*, 4, 101
- Otto, A., (1968) *Zeitschrift für Physik*, 216, 398
- Pizzo, P., Pozzan, T., (2007) *Trends Cell Biol.*, 10, 511
- Puustinen, A., Wikstrom, M., (1991) *Proc. Natl. Acad. Sci.*, 88, 6122
- Puustinen, A., Morgan, J. E., Verkhovsky, M., Thomas, J. W., Gennis, R. B., Wikstrom, M., (1992) *Biochem.*, 31, 10363
- Raether, H., (1988) *Surface Plasmon on Smooth and Rough Surfaces and on Gratings*, Springer, Berlin.
- Raguse, B., Braach-Maksvytis, V., Cornell, B. A., King, L. G., Osman, P. D. J., Pace, R. J., Wieczorek, L., (1998) *Langmuir*, 14, 648
- Redfean, E. R., (1967) *Methods in Enzymology*, 10, 381
- Rieske, J. S., (1967) *Methods in Enzymology*, 239
- Riistama, S., (2000) *Structural and Functional Studies of Bacterial Heme-Copper Oxidases*, Academic Dissertation, University of Helsinki
- Robelek, R., Lemker, E., Wiltschi, B., Kirste, V., Oesterhelt, D., Sinner, E.K., (2007) *Angewandte Chemie-International Edition*, 46(4), 605
- Rumbley, J. N., *Analysis of Heme-Copper Ligation, Quinol Activity and Ligand Binding Kinetics of Cytochrome bo₃ Quinol Oxidase from E.coli*, Dissertation Thesis (1995), University of Illinois at Urbana-Champaign
- Rumbley, J. N., Furlong Nickels, E., Gennis, R.B., (1997) *Biochim Biophys Acta*, 1340, 131-142
- Sackmann, E., (1996) *Science*, 271, 43
- Sambrook, J., Russell, D. W., (2001) *Molecular Cloning A Laboratory Manual*, 3rd Edt., Cold Spring Harbor Laboratory Press, NewYork.
- Saraste, M., (1999) *Science*, 283, 1488
- Schiller, S., Naumann, R., Lovejoy, K., Kunz, H., Knoll, W., (2003) *Angewandte Chemie International Edition*, 42, 208
- Sell, P. J., Neumann, A. W., (1966) *Angewandte Chemie*, 78, 321
- Sherer, T. B., Betarbet, R., Greenamyre, J. T., (2002) *Neuroscientist*, 8, 3, 192
- Singer, S. J., Nicolson, G. L., (1972) *Science*, 175, 720

Sinner, E. K., Knoll, W., (2001) *Curr. Op. Chem. Biol.*, 5, 6, 705

Spinke, J., Liley, M., Guder, H. J., Angermaier, L., Knoll, W., (1993) *Langmuir*, 9, 1821

Spirin, A. S., Swartz, J. R., (2008) *Cell-free Protein Synthesis*, WILEY-VCH Verlag GmbH & Co.

Subrahmaniam, Y., Alves, I. D., Salgado, G. F. J., Lau, P. W., Wysocki, R. J., Salamon, Z., Tollin, G., Hruby, V. J., Brown, M. F., Saavedra, S. S., (2005) *JACS Comm.*, 127, 5320

Tanford, C., (1980) *The hydrophobic effect: Formation of Micelles and Biological Membranes*, 2nd Edt., John Wiley & Sons Inc.

Taylor, R. W., Turnbull, D. M., (2005) *Nat. Rev. Genet.*, 6, 5, 389

Trumpower, B. L., (1990) *J. Biol. Chem.*, 265, 11409

Tsubaki, M., Mogi, T., Hori, H., Hirota, S., Ogura, T., Kitagawa, T., Anraku, Y., (1994) *J. Biol. Chem*, 269, 30861

Ulman, A., (1991) *An Introduction to Ultrathin Organic Films*, Academic Press, London.

van der Oost, J., Lappalainen, P., Musacchio, A., Warne, A., Lemieux, L., Rumbley, J., Gennis, R.B., Aasa, R., Pascher, T., Malmstrom, B.G., and Saraste, M., (1992) *EMBO J.*, 11, 3209

Vasilev, K., Knoll, W., Kreiter, M., (2004) *Journal of Chemical Physics*, 120, 3439

Vockenroth, I. K., (2007) *Investigation of Tethered Bilayer Lipid Membranes for Their Potential Use in Biosensing Devices*, Dissertation Thesis, University of Bath

Vockenroth, I. K., Atanasova, P. P., Jenkins, A. T. A., Köper, I., (2008) *Langmuir*, 24, 2, 496

Winterhalter, M., (2000) *Current Opinion in Colloid & Interface Science*, 5, 250

Yu, F., Yao, D., Knoll, W., (2003) *Analytical Chemistry*, 75, 2610

Zeviani, M., Di Donato, S., (2004) *Brain*, 127, 2153

Zhao, J., Tamm, L. K., (2003) *Langmuir*, 19, 1838

www.molgen.mpg.de/~soldatov/protocols/scripts/index.html